



# Assessing Neurophysiological Conditions using a Multimetric Approach (BioVRSea)

by

Deborah Cecelia Rose Jacob

Dissertation submitted to the School of Science and Engineering  
at Reykjavík University in partial fulfillment  
of the requirements for the degree of  
**Doctor of Philosophy**

June 2024

Thesis Committee:

Paolo Gargiulo, Supervisor  
Professor, Reykjavík University, Iceland

Hannes Petersen, Thesis Committee Member  
Professor, University of Iceland, Iceland

María Kristín Jónsdóttir, Thesis Committee Member  
Professor, Reykjavík University, Iceland

Giorgio Di Lorenzo, Thesis Committee Member  
Professor, University of Rome, Tor Vergata, Italia

Leandro Pecchia, Examiner  
Professor, Università Campus Bio-Medico di Roma, Italia

Copyright  
Deborah Cecelia Rose Jacob  
June 2024

ISBN: 978-9935-539-34-2  
Print version  
Assessing Neurophysiological Conditions using a Multimetric Approach  
(BioVRSea)

978-9935-539-35-9  
Electronic version  
Assessing Neurophysiological Conditions using a Multimetric Approach  
(BioVRSea)

ORCID ID: 0000-0003-3507-8003

The undersigned hereby certify that they recommend to the School of Science and Engineering at Reykjavík University for acceptance this Dissertation entitled **Assessing Neurophysiological Conditions using a Multimetric Approach (BioVRSea)** submitted by **Deborah Cecelia Rose Jacob** in partial fulfillment of the requirements for the degree of **Doctor of Philosophy (Ph.D.) in Biomedical Engineering**

.....  
date

.....  
Paolo Gargiulo, Supervisor  
Professor, Reykjavík University, Iceland

.....  
Hannes Petersen, Thesis Committee Member  
Professor, University of Iceland, Iceland

.....  
María Kristín Jónsdóttir, Thesis Committee Member  
Professor, Reykjavík University, Iceland

.....  
Giorgio Di Lorenzo, Thesis Committee Member  
Professor, University of Rome, Tor Vergata, Italia

.....  
Leandro Pecchia, Examiner  
Professor, Università Campus Bio-Medico di Roma, Italia

The undersigned hereby grants permission to the Reykjavík University Library to reproduce single copies of this Dissertation entitled **Assessing Neurophysiological Conditions using a Multimetric Approach (BioVRSea)** and to lend or sell such copies for private, scholarly or scientific research purposes only.

The author reserves all other publication and other rights in association with the copyright in the Dissertation, and except as herein before provided, neither the Dissertation nor any substantial portion thereof may be printed or otherwise reproduced in any material form whatsoever without the author's prior written permission.

.....  
date

.....  
Deborah Cecelia Rose Jacob  
Doctor of Philosophy



# Assessing Neurophysiological Conditions using a Multimetric Approach (BioVRSea)

Deborah Cecelia Rose Jacob

June 2024

## Abstract

Current diagnosis and longitudinal evaluation of many neurological disorders rely on subjective, questionnaire-based approaches rather than measured biomarkers of the disease. Deficits of postural control are frequently seen in such diseases and provide a route for more objective assessment. This thesis reports the work completed using the unique BioVRSea setup to assess those with a history of concussion and those with early-stage Parkinson's Disease and using a combination of neurophysiological (electromyography - EMG, electroencephalography - EEG, heart rate) and centre of pressure (CoP) measurements. The BioVRSea experiment is a challenging postural control task triggered by a moving platform and a virtual reality environment, during which the neurophysiological measurements are taken. In the first paper, measurements were performed on 54 professional athletes who self-reported their history of concussion or non-concussion. Biosignals and CoP parameters were analyzed before and after the platform movements, to compare the net response of individual postural control. The results showed that BioVRSea discriminated between the concussion and non-concussion groups. Particularly, EEG power spectral density in delta and theta bands showed significant changes in the concussion group and right soleus median frequency from the EMG signal differentiated concussed individuals with balance problems from the other groups. Anterior-posterior CoP frequency-based parameters discriminated concussed individuals with balance problems. In the second study on Parkinson's Disease, 11 early-stage Parkinson's subjects and 46 healthy over-50s took part in the experiment. Significant differences were found between the two groups in electromyographic and centre of pressure measurements. Correlation analysis of the EMG signal indicated opposite correlations in skewness in the right soleus muscle. In the second Parkinson's Disease study, 29 healthy and 9 early-stage Parkinson's Disease subjects were assessed. The results of our work show significant differences in several biosignal features, particularly in the right tibialis anterior, the ellipse area associated with the centre of pressure changes and the power spectral density changes in the alpha and theta bands of the EEG. This thesis shows the potential of BioVRSea as a quantitative means of developing a multi-metric signature capable of quantifying postural control and distinguishing healthy from pathological response.

# Mat á taugalífeðlisfræðilegum aðstæðum með notkun marga mælikvarða nálgun (BioVRSea).

Deborah Cecelia Rose Jacob

júní 2024

## Útdráttur

Núverandi greining og langtíma mat á mörgum taugasjúkdómum byggir á huglægri spurningalistamiðaðri nálgun frekar en mælingu á sjúkdómseinkennum. Skortur á líkamsstöðustjórnun er algengur í slíkum sjúkdómum og gefur þá tækifæri til hlutlægara mats. Þessi ritgerð greinir frá verkum sem framkvæmd voru með einstöku BioVRSea uppsetningunni til að meta þá sem hafa sögu um heilahristing og þá sem eru á byrjunarstigi Parkinsonsveiki með samblandi af taugasálfræðilegum (vöðvarafrit - EMG, heilarafrit - EEG, hjartsláttur) og þungamiðju (CoP) mælingum. BioVRSea tilraunin er krefjandi stöðustýringarverkefni sem framkvæmd er á hreyfanlegum vettvangi og sýndarveruleikaumhverfi, þar sem taugalífeðlisfræðilegar mælingar eru teknar. Í fyrstu greininni voru mælingar gerðar á 54 atvinnuþróttamönnum sem sögðust hafa sögu um heilahristing og þeim sem ekki höfðu sögu um heilahristing. Lífeðlisfræðileg merki og CoP breytur voru greindar fyrir og eftir hreyfingar til að bera saman heildarviðbrögð einstakra líkamsstöðustjórnunar. Niðurstöðurnar sýndu að BioVRSea greindi á milli heilahristinghópsins og samanburðarhópsins. Sérstaklega sýndi EEG aflþéttleiki í delta og theta böndum marktækar breytingar í heilahristingshópnum og miðtíðni í hægri soleus frá EMG merkinu greindi þá með jafnvægisvandamál frá öðrum hópum. Fremri-aftari CoP tíðnibundnar breytur greindu þá með jafnvægisvandamál. Í annarri rannsókn á Parkinsonsveiki tóku 11 einstaklingar á byrjunarstigi Parkinsons og 46 heilbrigðir yfir 50 ára aldur þátt í tilrauninni. Marktækur munur fannst á milli hópanna tveggja í vöðvarafrits- og þungamiðju mælingum. Fylgnigreining á EMG merkinu sýndi andstæða fylgni í skekkju í hægri soleus vöðva. Í annarri rannsókn voru 29 heilbrigðir og 9 einstaklingar á byrjunarstigi Parkinsons metnir. Niðurstöður okkar sýna marktækan mun á nokkrum lífeðlisfræðilegum eiginleikum, sérstaklega í hægri tibialis anterior, ellipse svæði tengt breytingum á þungamiðju og aflþéttleikabreytingum í alpha og theta böndum EEG. Þessi ritgerð sýnir möguleika BioVRSea sem meginlegt tæki til að þróa margþætt merki sem getur mælt líkamsstöðustjórnun og greint á milli heilbrigðra frá meinafræðilegri svörun.



# Acknowledgements

The work within this thesis could not have been completed without the funding of RANNÍS, grant number 239612-051: “Postural control signature: Advanced assessment and diagnostics using the BioVRSea paradigm”.

My deepest gratitude and thanks go to Prof. Gargiulo for answering my email back in 2019 and having me come to the lab to begin my Icelandic/Italian odyssey. Your patience, guidance and good humour will never be forgotten. And to all my coworkers in the lab who helped along the way during this thesis, especially to Romain, Marco, Lorena and Federica, it was a joy to work with you all and I thank you from the bottom of my heart for all your help and the many happy hours we spent together.

I also wish to express my gratitude to my supportive parents and bewildered friends in Ireland and Iceland, thanks for getting on the platform yourselves, or listening to me talk about it.

And finally, where would I be without my twins Nicoló Secondo and Claudio Mario Rech? What a good pair of lads.



# Preface

This dissertation is original work by the author, Deborah Cecelia Rose Jacob. Portions of the thesis text are used with permission from Jacob et al.[1]–[3] of which I am an author.

# Contents

<b>Acknowledgements</b>	<b>ix</b>
<b>Preface</b>	<b>xi</b>
<b>Contents</b>	<b>xii</b>
<b>List of Figures</b>	<b>xv</b>
<b>List of Tables</b>	<b>xvii</b>
<b>I Introduction to Postural Control and BioVRSea</b>	<b>1</b>
<b>1 Introduction</b>	<b>3</b>
1.1 Background . . . . .	3
1.1.1 Postural Control . . . . .	3
1.1.2 Concussion . . . . .	4
1.1.2.1 Diagnosis and Management of Concussion . . . . .	5
1.1.3 Parkinson's Disease . . . . .	7
1.1.3.1 Diagnosis and Management of PD . . . . .	7
<b>2 Methods</b>	<b>11</b>
2.1 BioVRSea Paradigm . . . . .	11
2.2 Neurophysiological Measurements . . . . .	13
2.2.1 Electroencephalography . . . . .	13
2.2.2 Electromyography . . . . .	13
2.2.3 Heart Rate . . . . .	14
2.2.4 Centre of Pressure . . . . .	15
2.3 Analysis and Extraction of Features . . . . .	15
2.3.1 EEG . . . . .	15
2.3.2 EMG . . . . .	16
2.3.3 CoP . . . . .	17
2.3.4 Heart Rate/ECG . . . . .	18
2.3.5 Questionnaire . . . . .	18
2.4 Compilation of Mastersheet . . . . .	19
2.5 Neurophysiology of BioVRSea . . . . .	19
2.5.1 EEG . . . . .	20
2.5.2 ECG . . . . .	21
2.5.3 EMG . . . . .	23
2.5.4 CoP . . . . .	23

## II Published Papers and Future Work 25

### 3 Papers 27

3.1	Towards defining biomarkers to evaluate concussions using virtual reality and a moving platform (BioVRSea) . . . . .	27
3.1.1	Abstract . . . . .	27
3.1.2	Introduction . . . . .	27
3.1.3	Methods . . . . .	28
3.1.3.1	Participants . . . . .	28
3.1.3.2	Written information and informed consent . . . . .	28
3.1.3.3	Concussion definition . . . . .	28
3.1.3.4	SCAT5 Questionnaire . . . . .	29
3.1.3.5	Virtual reality experiment . . . . .	29
3.1.3.6	Data acquisition . . . . .	30
3.1.3.7	EEG . . . . .	31
3.1.3.8	EMG . . . . .	31
3.1.3.9	Heart rate . . . . .	32
3.1.3.10	CoP . . . . .	32
3.1.4	Results . . . . .	33
3.1.4.1	Sports Concussion Assessment Tool (SCAT) 5 . . . . .	33
3.1.4.2	Centre of Pressure Measurements . . . . .	34
3.1.4.3	Electroencephalography Measurements . . . . .	36
3.1.4.4	Electromyography Measurements . . . . .	37
3.1.4.5	Heart Rate Results . . . . .	38
3.1.4.6	Classification Analysis . . . . .	38
3.1.5	Discussion . . . . .	40
3.2	Assessing Early Stage Parkinson’s Disease Using BioVRSea . . . . .	45
3.2.1	Abstract . . . . .	45
3.2.2	Introduction . . . . .	45
3.2.3	Methods . . . . .	46
3.2.3.1	Participants . . . . .	46
3.2.3.2	Written Information and Informed Consent . . . . .	46
3.2.3.3	Virtual Reality Experiment . . . . .	46
3.2.3.4	HR Analysis . . . . .	47
3.2.3.5	EMG Analysis . . . . .	47
3.2.3.6	CoP Analysis . . . . .	48
3.2.3.7	Correlation Analysis . . . . .	48
3.2.3.8	Statistical and Machine Learning Analysis . . . . .	48
3.2.4	Results . . . . .	49
3.2.4.1	Heart Rate Results . . . . .	49
3.2.4.2	EMG and CoP Results . . . . .	49
3.2.4.3	Machine Learning Results . . . . .	49
3.2.5	Discussion . . . . .	49
3.2.6	Limitations and Future Developments . . . . .	53
3.3	Adaptation Strategies and Neurophysiological Response in Parkinson’s Disease: BioVRSea Approach . . . . .	54
3.3.1	Abstract . . . . .	54
3.3.2	Introduction . . . . .	54
3.3.3	Methods . . . . .	59

3.3.3.1	Participants . . . . .	59
3.3.3.2	BioVRSea Experiment . . . . .	59
3.3.3.3	Heart Rate . . . . .	60
3.3.3.4	EMG Analysis . . . . .	60
3.3.3.5	CoP Analysis . . . . .	61
3.3.3.6	EEG Analysis . . . . .	61
3.3.4	Results . . . . .	62
3.3.4.1	Heart Rate . . . . .	62
3.3.4.2	EMG . . . . .	62
3.3.4.3	CoP . . . . .	62
3.3.4.4	EEG . . . . .	62
3.3.5	Discussion . . . . .	65
3.3.5.1	Heart Rate . . . . .	67
3.3.5.2	Muscle activation . . . . .	67
3.3.5.3	Center of Pressure . . . . .	67
3.3.5.4	Neural response . . . . .	67
<b>4</b>	<b>Summary and Conclusion</b>	<b>71</b>
4.1	Summary . . . . .	71
4.2	Conclusion . . . . .	75
	<b>Bibliography</b>	<b>77</b>
<b>A</b>	<b>Detailed Description of Features Calculated During Experiment</b>	<b>95</b>
A.1	EEG Features . . . . .	95
A.2	EMG Features . . . . .	95
A.2.1	EMG Formulas: . . . . .	96
A.3	CoP Features . . . . .	101
A.3.1	CoP Formulas: . . . . .	103
A.4	MOTION SICKNESS QUESTIONNAIRE . . . . .	105
A.4.1	Lifestyle Indexes . . . . .	105

# List of Figures

2.1	BioVRSea Experimental Setup. . . . .	12
2.2	Graphic showing the stance of participants during each phase of the experiment. . . . .	13
2.3	Setup of 64 channel EEG measurements system, with cap, amplifier (pink) and acquisition computer. . . . .	14
2.4	Base station for charging wireless EMG sensors . . . . .	14
2.5	Placement of EMG electrodes on the lower leg . . . . .	15
2.6	Force plates embedded into platform . . . . .	16
2.7	Outline of steps to rectify, filter and envelope the EMG signal. Raw EMG signals were filtered with an 8th order Butterworth filter, with a band pass ranging from 15 to 400 Hz. The signals were then rectified and then filtered with a 4th order Butterworth low pass filter with a cut-off frequency equal to 20 Hz. Finally, the resulting signals were filtered by means of a Savitzky-Golay filter. . . . .	17
2.8	Outline of the sections included as part of the questionnaire for the BioVRSea experiment. . . . .	19
2.9	Structure of Database . . . . .	19
2.10	Age breakdown of BioVRSea participants . . . . .	20
2.11	Sex breakdown of participants . . . . .	20
2.12	Absolute PSD distribution of the whole population behaviour. The "x" highlighted in green represents significant electrodes after Bonferroni correction. . . . .	22
2.13	Figure showing differences in Area of Poincare plot ellipse PRE stage of experiment for groups with a BioVRSea Effect and without BioVRSea Effect. . . . .	22
2.14	Box plot showing the significant differences in CoP ellipse area in the PRE and POST phases for unhealthy and healthy lifestyle index subjects . . . . .	24
3.1	Graphical Abstract and Experimental Paradigm . . . . .	30
3.2	Foot Position on Force Platforms . . . . .	32
3.3	SCAT 5 Results . . . . .	34
3.4	CoP statistical comparisons between Concussion, non-concussion and concussion with balance problems groups. . . . .	35
3.5	Spectral Analysis POST-PRE for Concussion Group in Delta (Left) and Theta (Right) Bands . . . . .	36
3.6	PSD results for subgroups - a. Difficulty concentrating, b. Pressure in the head, c. Fatigue and Low energy . . . . .	36
3.7	Spectral Analysis Results for Soleus Muscle . . . . .	38
3.8	Machine Learning Results with different Algorithms . . . . .	39
3.9	Setup and Graphical Abstract. . . . .	47

3.10	Skewness of the EMG signal in the right soleus muscle showed opposite correlations for each group for all but two features calculated . . . . .	50
3.11	Complexity Index in the Medio-Lateral Direction in the POST phase of the experiment comparing healthy (No) and PD (Yes) groups . . . . .	51
3.12	Symptoms and Stages before-after Parkinson’s diagnosis . . . . .	55
3.13	Quantitative and Qualitative Aspects in Parkinson Disease Diagnosis [184]	56
3.14	ASP Bands Analysis in different studies [83], [190]–[193]. . . . .	58
3.15	Ellipse Areas comparison between Parkinson and Healthy subjects in PRE-POST phases . . . . .	65
3.16	Absolute PSD Bands Analysis in Parkinson’s vs Healthy cohort for theta and alpha frequency band . . . . .	66
3.17	Mediolateral Complexity Index of Healthy (Blue) and Parkinson (Orange) Groups . . . . .	68
4.1	Graphic of Workflow for deciphering Brain Network States and Network Measures in Brain Connectivity - reproduced from [216] . . . . .	74



# List of Tables

2.1	BioVRSea Experimental Paradigm . . . . .	12
3.1	Summary of Participant Information . . . . .	28
3.2	SCAT5 Scores for Participants with a History of Concussion and those without a History of Concussion . . . . .	34
3.3	Significant Electrodes in Concussion and Concussion subgroups . . . . .	37
3.4	Machine Learning Results with SCAT5, PCS and SCAT5 and PCA combined. . . . .	51
3.5	Most Significant Features for Machine Learning Prediction . . . . .	52
3.6	Machine Learning Results . . . . .	52
3.7	Gold standard tests for assessing gait ability . . . . .	56
3.8	BioVRSea Experimental Paradigm . . . . .	60
3.9	Average and standard deviation for Heart Rates inside cohorts and between cohorts in PRE and POST phases . . . . .	62
3.10	EMG Features - This table shows the features that were significantly different between PD and Healthy groups in the Right Tibialis anterior muscle in the POST phase. . . . .	63
3.11	CoP Features Calculated - this table shows the features that were significantly different in the POST phase of the experiment when comparing the PD and Healthy groups . . . . .	64
3.12	Electrodes for theta band with corresponding p-values comparing the two cohorts in POST and PRE phases - bold shows they were significantly different in the POST phase of the experiment . . . . .	66
3.13	Electrodes for alpha band with corresponding p-values comparing the two cohorts in POST and PRE phases - bold shows they were significantly different in the POST phase of the experiment . . . . .	66
A.1	50 EEG features calculated according to band, region and relative or absolute . . . . .	95
A.2	EMG features . . . . .	96
A.3	35 COP features . . . . .	102
A.4	Motion Sickness Questionnaire based on SCAT5 . . . . .	107
A.5	Motion Sickness Index . . . . .	107
A.6	Percentages of subjects related to Lifestyle Index and Motion Sickness Proneness Index . . . . .	108
A.7	Percentages of subjects related to Lifestyle Index and BioVRSea Effect Index . . . . .	108
A.8	Percentages of subjects related to Motion Sickness Proneness Index and BioVRSea Effect Index . . . . .	108



## Part I

# Introduction to Postural Control and BioVRSea



# Chapter 1

## Introduction

### 1.1 Background

#### 1.1.1 Postural Control

Postural control (PC) denotes a feedback mechanism of the central nervous system that governs human upright stance, serving as a foundation for locomotion, task-oriented behaviors, and autonomic responses. The central nervous system processes this information, generating efferent signals—both somatic (muscular) and autonomic (e.g., blood pressure)—to bring about appropriate responses. The PC system is susceptible to dysfunction, stemming from either pathological conditions (resulting in diminished function) or physiological hyperstimulation (manifesting as increased function). In either scenario, the central nervous system promptly triggers adaptation and habituation mechanisms to ensure survival within the context of compromised (diseased) or heightened (physiological) dynamic environments. The perturbation of PC entails a dichotomous manifestation: either a decline, leading to vertigo and dizziness disorders, or an elevation, culminating in musculoskeletal ailments. These states invariably impede the quality of life for afflicted individuals.

Numerous investigations have demonstrated the susceptibility of PC to various influences. Both generalized and localized muscular fatigue elicit disturbances in PC, prompting compensatory responses to counteract fatigue-induced disruptions [4]. Cognitive processes play a vital role in maintaining equilibrium and robust PC, with the extent of involvement contingent upon task demands [5]. Any impairment affecting the systems (muscular, neural, or neurophysiological) essential for PC maintenance—be it due to pathological conditions, fatigue, or other afflictions—consequently disrupts PC, precipitating balance issues. Hence, advanced age precipitates a higher incidence of PC disturbances owing to age-related modifications in neural, sensory, and musculoskeletal domains [6]. Notably, age-related PC investigations highlight the escalating postural instability in the elderly [7], correlating with an increased propensity for falls.

Improvement of PC is attainable through targeted physical training strategies, as evidenced by the positive impact of specialized training on both dynamic and static balance tasks [8]. Numerous diseases and pathologies exert influence on neural and muscular systems, thereby perturbing PC. Parkinson's Disease (PD), a progressive neurodegenerative ailment, exemplifies this phenomenon. PD's cardinal symptoms encompass resting tremors, bradykinesia, rigidity, and/or postural instability. Clinical diagnosis requires the presence of at least two of these features, with histopathological confirmation remaining the definitive diagnostic criterion [9]. PC inadequacy emerges

as a notable consequence of the disease, compelling the need for quantitative measures to augment clinical assessments.

Similar observations are seen in individuals with a history of concussion. A concussion, or mild traumatic brain injury, arises from transient neurological impairment consequent to head trauma or transmitted force [10]. Acute concussion symptoms may encompass headaches, emotional volatility, loss of consciousness, amnesia, balance issues, and sleep disturbances [11]. While most concussion instances resolve spontaneously, some entail prolonged psychological, physical, and cognitive ramifications, elongating recovery periods. The absence of objective diagnostic tools necessitates a reliance on clinical assessments, which can be complex due to nonspecific symptoms. Research-wise, concussion evaluations commonly hinge on questionnaires adhering to the latest consensus on concussion definition [11].

PD and concussion both have an impact on the neuromuscular framework, consequently disrupting PC and heightening fall-related risks. Anxiety, a frequent comorbidity in balance disorders and motion sickness, has been linked to inferior balance scores [12]–[14]. Animal models suggest a potential vestibular link to anxiety, with balance training emerging as a prospective intervention [15]. Clinical diagnoses of these conditions remain qualitative, lacking quantitative assessments during PC tasks.

Given that PC encompasses a confluence of multifaceted mechanisms, a range of tools is at one’s disposal for the investigation, analysis, and assessment of neurophysiological parameters during experiments designed to induce PC disturbances. Primarily, it is imperative to recognize that PC is an intricate central nervous system system intertwined with cognitive processing. Our laboratory’s antecedent studies underscore the significance and role of cortical engagement in conjunction with PC tasks [16], [17]. Electroencephalography enables the capture of cerebral signals throughout PC tasks, offering an avenue to dissect these signals temporally, spectrally, and in terms of network dynamics. Such analyses serve to pinpoint neurological markers indicative of PC engagement.

Furthermore, PC is intrinsically linked with muscle activation, particularly within the lower extremities, to sustain the upright stance. Electromyographic sensors are harnessed to gauge muscular activity and derive parameters correlated with PC. Often, this coincides with the assessment of the center of pressure via force plates. Tracking center of pressure trajectories and concurrent electromyographic profiles over time is routine within gait and balance analysis. The electromyographic signals yield a plethora of metrics, encompassing spectral density, kurtosis, and skewness. Meanwhile, scrutinizing the stabilogram output of center of pressure exposes a gamut of geometric, temporal, and frequency-related parameters. The synthesis of these measurement modalities furnishes an intricate framework for quantifying the neurophysiological dimensions underpinning PC tasks.

By assembling a diverse cohort spanning various age brackets, encompassing both healthy individuals and those grappling with conditions such as PD, concussion, or anxiety, an enriched comprehension of these states can be attained. The comparative analysis of responses between healthy subjects and those afflicted by pathologies is poised to yield distinct neurophysiological patterns, which could potentially underpin the diagnosis and assessment of PC behaviors and anomalies.

### 1.1.2 Concussion

Adapted from [1]

A concussion, sometimes referred to as a mild traumatic brain injury (mTBI), is a short-lived functional neurological impairment caused by a blow to the head or by a force transmitted to the head [11]. Participation in sports is a risk factor for sustaining multiple concussions [18], with some sports presenting a greater risk than others[19], [20]. The possible acute symptoms of concussion can include headaches, emotionality, loss of consciousness, amnesia, problems with balance, and sleep/wake disturbance[21], [22]. Although most cases of concussions resolve spontaneously, they can have persistent psychological, physical, and cognitive complications and protracted recovery times[11], [19], [21]–[27].

### 1.1.2.1 Diagnosis and Management of Concussion

A definitive method for diagnosing a concussion remains elusive[11], and a universally precise definition of concussion is still lacking[28]. In the realm of concussion diagnosis, reliance on clinical assessment by medical professionals persists, albeit with inherent challenges due to the non-specific nature of symptoms[10] that could potentially be attributed to other mental or physical conditions. Within research contexts, concussion evaluations typically revolve around questionnaires constructed in line with the latest consensus on the concussion definition[10]. The Concussion Assessment Tool, fifth edition (SCAT5), has proven beneficial in assessing symptoms post-incident and monitoring recovery progress[10]. However, it is noteworthy that its exclusive use for diagnosis, much like other similar concussion assessment is cautioned against[29]–[32]. While medical records and clinical interviews are often considered the gold standard in concussion research [33], their reliance can lead to compromised accuracy as a significant number of concussion sufferers do not seek medical intervention[33]. The enigma of concussion pathology persists, and the exact manner in which alterations in neuronal function influence the emergence of concussion symptoms remains unclear[24]. Despite being diagnosable without evident structural damage, instances of structural damage post-concussion have been documented[10], potentially contributing to prolonged symptomatology[34]. While not a standard clinical practice, neuroimaging could potentially shed light on concussion symptoms and their relationship to functional brain changes (for a comprehensive review of functional MRI techniques in concussion studies, refer to[35]). Electrophysiological evaluations of concussions also hold promise. Electroencephalography (EEG), a non-invasive means of measuring electrical brain activity, provides insights into brain function associated with concussion pathology[24] and has been employed to discern functional changes post-concussion[35]–[40]. In comparison to many other brain imaging techniques, EEG is more feasible and cost-effective[39]. Although specialized training is still required, its accessibility for researchers and clinicians is notably higher compared to other modalities such as MRI and CT. A study examining steady-state visual-evoked potentials (SSVEP) in concussed athletes unveiled disparities in SSVEP responses compared to healthy counterparts[41], despite utilizing solely visual stimuli. Additionally, reduced brain network activation, gauged through EEG, has been linked to post-traumatic migraines in concussion patients, potentially reflecting symptom severity or persistence, given the correlation of post traumatic migraine with heightened severity and prolonged recovery[42]. Alterations in theta and alpha activity have also been correlated with concussion history[43]–[47]. However, due to methodological variances across studies, establishing EEG markers as return-to-play guidelines remains challenging[38], [48], [49]. Further exploration into the relationship between EEG and

subjective concussion symptoms is warranted. For EEG to substantiate return-to-play protocols, it is pivotal to encompass assessments beyond visual stimuli. Incorporating more demanding actions, such as physical movement, alongside EEG evaluation would better replicate real-world scenarios likely to induce concussion symptoms. Supported by evidence demonstrating a connection between concussion and modified PC[50], [51] EEG signals during postural tasks have indicated that concussion sequelae could persist for months following the injury[43], and in a singular instance, EEG alterations were detected even three decades post-concussion[52]. Additionally, EEG measures have shown reasonable predictive accuracy for concussions through machine learning techniques[53], suggesting the potential of EEG parameters as concussion biomarkers.

Among the most prevalent post-concussive symptoms are dizziness and balance issues[54]. Consequently, the objective assessment of PC becomes a logical avenue of exploration for those who have encountered a concussion, as PC[45], [46] hinges on inputs from visual and vestibular systems, along with the somatosensory system<sup>23</sup>, commonly affected by concussions. Notably, the center of pressure (CoP) has been investigated in the context of maintaining an upright stance, serving as a vital metric for postural stability[47] and potentially as an indicator of concussion[46]. Although evaluating PC and its correlation with concussion typically involves participants standing on a pressure plate, there is room for more advanced measures and analyses[55]. In a study by Degani et al.[56], individuals with a history of mTBI exhibited more significant, slower, and less predictable body oscillations compared to controls when assessing body CoP displacement through participants standing on a force plate while performing simple tasks. CoP displacement has also demonstrated correlation with EEG measurements in mTBI cases, even up to a year after injury[57]. PC assessments utilizing the sensory organization test (SOT) subsequent to mTBI[58] revealed discernible differences in PC dynamics for individuals with concussion history in comparison to control groups, extending from months to years post-injury. The link between concussion impacts and balance issues has been substantiated across numerous studies, with targeted quantitative methods focusing on sensorimotor and neural components proposed as the next phase in advancing understanding[59]. Given the connection between concussions and PC, electromyographic (EMG) recordings, though not commonly utilized in post-concussion symptom assessment[60], could potentially furnish biomarkers for concussions. EMG recordings can capture muscular activity essential for maintaining postural stability [61]. Anomalies have been identified in EMG signals, such as a pause post-motor evoked potential positively correlated with injury severity among athletes with concussions[62]. The tibialis anterior (TA) muscle, pivotal for stability control<sup>51</sup>, has been a focus of EMG recordings in PC studies[34], [63].

Blood flow and heart rate (HR) present other objective measures and have been found helpful in clinical settings when assessing individual differences in outcome after a concussion[64], [65]. Changes in HR variability in concussed athletes have been shown weeks or months after an incident[52], showing the potential of the autonomic nervous system (ANS) to function as a marker of concussion[65], [66]. However, results from HR studies are mixed, and it is recommended to use measures of HR variability only as a part of a multi-faceted approach<sup>46</sup>, considering sex and age[67]. A better understanding of how HR measures relate to concussions is needed as they could offer a cost-effective and non-invasive way to track concussion recovery[65].

Due to the complex etiology of concussive symptoms, a multi-faceted approach to concussion assessment and treatment is essential[29], including multiple concussion measures and techniques. As a part of a multi-faceted approach, virtual reality (VR)



offers a novel way to evaluate and manipulate PC and cortical activity[57]. VR gives an option to assess responses in a secure setting while exposing participants to a visually and physically demanding task. In recent years, VR has been recognized as a valuable tool, both as a stimulus and as a measurement tool offering new ways to study psychological and behavioral factors related to health[68], even showing promise in detecting and treating Alzheimer’s dementia[69]. In one study, EMG measures were acquired in a VR environment among high-risk concussion participants[70]. The experiment was a preliminary study to verify data in a VR environment. Results showed promise, although more research is needed. A 2020 study by Rao et al. [71] used VR, a moving platform, lower limb accelerometry, and EMG to detect subtle differences in balance between an mTBI group and a normal control group. Using these biometric measurements, walking and standing perturbation tests discriminated between the two groups. Results indicated that clinical assessment of concussion could be missing an important component, in this case, gait. By including movement, the assessment could be improved and with the addition of VR, the possibilities in manipulating and changing research settings in real-time greatly refined. The study also shows that a highly instrumented, multi-modal VR environment used in the performance of a demanding task can add important information that is not available in the clinical environment when assessing a concussion.

### 1.1.3 Parkinson’s Disease

Parkinson’s Disease (PD) is a progressive disorder of the nervous system characterized by muscle tremors, muscle rigidity, decreased mobility (bradykinesia), stooped posture, slow voluntary movements, and a mask-like facial expression. It may take time to diagnose because some of its symptoms are associated with the natural process of aging [72]. Globally, disability and death in PD are increasing faster than any other neurological disorder. The World Health Organization (WHO) reports that the prevalence of PD has doubled in the past 25 years and world estimates count over 8.5 million individuals with PD in 2019.

PC issues are often seen as the disease progresses, contributing to serious problems maintaining balance and upright stance, which greatly increases the risk of serious injury through falls. The mechanism of this loss of adequate posture is due to the complex interplay of Parkinson’s symptoms including reduced automatic postural adjustments, impaired sensory feedback integration, and altered muscle tone regulation.[73]

Objective diagnosis and management PD remains a challenge in the field of neurology, due to its complex clinical presentation and progressive course that significantly impacts the quality of life of affected individuals. However, in recent years efforts to improve diagnosis, evaluation, and longitudinal monitoring of PD are bearing fruit, aided by the convergence of multidisciplinary efforts, technological advancements, and a deeper understanding of the neurophysiological underpinnings of the disease. This progress is critical, given the increasing prevalence of PD in an aging global population and the urgent need for more accurate, accessible, and personalized approaches to its management.

#### 1.1.3.1 Diagnosis and Management of PD

The diagnosis of PD has historically relied on clinical assessment, primarily assessing cardinal motor symptoms such as bradykinesia, resting tremor, rigidity, and postural

instability. While these clinical criteria remain fundamental, there has been a growing recognition of the need for more precise and early diagnostic tools. Recent developments in neuroimaging, including magnetic resonance imaging (MRI) techniques such as diffusion tensor imaging (dMRI), diffusion kurtosis imaging, functional MRI, and susceptibility weighted imaging (SWI) have enabled a more detailed assessment of the underlying neuroanatomy. The use of DTI and DKI in particular has shown promise in identifying changes in the brain's microstructure, which may aid in diagnosing early-stage PD. [74]. Positron emission tomography (PET), and single-photon emission computed tomography (SPECT) are also used for imaging dopaminergic dysfunction. Furthermore, the identification of potential biomarkers in cerebrospinal fluid and blood samples has offered promising avenues for more objective and less invasive diagnostic procedures. For a recent overview of imaging techniques in PD, see [74]

Categorization of PD stages is predicated upon clinical observations, with clinical rating scales serving as the primary framework for quantifying symptoms and severity of the disease. The Hoehn and Yahr (HY), Unified PD Rating Scale (UPDRS) and its updated version by the Movement disorder society (MDS-UPDRS) are widely used clinical scales to assess, monitor and quantify the disease [75]. Clinical personnel assign a numerical score depending on the patient's performance of various postures, meaning the score depends heavily on the assessor skills and knowledge. Studies have shown that there is inter- and intra-observer variability present when using the MDS-UPDRS [76], [77]. In addition, the MDS-UPDRS relies on patient self-assessment in the first part of the exam, and subsequent assessment by the clinician. The process is lengthy, upwards of 30 minutes, with specialist official training required to keep variations in acquisition and interpretation to a minimum. [78] Motor symptoms play a crucial role in the diagnosis of PD, as they are considered the hallmark features of the condition and they feature heavily in the scales mentioned above. However, it is important to note that PD can also present with non-motor symptoms or sub-clinically noticeable motor symptoms. While motor symptoms are typically the first observable and most prominent features, there are cases where non-motor symptoms or cognitive changes may precede or accompany the motor symptoms. Therefore, the development of sensitive, early, and objective tests to both aid in diagnosis, treatment and ongoing assessment of the disease are crucial.

The pre-clinical phase denotes an absence of observable signs or symptoms, with genetic testing and counseling providing avenues for the identification of risk factors. The prodromal phase corresponds to a stage characterized by the nascent emergence of neurodegenerative alterations. Although symptoms in this phase are of a non-specific nature, the early detection of underlying changes facilitates timely intervention through nascent therapeutic modalities. Symptoms apparent in the early stages encompass mild tremors and mild ambulatory challenges, occasionally unilateral in nature, often accompanied by diminished facial expressivity. These manifestations generally exert limited impact on daily functioning and may not invariably manifest conspicuously [75]. In the intermediate stages, a decline in equilibrium and coordination becomes apparent, precipitating a state of moderate-to-severe impairment with discernible ramifications on daily life [75]. In the intermediate stages, a decline in equilibrium and coordination becomes apparent, precipitating a state of moderate-to-severe impairment with discernible ramifications on daily life [75]. Subsequently, the advanced stages entail pronounced challenges in standing and ambulation, even with external aids. Individuals within this stage are grappling with substantial debilitation [75].

The integration of neurophysiological tools could revolutionize PD management by providing objective, quantifiable biomarkers that are sensitive to early pathophysiological changes unseen in clinical assessments. By capturing the disease's progression at a neural level, these methods could substantially assist in the timely initiation of neuroprotective therapies and personalized medicine approaches, enhancing patient prognosis and quality of life. **Electroencephalography** (EEG) can detect damage in the central nervous system and alterations in neurophysiological activity associated with PD. In recent studies, quantitative analysis of EEG data identified significant differences in PD patients versus healthy subjects. In particular, the anterior cingulate and temporal lobe are areas with an established pathology in PD. Changes in cortico-cortical and cortico-thalamic coupling were observed as excessive EEG beta coherence in PD patients [79].

Map structure and functions of the brain are obtained measuring the signals produced by neural activity. Each region can have a particular influence according to the disease and the activation of an area can be considered important in the understanding of the progression of the disease. Although cortical EEG coherence can serve as a reliable measure of disease severity, the use of EEG to study PD has not been fully investigated. Neurophysiological signals provide instantaneous information and can aid in improving the accuracy of the diagnosis.

EEG signals have different specific frequency bands. Features in sub-bands are particularly important to characterize different brain states. The standard frequency bands of interest are  $\delta$ -band (0–4 Hz),  $\theta$ -band (4–8 Hz),  $\alpha$ -band (8–13 Hz), and  $\beta$ -band (13–30 Hz). Moreover, the quantification of EEG rhythms could provide an important biomarker for different neuropsychiatric and neurological disorders, such as schizophrenia, Alzheimer's disease, epilepsy, and Parkinson disease [80]–[82]. The combination of new analysis methods and EEG signal processing can contribute to the detection of early-stage PD. EEG reveals more important information underlying brain dysfunctions, which would be lost if analysis were restricted to traditional methods. Nowadays, many novel methods are suggested for EEG signal processing.

A recent study analyzed the EEG signals from 15 early-stage PD patients and 15 age-matched healthy controls during eyes-closed resting state [83]. Most EEG electrodes showed an increase in  $\theta$ -band relative power for PD patients, while several other electrodes decreased, such as in the frontal and occipital cortex (Fp1, Fp2, F7, F3, Fz, Oz). Moreover, an increase in  $\delta$ -band relative powers were reported, and a decrease in  $\alpha$ -band and  $\beta$ -band relative powers for PD patients compared with healthy patients. Other studies present higher spectral power in the low frequency domain of EEG, compared with controls. Also in these cases, subjects were in the resting awake condition with the eyes closed [84], [85].

Habituation and adaptation are part of a complex system to maintain or restore balance from any position or during motor activity. The central nervous system is fundamental in PC strategies and electroencephalography can underline the different cortical brain activities under different postural perturbations [16], [86]. PD usually interferes in this regulatory system, as can be clearly demonstrated by most motor symptoms, but to date, no study has yet been conducted on the analysis of postural kinematics in movement disorders. In a recent study from our lab, postural kinematics from HD-EEG have been measured during a postural perturbation applied to calf muscles.[16]The main changes in cortical activity were found in Absolute Spectral Power (ASP) over four frequency bands. For postural adaptation, increases in the  $\theta$  band in the frontal-central region for closed-eyes trials, and in the  $\theta$  and  $\beta$  bands in

the parietal region for open-eyes trials were reported. In habituation of the stance, no significant variations in ASP were observed during closed-eyes trials, whereas an increase in the  $\theta$ ,  $\alpha$ , and  $\beta$  bands were observed with open eyes [87]. Furthermore, open-eyed trials generally yielded a greater number of significant differences across all bands during both adaptation and habituation, suggesting that cortical activity during postural perturbation may be regulated with visual feedback. This clearly shows a correspondence in cortical activity and postural kinematics during postural perturbation, and could also be developed for pathological PC.

The utilization of sEMG in PD is instrumental in assessing muscle activity patterns that reflect the rigidity and bradykinesia characteristics of the disorder [88]. Through the evaluation of electrical activity produced by skeletal muscles, sEMG has proven efficacious in identifying abnormalities in motor unit recruitment and firing patterns, often disrupted in PD patients [89]. The modality's non-invasive nature coupled with its high temporal resolution makes it suitable for assessing the phasic muscle activities that are critical for maintaining postural stability, particularly during dynamic tasks. Investigations employing sEMG have revealed a reduced and delayed muscle response in PD patients, signifying impaired reflexive control [90].

While predominantly employed for cardiac assessments, ECG has relevance in PD research linked to autonomic dysfunction commonly seen in PD. The neurodegenerative processes in PD affect the autonomic nervous system, leading to various non-motor symptoms [91]. Anomalies in ECG, such as those related to heart rate variability, have been extrapolated to implicate the involvement of sympathetic and parasympathetic nervous systems in PD's pathogenesis [92]. Although not a direct measure of PC, ECG's insights into autonomic dysregulation can indirectly associate with the patients' ability to maintain postural stability, given the interplay between autonomic function and balance [93].

CoP measurements are integral to assessing postural sway, which encompasses the oscillations of the human body in various postures, especially in standing. In individuals with PD, there is typically an increase in sway path length and area, indicative of a diminished ability to maintain a stable upright position [94]. The analysis of CoP oscillations in both time and frequency domains allows for the identification of specific postural deficits in PD, such as reduced stability limits and increased reliance on hip strategies over ankle strategies for postural corrections, which is contrary to healthy adults who primarily use ankle strategies [95]. Anticipatory Postural Adjustments (APAs) are proactive mechanisms that facilitate balance maintenance in anticipation of self-initiated movements. In PD, the ability to generate adequate APAs is often impaired, leading to increased postural instability [96]. CoP-based analyses, particularly during task transitions (like sitting-to-standing or gait initiation), have revealed both temporal and spatial abnormalities in the anticipatory shift of CoP in PD patients. These findings suggest a compromised ability to prepare the postural system for movement, necessitating compensatory strategies that unfortunately still fall short of maintaining stability [97].

# Chapter 2

## Methods

### 2.1 BioVRSea Paradigm

BioVRSea is a PC paradigm based on virtual reality (VR) and a synchronised moving platform (Virtualis, Clapiers, France) which challenges the visual and motor systems of the participants. In the VR goggles is a simulation of a small boat at sea, while the platform moves in concert with the waves in the visual VR scene. The operator can set the frequency of the waves between 0.5 Hz and 3 Hz and the amplitude of the waves between 0 and 2 (these units are particular to the platform with 2 corresponding to around 45cm vertical displacement). During the simulation, the amplitude of the platform movements vary from 0% up to 75% of the platform's maximal displacement capacity. Two different protocols are used at random. The 'soft' protocol was defined as a wave frequency of 1 Hz with an amplitude of 0.6 while the 'hard' frequency was defined as a wave frequency of 3 Hz with an amplitude of 0.5. Participants wear a number of measurement devices to assess the quantitative neurophysiology associated with the experiment. This involves the placement of six wireless EMG sensors on the tibialis anterior (TA), gastrocnemius lateral (GL), and soleus (S) muscles of each leg and a heart rate sensor strapped around the chest. The participant is instructed to step onto the force plates on the platform after removing his/her shoes. The position of the feet is in bipedal stance with feet hip width apart, while standing on the force sensors. Finally, the participant dons the VR goggles. The participant stands quietly on the platform with their hands by their side observing a mountain view for the first 2 minutes of the experiment. Then, the scene in the VR goggles changes, beginning the sea simulation. The participants are instructed to remain standing quietly with their hands by their side for the first 35 seconds of the sea simulation. There is no platform movement in this part of the experiment, and it is called the PRE phase of the experiment. After 35 seconds of quiet standing watching the sea simulation, the participant holds onto the bars in front of them. The platform then begins synchronized movement with the sea scene in the VR goggles, with 25%, 50% and 75% of maximal wave amplitude. In this central part, each segment lasts 40 seconds and the participant holds the bars of the platform while continuing to observe the sea simulation. These three segments are together called the MOVE portion of the experiment. Finally, the platform stops and the participant is asked to remove their hands from the bars and stand quietly with their hands by their side for the final 40 seconds of the experiment. The sea scene is still observed by the participant for the final 40 seconds. This is called the POST phase of the experiment; it is performed identically to the PRE phase but

after the participant has experienced movement in the central part of the procedure. A table of the VR experiment protocol is shown below in Table 2.1, Fig. 2.1 shows a schematic of the experimental setup. A short video showing the experiment is available [here](#).

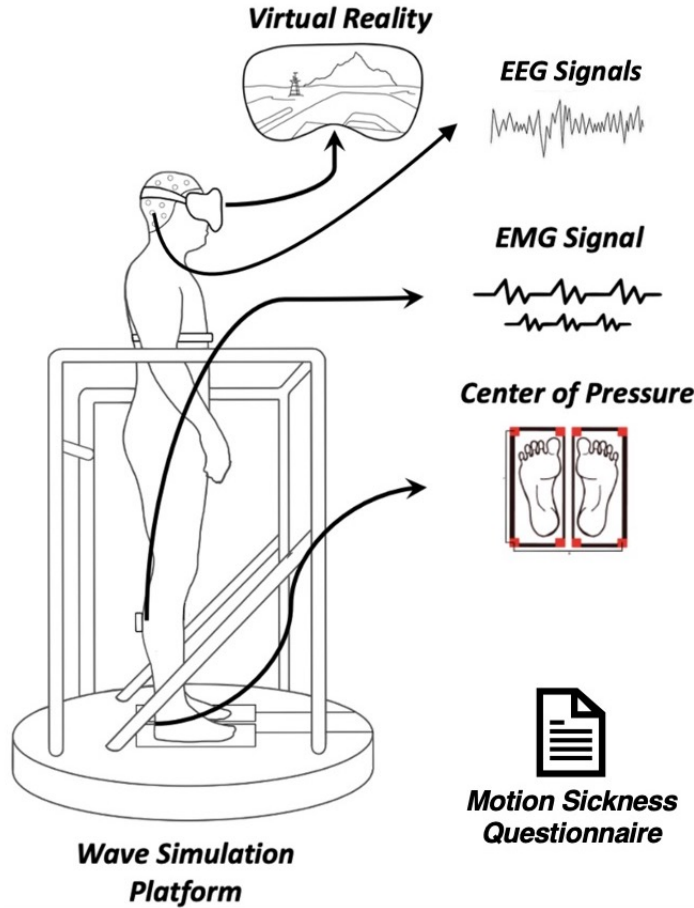


Figure 2.1: BioVRSea Experimental Setup.

Table 2.1: BioVRSea Experimental Paradigm

Time (s)	Segment	VR Scene	Position of Hands	Platform
0-120	Baseline	Mountains	by side	Stationary
120-160	PRE	Sea	by side	Stationary
160-280	MOVE	Sea	on bars	Moving
280-320	POST	Sea	by side	Stationary

The overarching experimental paradigm (PRE-MOVE-POST) is designed to compare two challenging states for PC as noted below and seen in Fig 2.2:

- Visual stimulation of PC system while performing upright stance - no movement of platform but VR scene is active (PRE)

- Movement of Platform in concert with VR Scene (MOVE)
- Visual stimulation of PC after movement (induced latent movement still present while performing upright stance (POST))

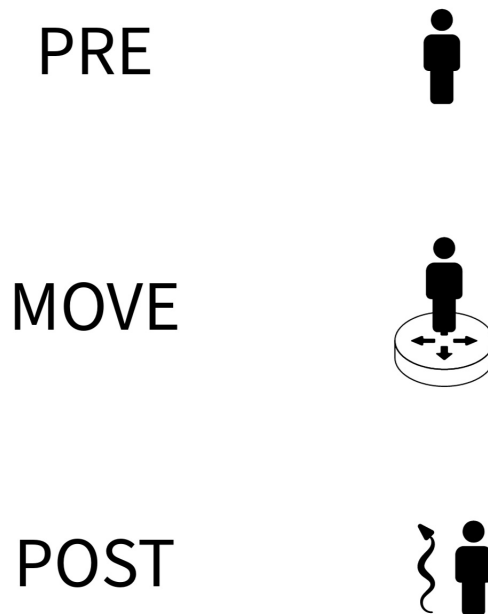


Figure 2.2: Graphic showing the stance of participants during each phase of the experiment.

## 2.2 Neurophysiological Measurements

### 2.2.1 Electroencephalography

Electroencephalographic (EEG) measurements were made using a 64-channel wet electrode setup from ANTNeuro (Hengelo, the Netherlands) sampling at 4096 Hz. The system is shown in Fig. 2.3, with connection to amplifier and acquisition computer (tablet). Prior to acquisition, each of the electrode contacts is filled with electroconductive gel via syringe until an impedance lower than  $20\Omega$  is reached.

### 2.2.2 Electromyography

Muscle electrical activities from the lower limbs was acquired using six wireless EMG sensors (sampling frequency of 1600 Hz) placed on the tibialis anterior (TA), gastrocnemius lateral (GL), and soleus (S) muscles of each leg (Kiso ehf, Reykjavik, Iceland). Each sensor wirelessly transmits (via Radiofrequency) to the base station (Fig. 2.4, which is itself connected via USB to the main acquisition computer. The base station also serves as a charging port for the sensors. Each sensor is fitted with single-use electrodes prior to a small amount of electroconductive gel on each electrode. The sensors are placed on the Tibialis anterior, gastrocnemius lateral and soleus muscles of each leg as in Fig. 2.5.



Figure 2.3: Setup of 64 channel EEG measurements system, with cap, amplifier (pink) and acquisition computer.



Figure 2.4: Base station for charging wireless EMG sensors

### 2.2.3 Heart Rate

Heart rate was measured using a chest heart sensor (Polar Electro, Kempele, Finland, sampling frequency 1000 Hz). This sensor was used in the papers included in this thesis and for the first 315 participants in the BioVRSea experiment. Subsequently we switched to an ECG sensor called BiosignalsPlux.

The BiosignalsPlux Explorer Kit consists of several components that enable the acquisition and analysis of ECG data. These components include a wireless 4-channel BioSignalsPlux HUB, sensors, a PLUX proven Bluetooth dongle, electrodes, and a medical-grade charger. The wireless 4-channel BioSignalsPlux HUB serves as the cen-





Figure 2.5: Placement of EMG electrodes on the lower leg

tral device for data collection. It wirelessly connects to the sensors and facilitates the transmission of ECG signals to the data acquisition system. The HUB is specifically designed for reliable and accurate ECG measurements. In the experimental setup, three ECG sensors are connected to the BioSignalsPlux HUB. To ensure precise ECG measurements, electrodes are used to establish electrical contact between the subject's body and the sensors. The electrodes are positioned on the subject from the Right Arm (RA) to the Left Foot (LF) following a specific placement protocol. This electrode placement scheme is designed to capture the electrical activity of the heart accurately.

#### 2.2.4 Centre of Pressure

Force Plate measurements were made using 4 sensors located under each foot platform. The sensors give information about the center of mass in the Antero-posterior and Medio-Lateral axis (Virtualis, Clapiers, France, sampling frequency 90 Hz).

## 2.3 Analysis and Extraction of Features

### 2.3.1 EEG

The EEG was recorded using a 64-electrode channel system. Data pre-processing and analysis were performed with Brainstorm ([98]) and Matlab2021b (MathWorks, Inc., Natick, 158 Massachusetts, USA), using the Automagic toolbox ([99]).

For each of the six tasks time segments, we removed the 5 first and 5 last seconds, to ensure the data quality and to avoid artefacts. The data were resampled to 1024 Hz. Automagic was used to automatically pre-process every dataset, with a manual inspection at the end. The data were notch filtered at 50 Hz. A high pass and low pass



Figure 2.6: Force plates embedded into platform

filter were set respectively to 1 Hz and 45 Hz. ICA MARA algorithm was used, with a variance of 20%. Finally, bad electrodes were interpolated. Each segment needing interpolation of more than 15% of the total amount of electrodes was rejected, and the associated individual was excluded from the experiment. Taking into account all the individuals comporting a complete EEG recording (208 individuals), rejected channels were  $2.4 \pm 10.1$  channels. After excluding subjects from the study, keeping only the 190 individuals with good signal quality, rejected channels were  $0.5 \pm 1.3$  channels.

From this complete EEG recording, the absolute and relative PSD were computed for each subject, using Welch's method ([100]), (1s Hamming window length, 50% overlap), for the following frequency bands: delta (1–4 Hz), theta (4–8 Hz), alpha (8–13 Hz), beta (13–30 Hz), low-gamma (30–45 Hz), known as the five main brain rhythms ([101], [102]). Welch's method is a PSD estimation method and is used to calculate the average periodogram of a time segment. Equation (2.1) defines the power spectral density, and (2.2) Welch's power spectrum, which is the mean average of the periodogram of each interval where it is computed.

$$S_l(\omega) = \frac{1}{M} \left| \sum_{n=0}^{M-1} w(n)x_i(n)e^{-j\omega n} \right|^2 \quad (2.1)$$

$$S(\omega) = \frac{1}{L} \sum_{l=0}^{L-1} S_l(\omega) \quad (2.2)$$

Then, the average power of the signal over each time segment is computed by integrating the PSD estimate, using the rectangle method. For each band, indices of relative power (RP) were obtained by expressing the absolute power (AP) in each frequency band as a percentage of the global absolute power obtained by summing the five frequency bands.

### 2.3.2 EMG

EMG data processing was performed using Matlab 2021b. EMG signals were filtered with an 8th order Butterworth filter, with a band pass ranging from 15 to 400 Hz.

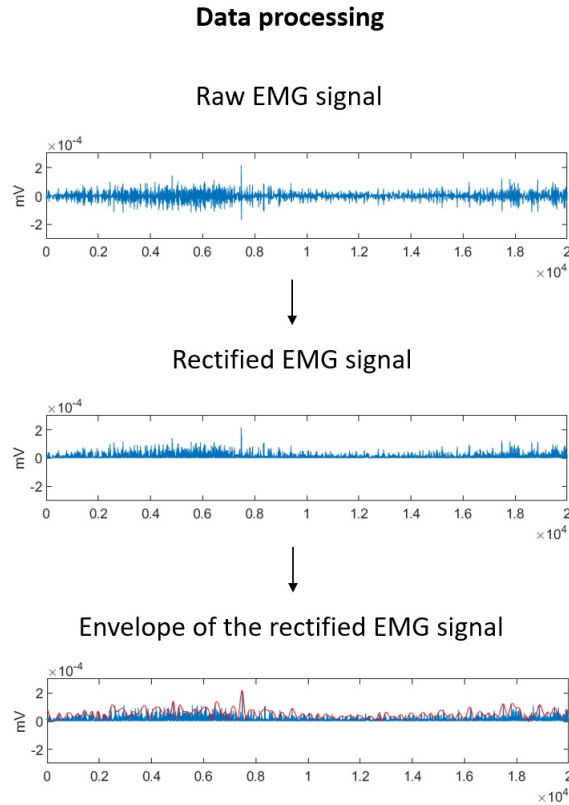


Figure 2.7: Outline of steps to rectify, filter and envelope the EMG signal. Raw EMG signals were filtered with an 8th order Butterworth filter, with a band pass ranging from 15 to 400 Hz. The signals were then rectified and then filtered with a 4th order Butterworth low pass filter with a cut-off frequency equal to 20 Hz. Finally, the resulting signals were filtered by means of a Savitzky-Golay filter.

The signals were then rectified and then filtered with a 4th order Butterworth low pass filter with a cut-off frequency equal to 20 Hz. Finally, the resulting signals were filtered by means of a Savitzky-Golay filter. Seven features were computed in the frequency domain and thirty-six features in the time domain for each muscle and each phase of the experiment. These features are listed in the appendix. Fig. 2.7 gives an overview of this process.

### 2.3.3 CoP

CoP measurements were made using 4 sensors located under each foot platform. The sensors give information about the center of mass in the Antero-Posterior and Medio-Lateral axis (Virtualis, Clapiers, France, sampling frequency 90Hz). The processing of the CoP data was performed using Matlab 2021b. During the experiment, the force platform records the movement of the Centre of Pressure (CoP), a projection of the center of mass of the subject on the plane of the machine, also called stabilogram. The CoP data was filtered with a Savitsky-Golay filter with window size 7. Included in the CoP analysis were a number of multi-scale entropy measurements, which have been shown to have great importance in the analysis of CoP data in discriminating between pathological subjects [103]. Multi-scale entropy measurements include features such as complexity index (CI), which indicate the complexity of the CoP signal as calculated

using multi-scale entropy methods. We extract several parameters from the stabilogram for evaluating the PC response of the subject during the experiment. The list of features extracted from the CoP is outlined in the appendix.

### 2.3.4 Heart Rate/ECG

The ECG data obtained from the BioSignalsPlux sensors are processed using the OpenSignals (r)evolution software, which is specifically designed for ECG sensor data analysis. This software provides real-time visualization and recording capabilities, facilitating the extraction and computation of various HRV parameters. All the implemented algorithms in the software adhere to established standards [104]. A total of 30 HRV features are obtained for each of the four phases of the experiment: baseline (BASE), pre-phase (PRE), move-phase (MOVE), and post-phase (POST). This results in a total of 120 features per subject, capturing the dynamics of heart rate variability across different stages of the BioVRSea protocol. The extracted features can be categorized into different types. Time domain analyses of heart rate variability are simple robust methods that use statistical or geometric techniques to quantify changes in heart rate. There are many different types of time domain analyses and these provide a global view of autonomic control of the heart [105]. There are many different types of time domain analyses and these provide a global view of autonomic control of the heart [104]. Frequency domain analysis of heart rate variability uses spectral analysis techniques to attempt to separate the effects of different components of the neuroendocrine system on fluctuations of heart rate. The renin–angiotensin–aldosterone system affects heart rate over a long period of time (seconds to minutes), the sympathetic nervous system over a short period of time (seconds) and the parasympathetic nervous system on a beat-to-beat basis (seconds) [104]. Frequency measurements estimate the distribution of power across three frequency bands: Very Low Frequency (VLF, between 0 and 0.04 Hz), Low Frequency (LF, between 0.04 Hz and 0.15 Hz), and High Frequency (HF, between 0.15 and 0.4 Hz) [105]. For each frequency band, features such as PEAK, POWER (in  $\text{ms}^2$ ), POWER (normalized units), POWER (percentage), and LF/HF ratio are extracted. These features provide information about the power distribution and balance between different frequency components of heart rate variability. Additionally, nonlinear parameters are computed to quantify the unpredictability and complexity of the ECG time series. These nonlinear parameters offer insights into the irregularity and intricate patterns present in the heart rate dynamics. By analyzing these 30 features across the different phases of the experiment, we can investigate the changes and patterns in heart rate variability induced by the BioVRSea protocol.

### 2.3.5 Questionnaire

Each participant is administered a questionnaire via Google Forms during the experiment. The questionnaire gathers data on their demographics (age, weight, height), lifestyle (alcohol intake, nicotine use, frequency of exercise etc.). The questionnaire also SCAT5 concussion questionnaire, the PHQ-9 anxiety and GAD-7 depression questionnaire, as well as a simulator sickness symptom questionnaire which is answered once prior to performing the experiment and then repeated afterwards. A visual overview of what is included in the questionnaire is shown in Fig 2.8. The whole questionnaire is reproduced as part of the appendix.

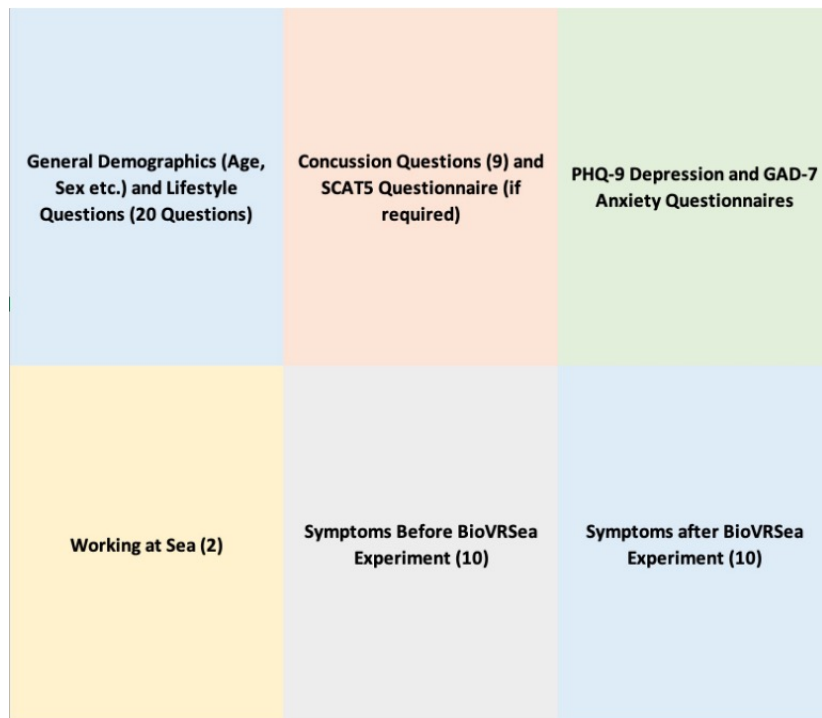


Figure 2.8: Outline of the sections included as part of the questionnaire for the BioVRSea experiment.

## 2.4 Compilation of Mastersheet



Figure 2.9: Structure of Database

All features have been compiled into a mastersheet for further analysis (e.g statistical and machine learning). The mastersheet has a structure as shown in Fig. 2.9. All features are recorded per phase (PRE, MOVE, and POST) for each subject.

## 2.5 Neurophysiology of BioVRSea

Approximately 400 participants have been measured using BioVRSea since the inception of the project in summer of 2020. An age and sex breakdown of the participants

is given in Figures 2.10 and 2.11. Our work strives to build a picture of a 'normative model' of experiment performance, while also delineating differences in neurophysiological parameters between different groups (i.e, sex, lifestyle, seasickness symptoms).

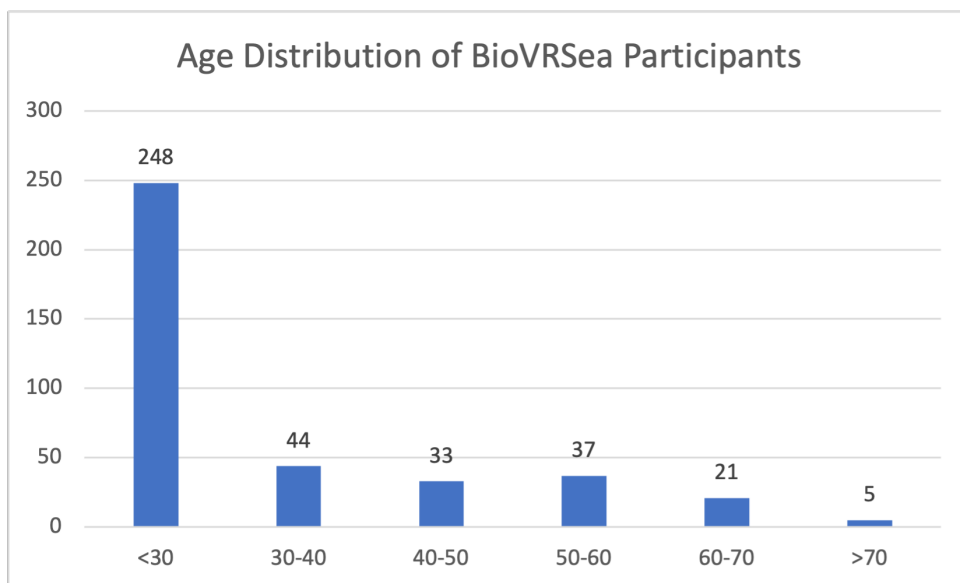


Figure 2.10: Age breakdown of BioVRSea participants

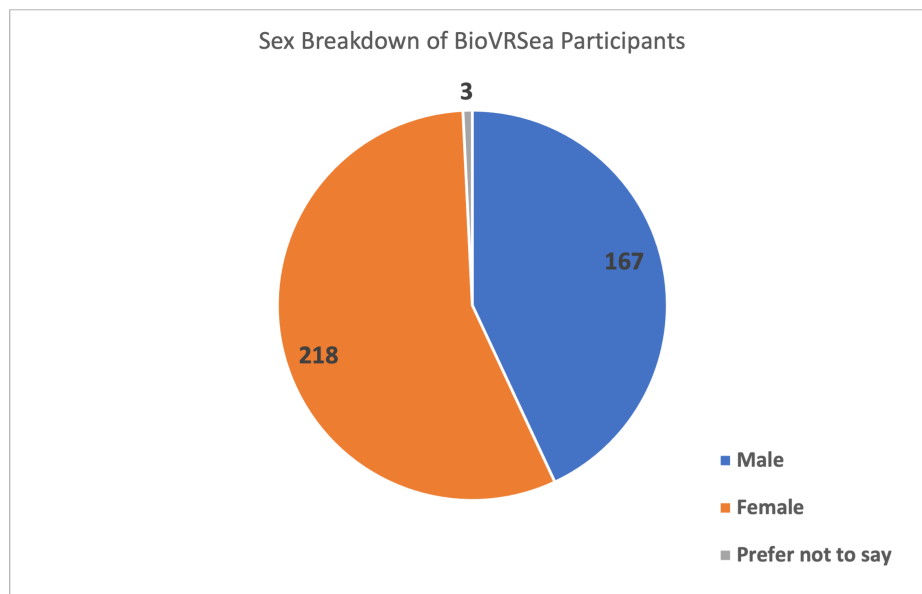


Figure 2.11: Sex breakdown of participants

Using electroencephalography, electromyography, electrocardiography and centre-of-pressure as our parameters, we have published work on the healthy response using EEG [106] and not yet published work showing EMG, ECG, and CoP as differentiators of neurophysiological response on the platform.

### 2.5.1 EEG

Electroencephalography (EEG) is a non-invasive and convenient tool for assessing brain response to an external stimulus. EEG is portable and much less expensive compared

to MRI, and, therefore, it is more accessible for researchers and clinicians. Both fMRI and fNIRS measure changes in blood flow in the brain, which is a proxy of neuronal activation. In contrast, EEG directly measures the changes of electrical signals generated from the cortex that arrive over the scalp. Balance and PC (PC) processes in the brain cortex can be evaluated using EEG while in an unperturbed stance or in challenging balance conditions. Event-related potentials (ERPs), which are stereotyped electrophysiological responses to a stimulus, have been used in many studies to distinguish the normal from the pathological response in many different population groups. The N1 response - a negative potential with a peak occurring approximately 100-150 ms after a perturbation is a prominent cortical potential related to loss of balance ([107] and [108]) and has been investigated to demonstrate the correlation between neurophysiological response and PC perturbation ([109]). A comprehensive review of ERPs (also called perturbation evoked potentials or PEPs) is found in [110]. The review mostly reports work in the amplitude assessment of PEPs but also reviews research performed in the frequency domain, where the spectral characteristics can reveal modulations of EEG activity between baseline and task-related activity ([111]).

However little work has been carried out in exploring the spectral response from EEG data, despite it being a common method for EEG signal analysis. ([112]). The same paper reports frontal and parietal theta power in a cohort of 32 healthy male participants to be correlated with continuous balance performance for balance tasks of varying difficulty. [16] used HD-EEG (256-channel) to measure cortical activity during vibratory proprioceptive stimulation, with significant changes in absolute power reported in the alpha and theta bands in adaptation to the stimulation.

In the 2022 paper by Aubonnet et al. [106], our group reported the healthy response to the BioVRSea experiment. This was the first step in constructing a normative model of neural response to the BioVRSea experiment. The initial investigation subtracted baseline activity from each task in BioVRSea and calculated the power spectral density in five EEG bands; delta (1–4 Hz), theta (4–8 Hz), alpha (8–13 Hz), beta (13–30 Hz), low-gamma (30–45 Hz). The results were the following: **The delta band** shows a power increase for every task, in the frontal and temporal areas. **The theta band** is the band showing less significance, mostly located in the parietal scalp during the platform movement, and has a quite small power decrease compared to BL. **The alpha band** shows significant changes over the whole scalp for all the tasks. Moreover, the alpha power for each task is lower than the baseline. **The beta band** shows significant differences in several areas. The occipital scalp area shows a power increase compared to the baseline, except for the PRE phase, and the fronto-parietal areas of the scalp have a global power decrease. **The low-gamma band** shows significant electrodes in the whole parietal, occipital and temporal scalps. Remodelling can be seen over the course of the experiment where the activity moves from the occipital lobe to more centro-frontal areas. The average power remains positive compared to BL throughout the whole experiment, as seen in Fig.2.12

### 2.5.2 ECG

Heart rate variability (HRV) is the time interval between two successive heartbeats and can be used clinical indicator of autonomic system dysfunction.[113] It is well known that during movement and postural changes, cardiac output is regulated by vestibulo-sympathetic responses [114]. PC challenges provide a route for studying heart biosignal alterations and their relationship with parameters involved in postural

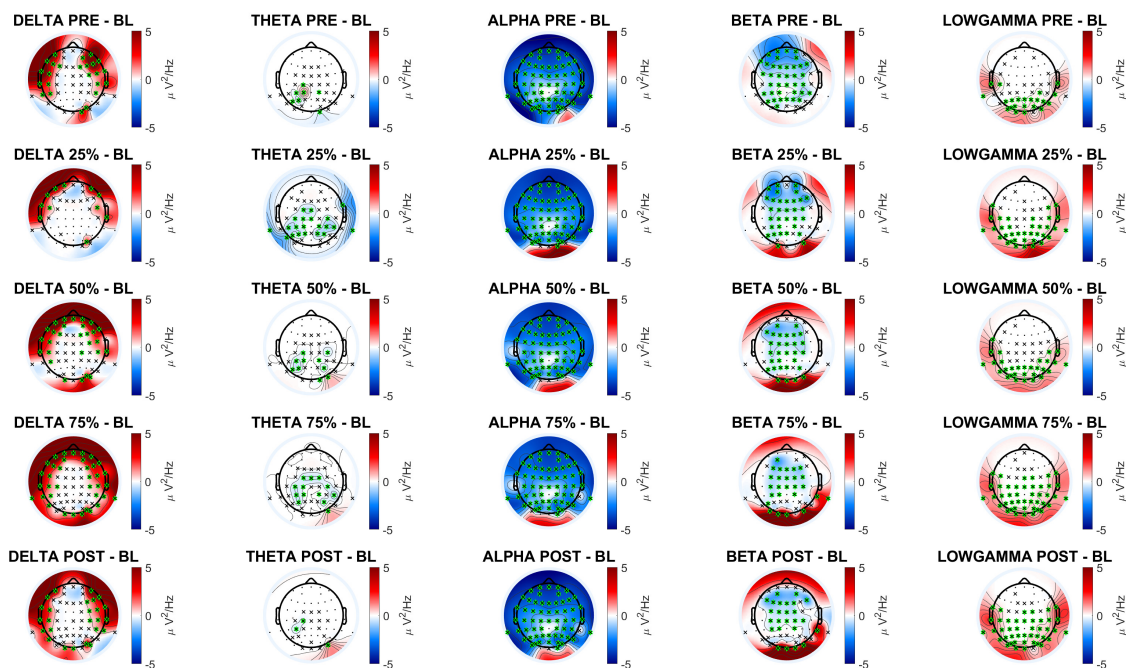


Figure 2.12: Absolute PSD distribution of the whole population behaviour. The "x" highlighted in green represents significant electrodes after Bonferroni correction.

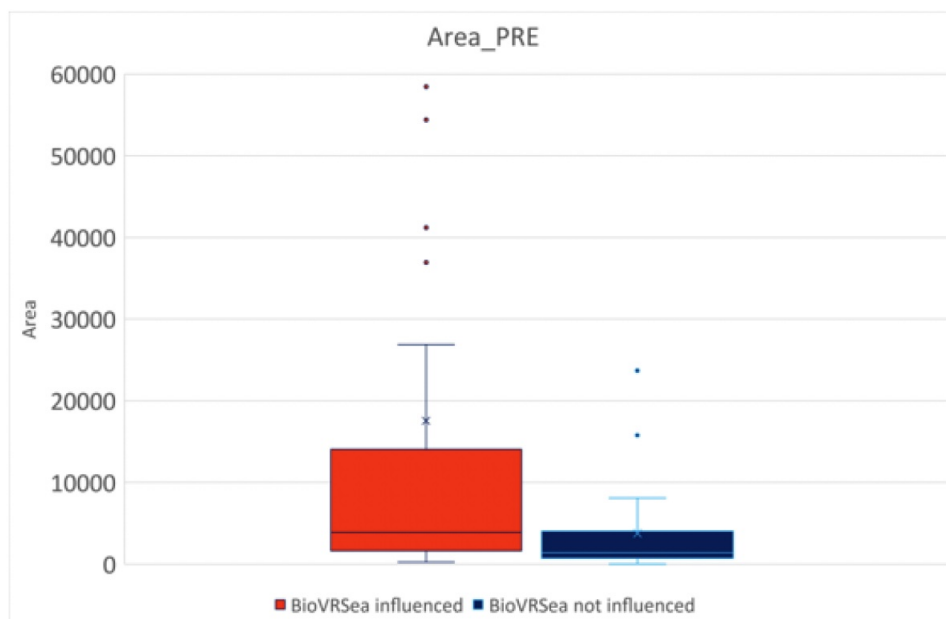


Figure 2.13: Figure showing differences in Area of Poincare plot ellipse PRE stage of experiment for groups with a BioVRSea Effect and without BioVRSea Effect.

strategies, such as EMG and CoP [115], [116]. During such a task, some individuals may experience a sensation of motion sickness. Heart rate and severity of motion sickness sensation have been shown to be linked [117]. Unpublished work by our group showed the relevance of ECG parameters to distinguish those who experienced a motion sickness effect during the BioVRSea experiment from those who didn't. The



work used machine learning on a cohort of 70 participants who reported their level of motion sickness before and after the BioVRSea experiment. Those that reported an increase in 3 or more symptoms after the experiment were considered to have a BioVRSea Index = 1, and those without any change in symptoms or fewer than 2 symptoms had BioVRSea Index = 0 (see Appendix for further information about the calculation of this index). The work showed the capability of ECG parameters, in the PRE, MOVE and POST phases, to predict the effect of the BioVRSea experiment on the symptoms of the subject. In particular the area of the Poincare plot to distinguish between groups along the lines of their levels of reported motion sickness in the PRE phase, as can be seen in Figure 2.13. The MOVE and POST phases both take the SD2 (standard deviation along the major axis of the Poincare plot) as an important feature to distinguish the groups, showing the overall utility of BioVRSea to detect altered responses based on neurophysiology and contribute new avenues for possible clinical measurement.

### 2.5.3 EMG

EMG is a powerful tool employed in the field of biomedical engineering to scrutinize the electrical activity produced by skeletal muscles. Particularly in studies related to lower limbs, EMG provides insights into the neuromuscular dynamics underlying human movement and PC. Lower limb muscles play a pivotal role in maintaining stability, locomotion, and overall body posture. [118] By analyzing the EMG signals of the lower limb muscle activation patterns, inter-muscular coordination, and the neuromechanical adaptations that occur in response to various postural challenges can be studied. Spectral analysis of EMG data reveals the frequency content of the signals, providing insights into muscle fatigue and contraction levels, while time-domain analysis can help discern the onset and duration of muscle activation. This information is instrumental for devising targeted rehabilitation strategies, improving assistive device design, and enhancing our understanding of the complex interplay between neural control and biomechanical constraints in maintaining upright posture.

Previous work from our group suggests that EMG parameters are useful in distinguishing between groups based on a lifestyle index calculated via questionnaire when taking the experiment [119]. This paper shows the potential of Machine Learning to classify groups of participants into distinct lifestyle classes using the parameters calculated during the BioVRSea experiment. EMG features improved the accuracy of classification when combined with CoP features, compared to classifying groups with CoP alone. This work clearly shows the potential for neurophysiological parameters for use in measuring healthy PC using a paradigm such as BioVRSea.

### 2.5.4 CoP

Unpublished work from our lab showed the capability of CoP features to distinguish between those with healthy or unhealthy lifestyles (as determined by the questionnaire administered during the experiment). In a similar vein to the work in the EMG paper mentioned above, CoP has shown promise for discriminating between groups based on lifestyle index, see Fig. 2.14. Those with a healthy lifestyle sway significantly less in both the PRE and POST phases of the experiment, compared to those with an unhealthy lifestyle index.

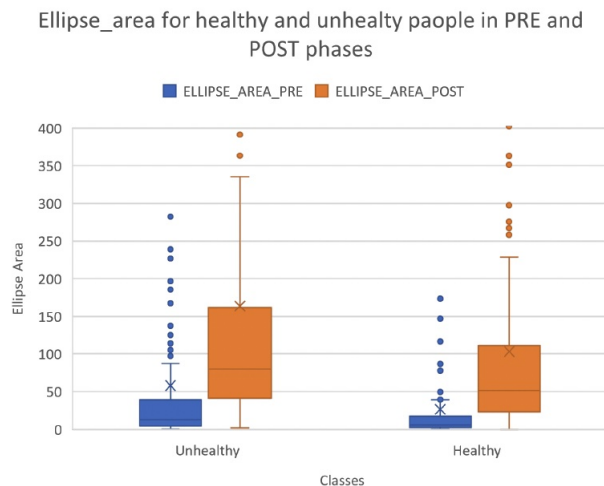


Figure 2.14: Box plot showing the significant differences in CoP ellipse area in the PRE and POST phases for unhealthy and healthy lifestyle index subjects

The work performed to date has shown that neurophysiological and centre of pressure features show promise to detect different responses based on lifestyle or self-reported symptoms related to our experiment. The ability of BioVRSea to quantitatively detect differences between groups of people underpins the hypothesis of this thesis that there may be a measurable difference using quantitative biomarkers (EEG, ECG, EMG and CoP) for neurophysiological disease using the PRE-MOVE-POST paradigms rather than the self-reported symptoms that are the gold standard of clinical assessment in the field.

## Part II

### Published Papers and Future Work



# Chapter 3

## Papers

### 3.1 Towards defining biomarkers to evaluate concussions using virtual reality and a moving platform (BioVRSea)

Adapted from [1].

#### 3.1.1 Abstract

Current diagnosis of concussion relies on self-reported symptoms and medical records rather than objective biomarkers. This work uses a novel measurement setup called BioVRSea to quantify concussion status. The paradigm is based on brain and muscle signals (EEG, EMG), heart rate and center of pressure (CoP) measurements during a postural control task triggered by a moving platform and a virtual reality environment. Measurements were performed on 54 professional athletes who self-reported their history of concussion or non-concussion. Both groups completed a concussion symptom scale (SCAT5) before the measurement. We analyzed biosignals and CoP parameters before and after the platform movements, to compare the net response of individual postural control. The results showed that BioVRSea discriminated between the concussion and non-concussion groups. Particularly, EEG power spectral density in delta and theta bands showed significant changes in the concussion group and right soleus median frequency from the EMG signal differentiated concussed individuals with balance problems from the other groups. Anterior–posterior CoP frequency-based parameters discriminated concussed individuals with balance problems. Finally, we used machine learning to classify concussion and non-concussion, demonstrating that combining SCAT5 and BioVRSea parameters gives an accuracy up to 95.5%. This study is a step towards quantitative assessment of concussion.

#### 3.1.2 Introduction

A concussion, or mild traumatic brain injury (mTBI), is a temporary neurological impairment resulting from head impact [11]. Participation in sports increases the risk of multiple concussions, with certain sports posing higher risks [18]–[20]. Symptoms may include headaches, emotionality, amnesia, balance issues, and sleep disturbances [21], [22]. While most concussions resolve spontaneously, some result in lingering complications [11], [23]–[27]. Diagnosing concussions is challenging due to non-specific

symptoms and the lack of a precise definition [10], [11], [28]. Tools like the SCAT5 aid in symptom assessment, though they shouldn't be used exclusively for diagnosis [10], [29], [30].

The pathology of concussions and the relationship between neuronal alterations and symptoms remain unclear [24]. Structural damage post-concussion, though diagnosable without evident structural damage, can contribute to prolonged symptoms [10], [34]. Neuroimaging and electrophysiological evaluations, such as EEG, can provide insights [24], [35], [36]. EEG is cost-effective and offers potential markers for concussion assessments, although more research is needed [38], [39], [41]–[43], [53].

Post-concussive symptoms include dizziness and balance issues [54]. Assessing postural control, such as the center of pressure (CoP), can indicate concussion [45]–[47], [56]–[58]. EMG recordings can also be used to assess postural stability and muscular activity [60]–[62]. Blood flow and heart rate variability have been explored as objective markers, although findings are mixed [64]–[67].

A comprehensive approach to concussion assessment and treatment is essential [29]. Virtual reality (VR) offers a novel method for evaluating postural control and cortical activity in a controlled environment, showing promise in distinguishing between mTBI and control groups [57], [68]–[71].

### 3.1.3 Methods

#### 3.1.3.1 Participants

Participants were all female athletes (N=54), competing at the highest level in Iceland in basketball (16.7%), handball (35.2%), soccer (38.9%), ice hockey (5.6%), or martial arts (3.7%). Mean age was 38.4 years (SD=7.7). Almost half of the participants had a history of concussion, 48.1% (n=26) half had no concussion history, 51.9% (n=28). Mean years since retirement was 4.3 years (SD=4.9). All participants had a college or a university diploma, 48% had an MA or an MS degree. This data is summarised in Table 3.1.

Table 3.1: Summary of Participant Information

	<b>History of Concussion (n=26)</b>	<b>No History of Concussion (n=28)</b>
Mean Age (SD)	30.5 (6.9)	29.8 (8.2)
Retired %	69.2 (18)	57.1 (16)*
Active %	30.8 (8)	39.3 (11)

#### 3.1.3.2 Written information and informed consent

All participants were provided written information about the study prior to signing an informed consent document. The study protocol was approved by the Icelandic National Bioethics Committee (no: 17–183-S1).

#### 3.1.3.3 Concussion definition

Participants were read a concussion definition and were asked if they had sustained a concussion. The definition was based on the Berlin Consensus statement on concussion in sport from 2016[10], [120], [121].

#### 3.1.3.4 SCAT5 Questionnaire

All participants completed the symptoms scale from The Sport Concussion Assessment Tool 5 (SCAT5) [27], [36], [120] before the experiment. The overall score is calculated by the sum of each participant's responses. The SCAT5 has been recognized as a concussion assessment tool [10]. However, the SCAT5 should not be used as a diagnostic tool but as part of an assessment battery [36]. The SCAT5 symptoms checklist has not been validated in a Icelandic sample only the SCAT 3 [122]. The scale has 22 items, each item scoring from 0 to 6, indicating the severity of the symptom [36]. In this study, it was hypothesized that the Icelandic versions of the SCAT5 symptoms checklist, could be used to differentiate between concussed and non-concussed athletes, it was used to validate the self-reported concussion status and assess for each group the changes of some physiological conditions associated with our experiment.

#### 3.1.3.5 Virtual reality experiment

The participants were then prepared for the virtual reality and physiological measurement part of the experiment. This involved the placement of a wet 64-electrode EEG cap (Sampling frequency 4096 Hz, ANTNeuro, Hengelo, The Netherlands), six wireless EMG sensors (Sampling frequency 1600 Hz Kiso ehf., Reykjavík, Iceland) on the tibialis anterior (TA), gastrocnemius lateral (GL), and soleus (S) muscles of each leg, and a heart rate sensor (sampling frequency 1 Hz, PolarBeat, Kempele, Finland) strapped around the chest. The EEG amplifier (ANTNeuro, Hengelo, The Netherlands) was connected to the cap and placed in a backpack with a tablet used for EEG signal acquisition. The participant put on the backpack and was instructed to step onto the force plates after removing their shoes. The position of the feet was in bipedal stance with feet hip width apart, while standing on the force sensors (Sampling frequency 90 Hz, Virtualis, Clapiers, France). The force sensors on the moveable platform (Virtualis, Clapiers, France). Finally, the participant dons the VR goggles.

The experimental protocol was then explained to the participant. The explanation included that they should stand quietly on the platform with their hands by their side observing a mountain view for the first 2 min of the experiment. Then, the scene in the VR goggles would change, beginning the sea simulation. The participants were instructed to remain standing quietly with their hands by their side for the first 35 s of the sea simulation. There was no platform movement in this part of the experiment, and it is called the PRE phase of the experiment. After 35 s of quiet standing watching the sea simulation, the participant was instructed to hold onto the bars in front of them. The platform then began synchronized movement with the sea scene in the VR goggles, with 25%, 50% and 75% of maximal wave amplitude. In this central part, each segment lasted 40 s and the participant held the bars of the platform while continuing to observe the sea simulation. Finally, the platform stopped moving and the participant was asked to remove their hands from the bars and attempt to stand quietly with their hands by their side for the final 40 s of the experiment. The sea scene was still observed by the participant for the final 40 s. This is called the POST phase of the experiment; it is performed identically to the PRE phase but after the participant has performed movement in the central part of the procedure. A table of the VR experiment protocol is shown below in Fig. 3.1. Each participant took part in a single trial according to the experimental protocol.

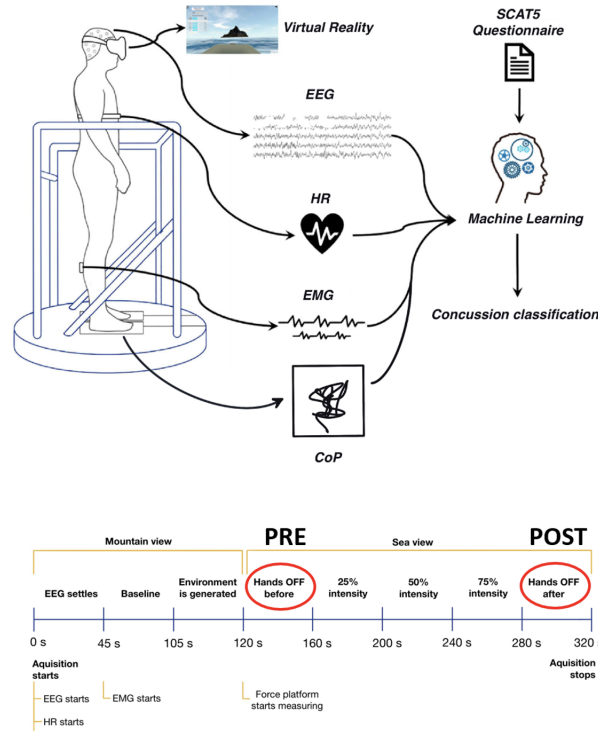


Figure 3.1: Graphical Abstract and Experimental Paradigm

The operator can set the frequency of the waves between 0.5 Hz and 3 Hz and the amplitude of the waves between 0 and 2. During the simulation, we vary the amplitude of the platform movements from 0% up to 75% of the platform’s maximal amplitude. Two different protocols were used at random throughout the study. The ‘soft’ protocol was defined as a wave frequency of 1 Hz with an amplitude of 0.6 while the ‘hard’ frequency was defined as a wave frequency of 3 Hz with an amplitude of 0.5. Each participant experienced either the hard or soft protocol once while taking part in the experiment.

Randomly selected amplitude of the experiment (soft or hard protocol) is made to mimic the variety of “sea behavior,” to cover a wide possibility to trigger a postural control response.

### 3.1.3.6 Data acquisition

During each protocol, muscle, brain, heart, and CoP data were acquired using the following technologies:

**Brain electrical activity** was measured using a 64-channel wet electrode cap (sampling frequency of 4096 Hz) from AntNeuro, Hengelo, the Netherlands. **Muscle electrical activities** from the lower limbs was acquired using six wireless EMG sensors (sampling frequency of 1600 Hz) placed on the tibialis anterior (TA), gastrocnemius lateral (GL), and soleus (S) muscles of each leg (Kiso ehf, Reykjavik, Iceland). **Heart rate** was measured using a chest heart sensor (Polar Electro, Kempele, Finland, sampling frequency 1000 Hz). **Force Plate measurements** were made using 4 sensors located under each foot platform. The sensors give information about the center of mass in the Antero-posterior and Medio-Lateral axis (Virtualis, Clapiers, France, sampling frequency 90 Hz).



Post processing and calculations The data from each measurement were divided into 6 segments, corresponding to each stage of the protocol. Data for the EEG, EMG and CoP were analyzed by calculating POST–PRE (POST minus PRE) paradigm.

Division into subgroups by symptoms Subjects from the concussion group were further divided into subgroups for quantification of some symptoms from the SCAT5 questionnaire. For instance, CoP measures may be different among the concussion participants that reported balance problems, compared to those that did not/non-concussion group. The following symptom-based subgroups were formed from the concussion participants for the following measurements:

For EEG: Pressure in the head symptom group (17 subjects), Fatigue/Low Energy symptom group (19 subjects), difficulty concentrating symptom group (16 subjects).

For HR: Nervous/Anxious group (20 subjects), Fatigue/Low Energy Group (19 subjects).

For EMG: Balance problem symptoms group (14 subjects).

For CoP: Balance problem symptom group (14 subjects).

### 3.1.3.7 EEG

The EEG analysis was performed on the spectral domain. The focus was put on the difference between the PRE and POST segments. The considerable electrodes were identified between those two segments.

The EEG was recorded using a 64-electrode channel system with an electrooculogram (EOG) electrode placed below the right eye and a ground electrode placed on the left side of the neck. Data pre-processing and analysis were performed with Brainstorm [123] and Matlab 2020b,[124] using the Automagic toolbox [125].

For each segment, we removed the 5 first and 5 last seconds, to ensure the data quality and to avoid artefacts. The data were resampled to 1024 Hz. Automagic was used to automatically pre-process every dataset, with a manual inspection at the end. The ICA MARA algorithm was used, with a variance of 20%. The data were notch filtered at 50 Hz. A high pass and low pass filter were set respectively to 1 Hz and 45 Hz. Finally, the bad electrodes were interpolated. Each segment was on average interpolated up to 10%.

The power spectral density (PSD) was computed for each epoch with ‘Welch’s method, with the following frequency bands: delta (1–4 Hz), theta (4–8 Hz), alpha (8–13 Hz), beta (13–30 Hz), low gamma (30–45 Hz). The relative power of each band was then computed obtaining a total of 5 EEG-related features.

### 3.1.3.8 EMG

Two types of EMG analysis were performed on the participants data. The area under the rectified and smoothed EMG curve was calculated for each electrode, as well as spectral analysis of each signal.

EMG data processing was performed using Matlab 2020a [124]. The EMG signal was filtered with a 50th order FIR bandpass filter with cut-off frequencies at 40 and 500 Hz. The integral of the rectified EMG signal for each leg was calculated, resulting in 1 EMG area measurement per muscle for each segment of the acquisition. The area under the EMG curve indicates the excitability and neural drive to the muscle, preceding muscle contraction [126].

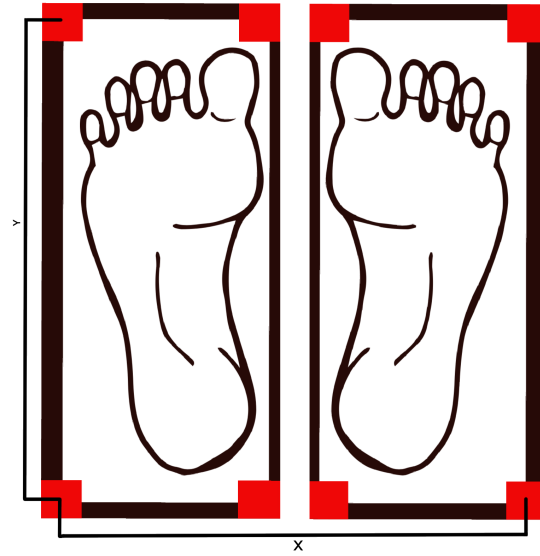


Figure 3.2: Foot Position on Force Platforms

If the two phases, namely PRE and POST, last 40 s we considered a central 30-s time window for each of the two phases to exclude the effects of the transition between phases. Successively, we performed in these time windows an electromyography (EMG) spectral analysis through the analysis of the signal power distribution calculated by the Fast Fourier Transformation (FFT) algorithm and therefore computing the total power spectrum of the EMG signal. For each of the two resulting total power spectra, one for the PRE and the other one for the POST, four frequency-domain parameters were extracted: Total Power, kurtosis, skewness, and median frequency.

The total power is the integral under the spectrum curve which increases with the force of contraction [127]. The kurtosis is a measure of how outlier-prone a distribution is; we used a kurtosis function that considers the following assumptions: the kurtosis of the normal distribution is 3 and the kurtosis is biased. Skewness is a measure of the data's asymmetry around the sample mean; we used a skewness function that considered a biased version. Kurtosis and skewness were chosen because they allow evaluation of any changes in the EMG spectrum. Studies show their valuable contribution in the EMG analysis [128]–[130]. The median frequency is the frequency that divides the total power area into two equal parts. The median frequency was chosen considering its usefulness in describing fatigue changes [131], [132] including the soleus and gastrocnemius muscles. The analysis of median frequency has also been useful in diagnosis of various disorders [133]. EMG analysis and feature extraction were carried out through MATLAB R2020a [124].

### 3.1.3.9 Heart rate

The heart rate data were averaged for the 40 s PRE and POST stages and the standard deviation computed.

### 3.1.3.10 CoP

Figure 3.2 shows a schematic of the foot position on the force plate.

The processing of the CoP data was performed using Matlab 2020a [124]. During the experiment, the force platform records the movement of the Centre of Pressure (CoP), a projection of the center of mass of the subject on the plane of the machine, also called stabilogram. The CoP data was filtered with a Savitsky-Golay filter with window size 7.

We extracted several parameters from the stabilogram for evaluating the postural control response of the subject before (PRE) and after (POST) the perturbation caused by the movement of the platform (25%, 50%, 75%) and the visual cues provided by the VR goggles.

During the PRE and POST phases, the platform is not moving and the subject experiences only the visual cues provided by the movement of the waves. In other words, we are evaluating how the postural control changes the COP and if certain conditions can affect this complex biological system.

The most important geometrical features extracted are the 95% confidence ellipse (axes length, orientation, and area), the mean root square distance from the center (RDIST) [134], the total excursion (TOTEX) and the position of extreme points (Anterior, Posterior, Left, Right). TOTEX is computed on support plane, on the Antero-Posterior Axis (AP) and Medio-Lateral Axis (ML).

In addition to geometrical features, we computed the standard deviation and sample entropy [31] of ML and AP signals and heading change [30]. Following [32], [135] AP and ML Complexity Index (CI) and Multivariate CI are obtained from the multi-scale entropy with time scales 1 to 6.

Moreover, we consider the difference between consecutive points to evaluate the Mean Velocity (MV) on the support plane and on each individual axis.

Finally, to understand any link between the chosen set of parameters and the aim of this study we considered the POST features minus the PRE features, and we performed a Wilcoxon signed-rank test to assess the relationship between features and subgroups under analysis. We also tested for statistically significant differences between PRE and POST for each individual variable.

### 3.1.4 Results

Symptom or behavioral assessment with SCAT5 was performed prior to the instrumented VR experiment and is reported below, followed by the neurophysiological and classification results.

#### 3.1.4.1 Sports Concussion Assessment Tool (SCAT) 5

We used the SCAT5 to validate the self-reported concussion status, and to assess the changes in physiological conditions associated with our experiment. An independent t-test showed a significant difference between severity scores on the SCAT5 when comparing the concussed and the non-concussed athletes. Those with a history of concussion reported more severe concussion symptoms as assessed by the SCAT5 compared to those with no history of concussion as seen in Table 3.2.

A closer look was taken at types of symptoms in the two groups. As seen in Fig. 2, 21% of participants with no concussion history reported feeling nervous and anxious before going into the VR environment compared to 88% of participants with a history of concussion (Fig. 3.3). The symptom most often reported among those without a concussion history was a headache, the only symptom above 30% (32%). Only

Table 3.2: SCAT5 Scores for Participants with a History of Concussion and those without a History of Concussion

History of Concussion		
Number	Mean	SD
26	36.47	23.71
No History of Concussion		
Number	Mean	SD
28	3.71	4.5

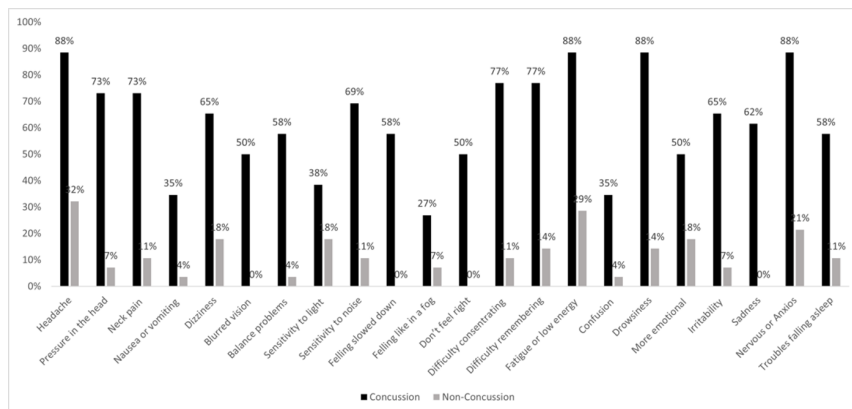


Figure 3.3: SCAT 5 Results

one symptom was reported by under 30% of participants with concussion history, the symptom feeling like in a fog. The most reported symptoms in the concussion group were headache, fatigue/low energy, drowsiness and nervous/anxious.

### 3.1.4.2 Centre of Pressure Measurements

All CoP parameters were studied as the difference of their values POST–PRE. In these two phases the subjects experienced the same environmental condition with the difference that in POST the subjects had to adapt to the induced movement provided from the previous phase where the platform was moving.

#### CoP analysis

We extracted several parameters from the stabilogram for evaluating the postural control response of the subjects before (PRE) and after (POST) the joined perturbation caused by the movement of the platform (25%, 50%, 75%) and the visual cues provided by the VR goggles.

Six features from the displacement and velocity analysis showed significant differences (all  $p < 0.05$ ) between the PRE and the POST stages for all groups.

- TOTEX - Total Excursion
- MDIST AP - Mean Distance in the Anteroposterior direction
- MVELO - Mean velocity
- ELLIPSE MAIN AXIS - The length of the main axis of 95% confidence ellipse
- SD AP -Standard Deviation in the AP direction

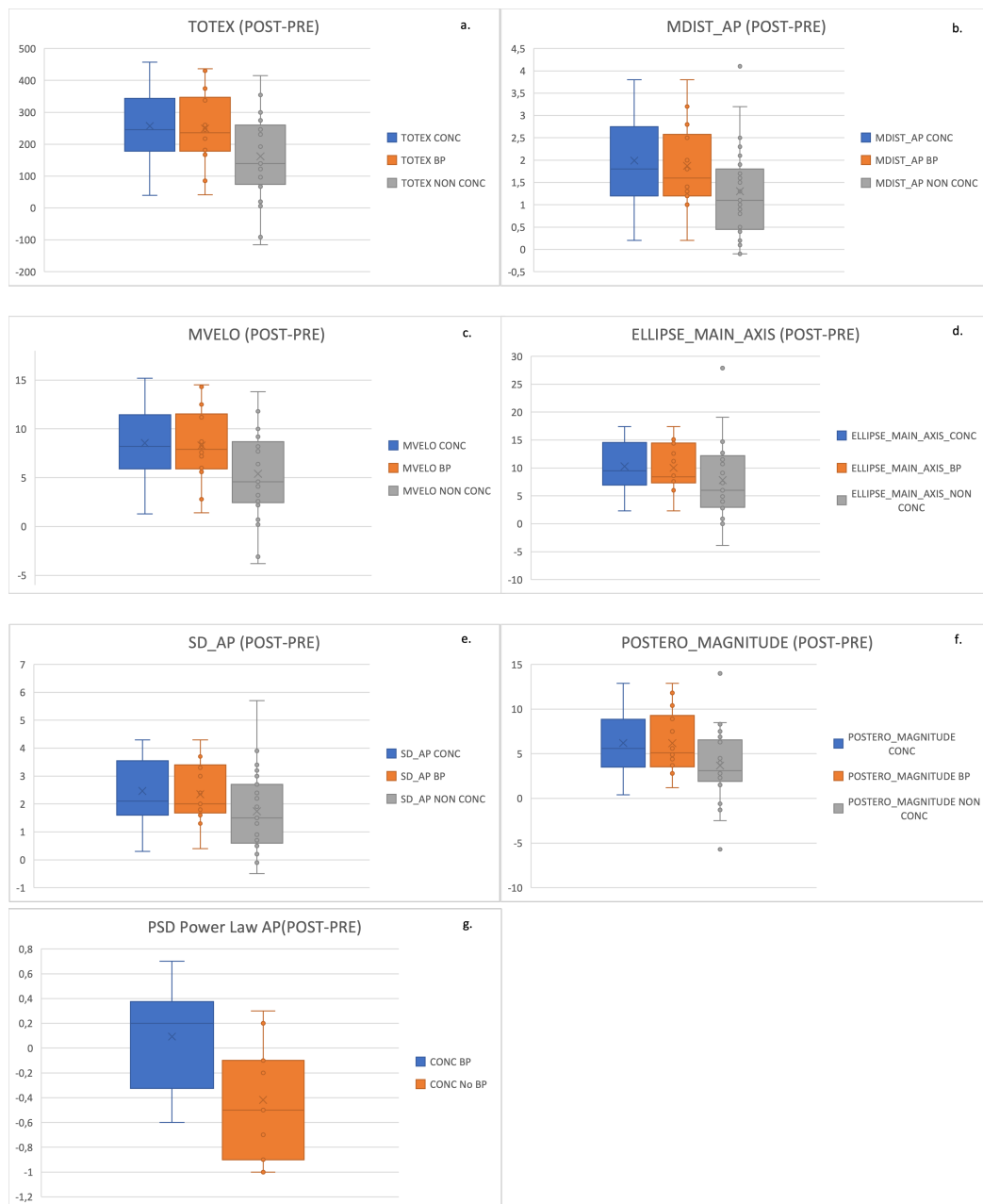


Figure 3.4: CoP statistical comparisons between Concussion, non-concussion and concussion with balance problems groups.

- POSTERO MAGNITUDE - Posterior extreme point distance

The concussion group exhibited larger changes from PRE to POST for all six features compared to the non-concussion group.

One feature in the spectral analysis, PSD EXP AP – Power Spectral Density (PSD) Power Law Exponent for the AP signal showed statistical significance ( $p=0.019$ ) while comparing the concussion subgroup experiencing balance problems compared with concussion subgroup not experiencing balance problems. This can be seen in Fig. 3.4

Calculation of features in both the anterior–posterior and medio-lateral directions were made, along with sample and multiscale entropy features, however they did not show any significant differences between PRE and POST, and are not reported on here.

### 3.1.4.3 Electroencephalography Measurements

Figure 3.5 shows the results from the EEG analysis performed in the frequency domain. The figure shows the difference POST–PRE for the concussion group for the delta and theta band, the only bands that were significantly different. The ‘x’ represents the electrodes for which we found significant differences for each band.

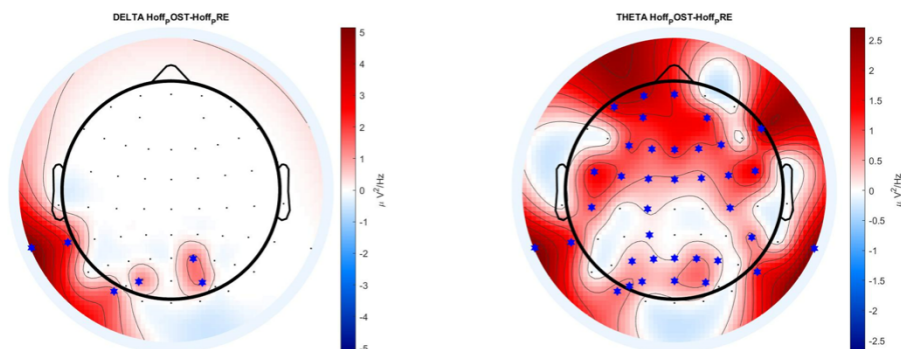


Figure 3.5: Spectral Analysis POST-Pre for Concussion Group in Delta (Left) and Theta (Right) Bands

The difference was highlighted by an increase of power and significant evolution in the theta band mostly, and delta band for the concussion group ( $p = 0.038$ ), the theta band showing significantly higher POST power than PRE. The theta band displayed an important number (37 out of 64) of significant electrodes ( $0.032 < p < 0.047$ ) (t-test, corrected with false discovery rate (FDR), Benjamini–Hochberg method), in the frontal (18 out of 64 electrodes) and occipital (11 out of 64) cortex. The non-concussion group did not display any significant results for this experiment. We then

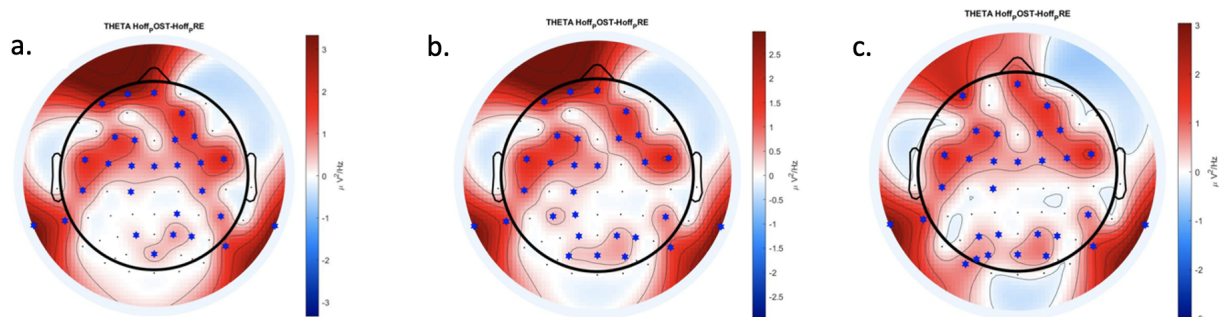


Figure 3.6: PSD results for subgroups - a. Difficulty concentrating, b. Pressure in the head, c. Fatigue and Low energy

divided the concussion group into subgroups based on symptoms identified from the SCAT5 questionnaire. We analyzed the Difficulty concentration symptoms group (16 individuals), the Pressure in the head symptoms group (17 individuals), Fatigue and low energy group (19 individuals).

Figure 3.6 shows the results from the EEG analysis performed in the spectral domain. The figure shows the difference POST–PRE for the concussion subgroups, for the theta band, the only band that presented significance. Figure 3.6 shows from

Table 3.3: Significant Electrodes in Concussion and Concussion subgroups

	<b>Significant Delta Band Electrodes</b>	<b>Significant Theta Band Electrodes</b>
Concussion Group	M1 P2 PO3 PO4 TP7 PO7	Fp1 Fpz F3 Fz F4 F8 FC5 FC1 FC2 FC6 M1 C4 M2 CP1 CP6 P3 Pz P4 P8 Poz AF7 AF3 AF4 F1 F2 FC3 FCz FC4 C5 C1 P1 P2 PO5 PO3 PO4 TP7 PO7
Difficulty Concentrating Subgroups	-	Fp1 Fpz F3 F4 FC5 FC1 FC2 FC6 M1 C4 M2 CP2 CP6 P4 P8 Poz AF7 AF4 F1 F2 FC3 FCz FC4 C5 C1 P1 P2 TP7
Pressure in the head subgroup	-	Fp1 Fpz F3 F4 FC5 FC1 FC6 M1 M2 CP1 CP6 P4 P8 Poz AF7 AF4 F1 F2 FC3 FCz FC4 C5 C1 CP3 P1 P2 PO3 PO4 TP7
Fatigue and low energy subgroup	-	Fpz F3 F4 FC5 FC1 FC2 FC6 M1 M2 CP6 P3 P4 P8 Poz AF7 AF4 F1 F2 FC3 FCz FC4 C5 C1 P1 P2 PO3 PO4 TP7 PO7

left to right the results for the a. Difficulty concentrating group, the b. Pressure in the head group, the c. Fatigue and Low energy group.

Figure 3.6 reveals that the subgroups present significant differences (0.008 p 0.049) for the theta band, with a global increase mostly in the frontocentral cortex (16 significant electrodes for difficulty concentrating, 15 for pressure in the head, and 14 for fatigue and low energy) for all of them, as well as an increase in the occipital lobe for the Pressure in the head (8 significant electrodes) and Fatigue and low energy (10 significant electrodes) subgroup. Other symptoms groups were analyzed, such as headache (20 individuals), dizziness (14 individuals), balance problem (13 individuals) and more emotional group (11 individuals). These subgroups did not present any significant findings; therefore, their results will not be displayed.

3.3 summarizes the significant electrodes (0.008 p 0.049) of Delta and Theta band, for the concussion group and the three subgroups detailed.

### 3.1.4.4 Electromyography Measurements

**Spectral Results** Total power, kurtosis, skewness, and median frequency were calculated for each muscle in the concussion and non-concussion groups in both the PRE and POST stages of the experiment. For these POST–PRE results, the muscle that best discriminated the concussion and non-concussion groups was the soleus muscle, for all features except median frequency. Two subgroups from the concussion group were also analyzed, based on their responses to the SCAT5 symptom questionnaire: those experiencing balance problems (BP) and those not experiencing balance problems (No BP). Median frequency results for the right soleus of the BP group showed significance (p=0.0075) in the POST phase of the experiment when compared to the no BP group. The POST–PRE results in the median frequency of concussion, non-concussion and BP groups were not significant. Median frequency results for the soleus

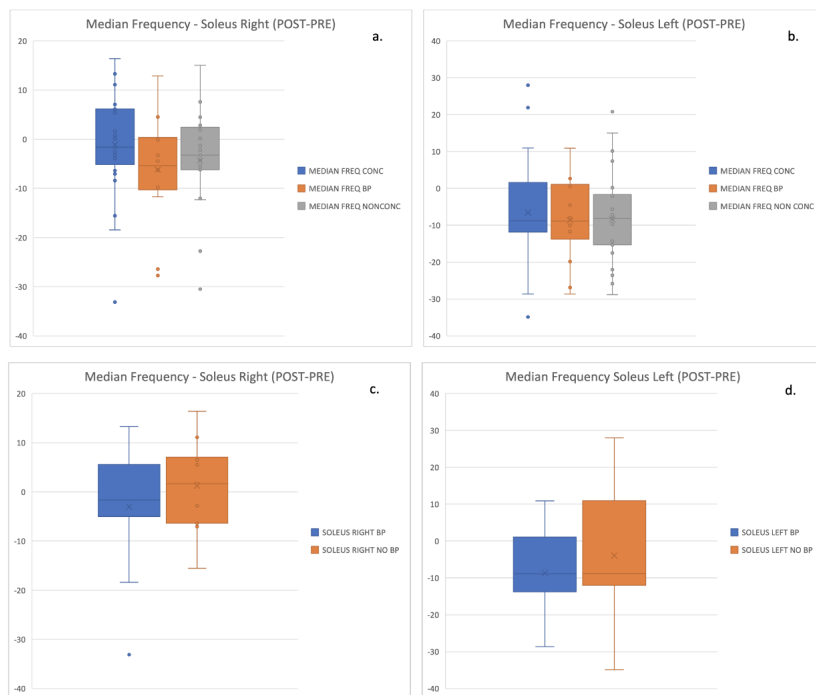


Figure 3.7: Spectral Analysis Results for Soleus Muscle

are presented in Fig. 3.7. **EMG Area** The changes (POST–PRE) in the area under the EMG signal were not significant for any group, nor do the area measurements show any differentiation between the concussion and non-concussion group.

### 3.1.4.5 Heart Rate Results

Heart rate was measured in beats per minute (bpm) PRE and POST for each participant. The non-concussion participants experienced a minor, non-significant, change in heart rate. The concussion group participants experienced a larger change in heart rate from PRE to POST. However, the difference between POST and PRE (POST–PRE) was not significant for the concussion group.

### 3.1.4.6 Classification Analysis

Three different features selections were used as predictive features to demonstrate the capability to classify concussed and non-concussed athletes through a supervised machine learning approach and a 10 k-fold cross validation. Tree-based, linear-based and simplified artificial neural networks algorithms were used to consider different algorithmic strategies for the classification. Table 3.4 shows the accuracy, sensitivity and specificity obtained with the 9 PCA features: the highest accuracy of 72.7 was reached with a Random Forest (RF) model. In contrast, the most heightened sensitivity of 57.9 was achieved with Gradient Boosting (GB), another tree-based model. Table 3.4 shows the results from the SCAT5 features models, with RF and the linear-based Support Vector Machine (SVM) model having the highest accuracy of 88.6 and the simplified artificial neural networks of the Multilayer Perceptron (MLP) model having the highest sensitivity of 89.5. The best results were achieved by merging the two features sets with all the models exceeding 90 in accuracy except (GB), getting a significant 95.5 with SVM and 93.2 with Ada Boosting (ADA-B) (Fig. 3.8). All the sensitivity and



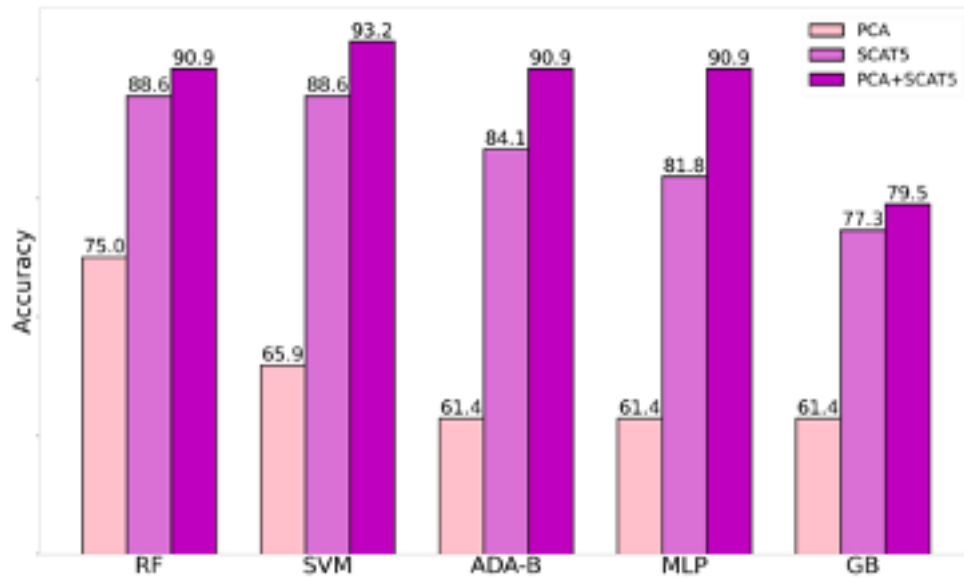


Figure 3.8: Machine Learning Results with different Algorithms

specificity results for all the models with the combined feature selection are noteworthy. It is also worthy of underlining that the linear model SVM is the one from which the best accuracy is obtained with the 31 features. At the same time, the one based on the artificial neural network MLP gives the best sensitivity of 96.0. Tree-based models work with good results apart from the GB, which, in all cases, is the one with the least significant accuracy results.

### 3.1.5 Discussion

The results of this study support a novel method in concussion assessment by evaluating self-reported concussion symptoms and history against neural and postural responses acquired in a BioVRSea environment, with machine learning used to demonstrate the classification ability of this model. We hypothesized that (1) The Icelandic versions of the SCAT5 symptoms checklist, although not a diagnosis tool, can be used to differentiate between concussed and non-concussed athletes, (2) changes of CoP, heart rate, EMG and EEG data can quantitatively measure concussion and concussion symptoms, and (3) machine learning techniques using SCAT5, and neurophysiological parameters can improve assessment of concussion.

Participants in this study were all female athletes, either with a self-reported history of concussion or no history of concussion. Participants were matched in age and divided almost equally among the two groups. The participants with a history of concussion had a significantly higher score on the concussion symptom scale (SCAT5). The symptoms on the SCAT5 scale are non-specific to concussion, meaning that symptoms can be seen in those with no history of concussion [136]. Nevertheless, the SCAT5 has been recognized as a concussion assessment tool and is used to assess symptoms after a concussion [10]. Only the Icelandic version of the SCAT3 has been validated in an Icelandic sample, with more studies being recommended[122]. The scale was therefore administered to all the athletes to assess if it differentiated between those with and without a history of concussion. Results supported that it did. The most frequently reported symptoms among those with a concussion history were headaches, fatigue and low energy, drowsiness and nervousness, and the symptom reported by the fewest was feeling like in a fog, reported by almost 30%. This is in stark contrast to the non-concussion group where the most frequently reported symptom, headache, was reported by 32% and was the only symptom reported by more than 30%. This was expected as headache is the most common post-concussive symptom, followed by troubles with memory and concentration, dizziness, and balance problems. In addition, results show that the correlation between concussion count (no concussion vs. concussion) and symptoms severity score was significant with concussion history resulting in a higher severity score for concussion symptoms.

To quantify concussion symptoms, changes of CoP, heart rate, EMG and EEG measures were analyzed against reported concussion history and by concussion subgroups represented by specific symptoms reported on the SCAT5. CoP features showed a larger change in six features in the displacement and velocity analysis. Other studies support these results, having previously found that subjects who have experienced concussions show alterations in displacement and velocity CoP beyond the date of clinical recovery or return to play[137]. According to results from a study [138], the disruption induced in the Postural Control (PC) by a concussion may be observed from the CoP even months after the injury. Since there are many mechanisms involved in maintaining the stability of the body, the stabilogram is a good candidate to evaluate impairments in case of concussions. To evaluate any decrease in the static stability we considered the following: TOTEX, as a decreased instability may lead to an increased movement compared to more stable subjects; RDIST follows a similar rationale, accounting also for the distance from the center as a measure of instability; MVELO [139] accounts for both spatial and frequency components, and the velocity may have a significant role in anticipatory movement response [140], [141]; The Main Axis of the 95% confidence ellipse [134] indicates the magnitude of the principal com-

ponent of motion, a greater axis length is associated to a decreased stability; and SD AP reflects the variability in the Antero-Posterior Signal [139]. We decided to include the Postero Magnitude feature to assess whether extreme and rare oscillations may be signs of postural control impairments although further research should investigate this phenomenon better. Finally, we investigated the AP and ML signals in the frequency domain computing the Power Spectral Density (PSD) with Fast Fourier Transform (FFT) and used the log-log plot to compute the exponent of the PSD power law. The only statistically significant difference was on AP direction when comparing concussion subgroups related to balance problems, thus the AP direction may have a critical role in maintaining balance compared to ML direction in case of concussion.

The EEG results indicated a significant difference (at some frequency bands) between those with a history of concussion and those with no history of concussion when participants had to maintain postural control and balance. Activity on the theta band was increased in those with a history of concussion. The theta wave activity has been associated with the ability to encode new information, and is correlated with cognitive performance, memory in particular [142], [143], and may appear normal during relaxed wakefulness [144]. Theta activity has been observed to increase during cognitive tasks compared to motor tasks, indicating an active role in problem solving [145] and has been associated with tasks that need more attention and cognitive demands [145]. An increase in theta among those with a history of concussion when compared to those with no history of concussion may indicate a need for more attention and cognitive effort than those who do not have a history of concussion. The increase in theta was additionally present in concussion subgroups among participants that reported having difficulty concentrating, feeling pressure in the head, and feeling fatigue and low energy. Further supporting their reports of concussion symptoms and offering an objective way to assess post-concussive symptoms. Concussion history has been connected to cognitive impairment [146], [147] like attention and reaction [148], [149] and cognitive fatigue has been suggested as a sub-type of concussion [150]. The increase in theta may support this type of cognitive malfunctioning and indicates that the task was more demanding for those with a history of concussion. It is worth mentioning that theta increase has also been found in the frontal and central regions for postural control adaptation and habituation [16], highlighting its activation during balance and postural control disturbance [151].

EMG area measures showed differences between the two groups based on signals from the tibialis anterior (TA) when participants had to maintain postural control in the PRE and POST stages. The calf muscles are active agonists in upright posture [152], driving the main action of maintaining upright balance. Those with a history of concussion showed a trend towards higher muscle activation in the TA when maintaining balance POST, although the difference was not significant. This could indicate postural control and balance problems, resulting in a more active muscle when trying to stabilize in an unstable environment. Impaired postural control has been connected to concussion history [153], as well as impairment in visual and vestibular systems [10], [154], [155]. Concerning the EMG spectral analysis, all the features computed, namely Total Power, Kurtosis, Skewness, and Median Frequency, showed a stronger statistically significant difference between PRE and POST in the concussion group compared to the non-concussion group. Among the muscles analyzed, the soleus showed the maximum discriminative power to differentiate between the two groups and a coherence between the results obtained from right and left sides. Indeed, for the concussion group, all the features, except the median frequency, exhibited a strong, statistically

significant difference between the PRE and POST while non statistically significant differences were found in the same features for the non-concussion group. For both groups, no difference in median frequency was found, which implies that the task did not lead to muscle fatigue. In the concussion group a more symmetrical, Gaussian-like, spectrum shape was observed in the POST compared to the PRE, as indeed kurtosis and skewness showed statistically lower values. Finally, in the concussion group a statistically higher Total Power was found in the POST compared to the PRE suggesting an increase in the muscle contraction force. The further statistical analysis, aimed to compare within the concussion group subjects who experienced balance problems versus subjects who did not experience balance problems, showed once again the significant discriminative power of the right soleus muscle. In fact, in this analysis, contrary to the previous one, the median frequency feature has proved to be the most significant feature being able to discriminate concussed subjects (of which are 92% right-handed) with and without balance problems in the post phase. We can conclude that the median frequency features together with the other spectral features – namely Total Power, Kurtosis and Skewness—could be potential biomarkers to predict and explain concussion and its related symptoms (e.g., balance problems).

Output from heart rate (HR) sensors showed that those with a history of concussion had a higher HR than those with no history of concussion when postural control and balance were also considered. The HR variance was higher for both groups before the balancing/postural control task began in the VR. HR was higher for both groups at the start of the task and may be due to stress regarding the unknown task at hand. However, despite the HR being higher for both groups, the variance was higher for those with a history of concussion. On average, the HR was high in the hands-off part of the VR task and lowered when participants could hold on to the handle in front of them. HR measures have shown potential as an additional measure to potentially index the ANS in reaction to concussion [52], [66], [67]. These results support the possibility that HR rate measures could give added information when mapping out physical markers of concussion.

ML results are promising and demonstrate that concussion can be assessed by the biometric measurements from BioVRSea and SCAT5, especially if combined. The use of only neurophysiological measures allows a decent classification accuracy of almost 73% with RF, which demonstrate the ability of the BioVRSea multi-biometric system not only to evaluate sick and not motion sick people as previously published [156] but also to individuate concussed and not concussed athletes. These results increase if the BioVRSea features are combined with the SCAT5 features. The latter alone can produce an 88.6% accuracy, which is remarkable but not innovative. The novelty of the results is the successful combination of measured and self-reported parameters as seen in Table 3.8 with an accuracy of 95.5%. Furthermore, the combination of these two different measurement approaches provides a novel tool that can be implemented also for monitoring effect of treatment, to develop rehabilitation strategies, or even to support insurance assessment.

Discussing the different algorithmic approaches, we can state that the linear system works better when the SCAT5 features are involved. In [157], SVM was also used for a similar purpose with a larger but unbalanced dataset. Our dataset is smaller and includes fewer features, but they are quicker to assess, and the balanced number of concussed and not-concussed subjects strengthens the obtained classification accuracy. SVM was also successfully performed in [158] for an individual-level concussion detection starting from only EEG features: this can suggest that as a probable future

development of the ML concussion analysis, a focus on more specific EEG features can be performed to understand better how the BioVRSea system can eventually mitigate or improve concussion influence on the brain. The tree-based algorithmic models confirm that the BioVRSea multimetric measurements can be better processed with this approach, like in [156]. The simplified neural network MLP suggests us that a more complicated neural network model can be, with a larger population, worth trying to increase the classification ability of the model.

This study has several important strengths, as well as several limitations. It is challenging to confirm concussions, especially when carrying out a retrospective study. Using medical records to confirm concussion is the gold standard [33]. However, high-risk groups like athletes do not always seek out medical assistance [159], [160]. Medical records could therefore be inaccurate and could result in misclassification of a participants' concussion history. In this study, participants were asked how many concussions they had received after being given a concussion definition. This increases the reliability of self-reporting [120], [160], [161]. A strength is that new technological advances were used to assess concussion symptoms, finding quantitative patterns related to brain, muscles, and CoP which were able to discriminate conditions such as balance problems, difficulty concentrating, pressure in the head, and fatigue/low energy. VR technology was used to provide a secure environment where responses to a postural control task was studied. Finally, the main strength of this work is the multi-faceted approach to assess concussion as recommended in the scientific literature [29].

One limitation to this study is that participants were not asked about prior balancing problems like inner ear problems before they participated. As Manley [146] pointed out there are several methodological limitations in concussion research; one is that most studies do not include the possibility of a third variable affecting the outcome, e.g., substance use, genetics, family history, and mental and cognitive health [146]. In this study, both groups were athletes; some retired and others active, they are all females, and mean age and level of education are similar. Groups are, therefore, well matched in other respects.

As participants were all actively or historically involved in contact sports and as such this is a group at elevated risk for receiving sub-concussive injuries throughout their careers [162], [163]. The comparison between the concussion and non-concussion groups is not a comparison between a concussion group and a normal population. Both groups will likely have received repeated head and body impacts, with possible sub-concussive blows. Sub-concussive blows can result in concussion symptoms, including problems with balance [164], [165] or the neck [166], but neck proprioception is extremely important in postural control. Neck injury not related to a concussion is also a possibility in this groups and should be considered in future studies. Having all participants possibly exposed to injuries affecting postural control and dizziness is both a strength and a limitation. It's a limitations as some participants in the non-concussion group could belong to concussion group, the only clear distinction when placing participants in groups for analysis is their report of concussion history. On the one hand, because the groups are so similarly matched this type of injuries are controlled for. Measures evaluated in this paper could therefore be differentiating between the concussed vs non-concussed.

Hormonal influences were also not studied in this experiment. There is robust evidence in animal models, that higher estrogen and progesterone levels at time of injury can have a neuroprotective effect in the female animal, particularly in the proestrus phase of the cycle [167].

The limited number of participants limits the ML algorithm's predictive capabilities, but the balanced number of concussed and not-concussed subject is a strength. Recruitment of more participants in the future could improve the results in terms of accuracy, and more complicated algorithmic models can be implemented.

## 3.2 Assessing Early Stage Parkinson's Disease Using BioVRSea

Adapted from [2].

### 3.2.1 Abstract

Parkinson's Disease is among the most prevalent neurological diseases in the world today. Typically characterised by cognitive problems and impairments in motor function, there remains no known cure for the disease. Treatments generally take the form of medication and/or surgical intervention in combination with physical therapy. Deficits in postural control are commonly seen in Parkinson's sufferers. Our work using the unique BioVRSea setup aims to assess early-stage Parkinson's using a combination of neurophysiological (Electromyography and Heart Rate) and centre of pressure (or sway) measurements. Eleven early-stage Parkinson's subjects and 46 healthy over-50s took part in the experiment. Significant differences were found between the two groups in electromyographic and centre of pressure measurements. Correlation analysis indicated opposite correlations in skewness in the right soleus muscle. Finally, machine learning was able to predict with a maximum of 94.6% accuracy whether a subject belonged to the healthy or Parkinson's group based on their measurements from the experiment. Our results are a first step in a prototype of the quantitative evaluation of early-stage Parkinson's.

### 3.2.2 Introduction

Parkinson's disease (PD) is a progressive neurodegenerative disorder caused by the loss of dopaminergic innervation of the basal ganglia. The disease has a high global prevalence, with approximately 1% of those over 60 suffering from PD [168]. No cure is available for PD, clinical intervention is made with intention to manage the symptoms of the disease through medication, surgery and/or physical therapy. There is a constellation of PD symptoms, however often the first noticeable signs of the disease are apparent in the motor system. The main motor symptoms of PD are resting tremor, bradykinesia, rigidity and/or postural instability. Diagnosis of the disease is made on the presence of two of these four clinical features, with histopathological confirmation being the only definitive diagnosis of the PD [9]. Lack of adequate postural control is a hallmark feature of those suffering with PD, especially as the disease progresses. Parkinson's patients are therefore prone to falls, the likelihood of which increases with the severity of the disease [169]. Maintenance of human upright posture is a naturally unstable state requiring constant dynamic feedback from somatosensory, vestibular, and visual systems to maintain equilibrium and provide proper alignment of body parts with respect to gravity. Physiological correlates of postural control have been reported, predominantly using Centre of Pressure (CoP) features such as displacement, velocity, and frequency of sway during quiet stance or dual-task performance. Those suffering from PD show differences in CoP parameters and balance strategies compared to healthy groups [170]–[172]. Virtual reality (VR) has been used successfully in the assessment of balance in PD patients [173]. We have built a special measurement environment known as BioVRSea, using VR, a moving platform and acquisition of multiple biosignals (see [156] and Fig. 3.9). In this paper, we measure neurophysiology (elec-

tromyography (EMG) and heart rate (HR)) and CoP responses of 11 early-stage PD patients (both with and without postural instability) and 40 healthy participants over the age of 50. Our hypothesis is that the response of the participants to BioVRSea will be different between the PD and healthy groups. This can be visualized using correlation matrices of the quantities measured in the experiment (EMG, HR, and CoP) in the PD group and the healthy over -50s group. Machine Learning is also useful in this case to try to correctly classify the participants into PD and healthy groups and to extract the most important features from our measurements for this prediction. Identifying features where PD sufferers differ in their responses from healthy controls may provide insight into routes for targeted rehabilitation and training to improve postural control and other symptoms experienced through illness. Studies demonstrating the utility of machine learning in PD have been published [174], including one that has been used to monitor the impact of rehabilitation on a group of PD sufferers, with clearly quantifiable differences between pre-rehab and post-rehab measurements [175], and even a study reporting the link between cognitive impairment and gait patterns of PD patients, using machine learning [176].

### 3.2.3 Methods

#### 3.2.3.1 Participants

Eleven early-stage PD participants (9 male, 2 female,  $62.3 \pm 12.4$  years) and 46 healthy controls over-50 (20 male, 26 female,  $55.7 \pm 11.6$  years) took part in the BioVRSea experiment. All PD participants were taking the drug Levodopa.

#### 3.2.3.2 Written Information and Informed Consent

All participants were provided with written information about the study prior to signing a declaration of informed consent document. The study protocol was approved by the Icelandic National Bioethics Committee (no: 17-183-S1).

#### 3.2.3.3 Virtual Reality Experiment

The participants were prepared for the VR and physiological measurement part of the experiment. This involved the placement of six wireless EMG sensors on the tibialis anterior (TA), gastrocnemius lateral (GL), and soleus (S) muscles of each leg and a heart rate sensor strapped around the chest. The participant was instructed to step onto the force plates on the platform after removing his/her shoes. The position of the feet was in bipedal stance with feet hip width apart, while standing on the force sensors. Finally, the participant dons the VR goggles. The experimental protocol was then explained to the participant. The explanation included that they should stand quietly on the platform with their hands by their side observing a mountain view for the first 2 minutes of the experiment. Then, the scene in the VR goggles would change, beginning the sea simulation. The participants were instructed to remain standing quietly with their hands by their side for the first 35 seconds of the sea simulation. There was no platform movement in this part of the experiment, and it is called the PRE phase of the experiment. After 35 seconds of quiet standing watching the sea simulation, the participant was instructed to hold onto the bars in front of them. The platform then began synchronized movement with the sea scene in the VR goggles, with 25%, 50% and 75% of maximal wave amplitude. In this central part,



### 3.2. ASSESSING EARLY STAGE PARKINSON'S DISEASE USING BIOVRSEA47

each segment lasted 40 seconds and the participant held the bars of the platform while continuing to observe the sea simulation. Finally, the platform stopped moving and the participant was asked to remove their hands from the bars and attempt to stand quietly with their hands by their side for the final 40 seconds of the experiment. The sea scene was still observed by the participant for the final 40 seconds. This is called the POST phase of the experiment; it is performed identically to the PRE phase but after the participant has performed movement in the central part of the procedure. In previous work, we have compared the identical PRE and POST phases in order to determine how well different populations can perform unassisted standing under conditions of sensory conflict after exposure to the complex postural control task of the moving platform and VR scene [1]. As previously stated, our hypothesis is that the response of the participants to BioVRSea will be different between the PD and healthy groups, in this case we look across all phases of the experiment. Fig.3.9 shows a schematic of the experimental setup. Each participant took part in a single trial according to the experimental protocol. Measured data was post-processed in Matlab and analysis was made in all phases of the experiment. Each analysis pipeline for a particular measurement is explained below.

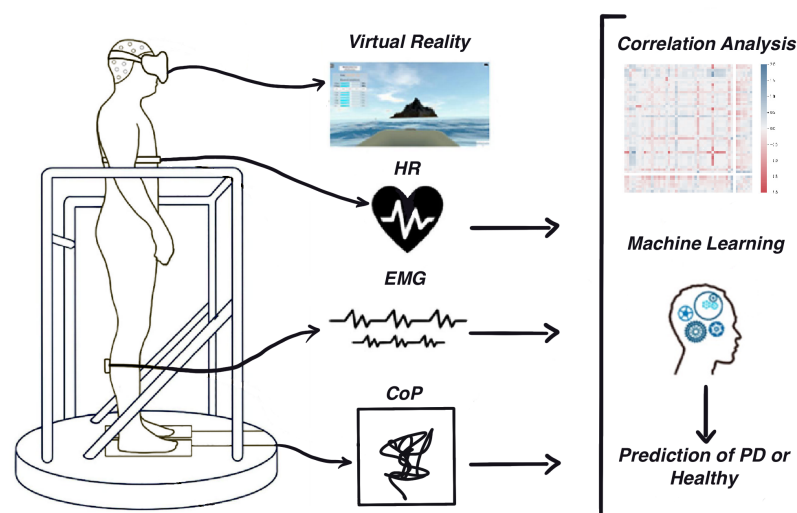


Figure 3.9: Setup and Graphical Abstract.

#### 3.2.3.4 HR Analysis

Heart rate was measured using a chest heart sensor (Polar Electro, Kempele, Finland, sampling frequency 1000 Hz). The HR was sampled at 1Hz and the average HR for each section of the experiment was calculated.

#### 3.2.3.5 EMG Analysis

Muscle electrical activities from the lower limbs were acquired using six wireless EMG sensors (sampling frequency of 1600 Hz) placed on the tibialis anterior (TA), gastrocnemius lateral (GL), and soleus (S) muscles of each leg (Kiso ehf, Reykjavik, Iceland). EMG data processing was performed using Matlab 2021b. EMG data were filtered

using a 4th-order Butterworth filter. Seven features were computed in the frequency domain and thirty-six features in the time domain. These features are listed in the appendix.

### 3.2.3.6 CoP Analysis

CoP measurements were made using 4 sensors located under each foot platform. The sensors give information about the center of mass in the Antero-posterior and Medio-Lateral axis (Virtualis, Clapiers, France, sampling frequency 90Hz). The processing of the CoP data was performed using Matlab 2021b. During the experiment, the force platform records the movement of the Centre of Pressure (CoP), a projection of the center of mass of the subject on the plane of the machine, also called stabilogram. The CoP data was filtered with a Savitsky-Golay filter with window size 7. Included in the CoP analysis were a number of multiscale entropy measurements, which have been shown to have great importance in the analysis of CoP data in discriminating between pathological subjects [177]. Multiscale entropy measurements include features such as complexity index (CI), which indicate the complexity of the CoP signal as calculated using multiscale entropy methods. We extract several parameters from the stabilogram for evaluating the postural control response of the subject during the experiment. The list of features extracted from the CoP is outlined in appendix.

### 3.2.3.7 Correlation Analysis

The correlation matrix for a given biosignal and for a given phase was calculated using the pair-wise correlations between features for this biosignal in this phase. The correlation score used was the Pearson correlation coefficient. It is computed following this formula :

$$\rho_{x,y} = \frac{cov(X,Y)}{\sigma_x \sigma_y} \quad (3.1)$$

Correlation matrices from the healthy group and the PD group were then subtracted from one another in order to highlight the most prominent differences between the two groups for a given feature and stage of the experiment.

### 3.2.3.8 Statistical and Machine Learning Analysis

P-values for all the features of EMG, CoP and HR in all the tasks (baseline, PRE, 25%, 50%, 75%, POST) were computed to see if there are statistical differences between PD and healthy participants. The features are quantitative measurements and condition is qualitative (2 conditions: Healthy or PD). The Student t-test was used for normal distribution and Mann-Whitney test for non-normal distribution to test for statistically significant differences between the two groups. A number of different machine learning classification algorithms were applied in order to find one that could maximize the possibility of distinguishing the healthy group and the PD group. The algorithms were: Medium Tree-based, Logistic Regression, Gaussian Naive Bayes, Subspace Discriminant, Medium Neural Network, and weighted k-Nearest Neighbour.

Machine learning was carried out in Matlab using the Classification Learner App from Statistics and the Machine Learning Toolbox.

### 3.2.4 Results

#### 3.2.4.1 Heart Rate Results

Heart rate results did not show any significant differences between the two groups and will not be discussed further in this paper.

#### 3.2.4.2 EMG and CoP Results

Comparisons were made between the correlation matrices for the PD and healthy groups for each measurement (EMG, HR and CoP), and in each phase of the experiment, including also the differences between each phase of the experiment, e.g. POST-PRE to compare net postural control response following the sea simulation. EMG results from the soleus muscle taking the difference between the responses from the POST and PRE stages showed skewness of the signal to be oppositely correlated with other parameters when comparing the healthy and PD groups, see Fig. 3.10. The CoP results showed that Complexity Index (CI) in the medio-lateral direction in the POST stage was one of the most important features showing a significant difference between the two groups (see Fig. 3.11).

#### 3.2.4.3 Machine Learning Results

Statistical analysis and Machine Learning was carried out using Matlab. There are 11 features from our neurophysiological assessment that have a p-value  $< 0,001$  (99,9% confidence that there are significant differences between Healthy and PD patients). We used these 11 features as the basis for the consequent machine learning analysis. We split the sample randomly four times (70% train data, and 30% test data). ML analysis was able to discriminate between the healthy and PD group using 11 features from the measurements made (10 features from the CoP and 1 from the EMG) which had p values  $< 0.001$  and a weighted k-nearest-neighbour algorithm. Our analysis obtained a maximum of 94.6% accuracy, 85.4 % recall (correctly classifying PD), and specificity of 97.7 (correctly classifying healthy participants). The 11 features are listed in Table 3.5. Table 3.6 shows an overview of the algorithms used in the machine learning analysis and their respective results.

### 3.2.5 Discussion

Our hypothesis was that the physiological response of the participants to BioVRSea will be different between the PD and healthy groups. We showed this using correlation matrices of the quantities measured in the experiment in the PD group and the healthy over -50s group. Statistical analysis also showed very significant ( $p < 0.001$ ) for 11 features from our measured data set. Machine Learning was able to classify the participants into PD and healthy groups, achieving a maximum of 94.6% accuracy using the dataset acquired during the BioVRSea experiment. Considering the measured signals in the experiment, EMG analysis showed opposite trends in regard to the right soleus muscle when comparing the net response of healthy and PD participants. The soleus muscle is an important plantarflexor muscle (to extend the foot) and is crucial

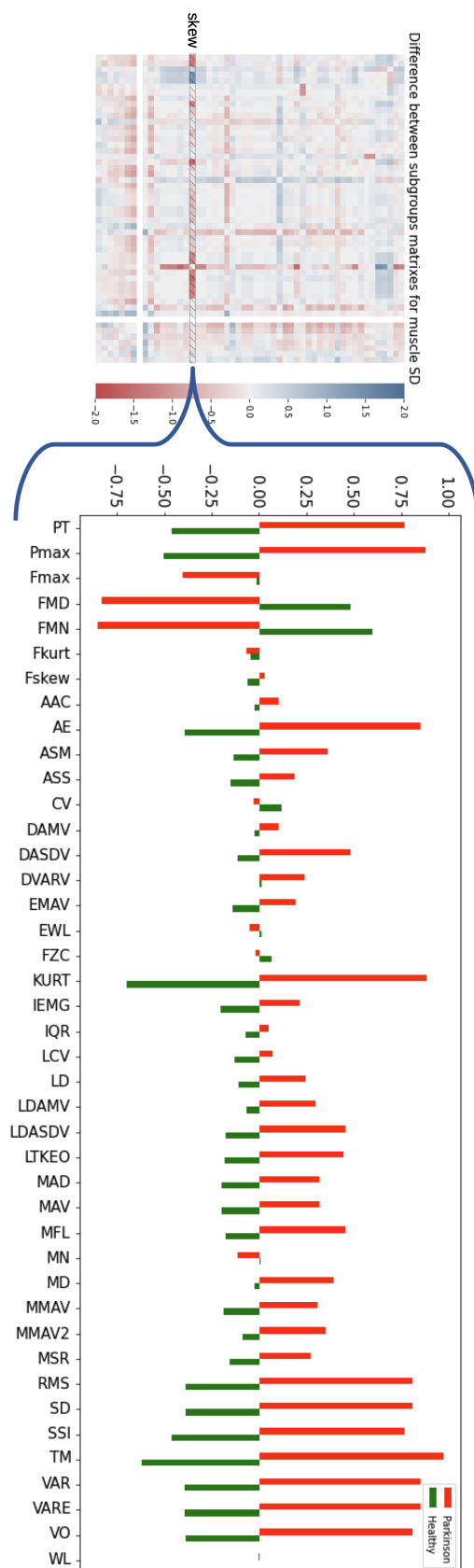


Figure 3.10: Skewness of the EMG signal in the right soleus muscle showed opposite correlations for each group for all but two features calculated

Algorithm	Accuracy	Sensitivity	Specificity
<b>PCA Features (9)</b>			
RF	72.7	68.4	76.0
SVM	61.4	30.8	92.0
ADA-B	68.2	57.9	76.0
MLP	70.5	63.2	76.0
GB	63.6	73.7	56.0
<b>SCAT5 Features (22)</b>			
RF	88.6	84.2	92.0
SVM	88.6	84.2	92.0
ADA-B	84.1	73.7	92.0
MLP	81.8	89.5	76.0
GB	77.3	78.9	76.0
<b>PCA + SCAT5 Features (31)</b>			
RF	90.9	89.5	92.0
SVM	95.5	94.7	96.0
ADA-B	93.2	94.7	92.0
MLP	90.9	96.0	86.0
GB	79.5	78.9	80.0

Table 3.4: Machine Learning Results with SCAT5, PCS and SCAT5 and PCA combined.

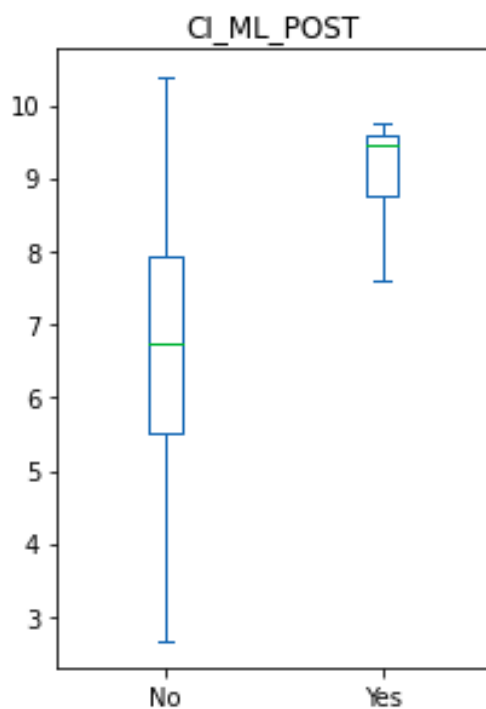


Figure 3.11: Complexity Index in the Medio-Lateral Direction in the POST phase of the experiment comparing healthy (No) and PD (Yes) groups

Table 3.5: Most Significant Features for Machine Learning Prediction

Total Power in POST-Baseline in Left TA
Mean ML distance in POST
RMS distance in ML POST Task
Sample Entropy in ML in 50%
Sample Entropy in ML in POST
Complexity Index in ML in 50%
Complexity Index in ML in POST
Minor Axis Ellipse in POST
SD in ML in POST
Multivariate complexity index in POST
Right magnitude in 75%

Table 3.6: Machine Learning Results

<b>Algorithm</b>	<b>Accuracy</b>	<b>Recall</b>	<b>Specificity</b>
Tree Medium	80.4%	54.2%	90.8%
Logistic Regression	87.5%	75%	91.1%
Gaussian Naive Bayes	92.9%	79.2%	97.7%
Weighted kNN	94.6%	85.4%	97.7%
Subspace Discriminant	87.5%	81.3%	92.1%
Medium Neural Network	94.6%	85.4%	97.9%

in its function as an active agonist muscle in maintaining upright postural control to keep the body from toppling forward [178]. Our results show that the skewness of the signal from the right soleus muscle is oppositely correlated with the other parameters when comparing the PD and healthy over-50s group. Although there is no direct physiological meaning known for this particular statistical feature of a signal, it is interesting that a muscle so heavily involved in upright postural control shows completely opposing trends when comparing the POST-PRE (net postural response) of the two groups. CoP Analysis revealed significant differences in 10 features, the most significant of which is the difference in CI in the medio-lateral direction in the POST phase of the experiment. Decreases in complexity of CoP signal have been documented in pathological subjects (multiple sclerosis specifically) previously, in addition to those who are aging [177]. Our results however indicate the opposite trend, a higher CI in the pathological group. Gait analysis has revealed higher CI for PD compared to healthy controls,[179] however no standing CoP measures have been reported for PD in the literature. Machine learning literature has been actively contributing to the field of PD research in recent years. Our results, using a majority of CoP data relating to a postural control task was able to discriminate between PD and healthy groups with 94.6% accuracy. CoP data used in conjunction with machine learning classification has shown similar accuracy results when comparing Parkinson's disease groups with

healthy controls ([180], [181]). This work is the first prototype of quantitative evaluation of early-stage PD. Even though we only measured 11 patients, analysis of the signals acquired by BioVRSea shows an objective and predictable difference between the PD and healthy groups. It is particularly relevant that our model can predict the early-stage condition of Parkinson's disease. BioVRsea paradigms could be used to monitor a patient's condition and indicate hazardous situations, such as changes in CoP which are associated with an increased risk of falls. [182].

#### 3.2.6 Limitations and Future Developments

The study only recruited 11 PD patients. It is difficult to draw very robust statistical conclusion from such a small group of measurements, however our intention is to continue to enroll more PD patients and follow-up those who have already been measured to see the evolution of the features measured throughout the course of the disease. Our feature selection is based on p-values, which is not an ideal way to select the features for input to machine learning algorithms. However, we chose this method as an initial dimensionality reduction method, and the results were good compared to no feature selection. Of course, there may be other, non-linear relationships that are not captured with this method of feature selection. EEG was also acquired during the experiment and has not been analysed yet. it would be interesting to include the whole battery of neurophysiological data in order to strengthen our results.

### 3.3 Adaptation Strategies and Neurophysiological Response in Parkinson's Disease: BioVRSea Approach

Adapted from [3].

#### 3.3.1 Abstract

There is accumulating evidence that many pathological conditions affecting human balance are consequence of postural control (PC) failure or overstimulation such as in motion sickness. Our research shows the potential of using the response to a complex postural control task to assess patients with early-stage Parkinson's Disease (PD). We developed a unique measurement model, where the PC task is triggered by a moving platform in a virtual reality environment while simultaneously recording EEG, EMG and CoP signals. This novel paradigm of assessment is called BioVRSea. We studied the interplay between biosignals and their differences in healthy subjects and with early-stage PD. Despite the limited number of subjects (29 healthy and 9 PD) the results of our work show significant differences in several biosignals features, demonstrating that the combined output of posturography, muscle activation and cortical response is capable of distinguishing healthy from pathological. The differences measured following the end of the platform movement are remarkable, as the induced sway is different between the two groups and triggers statistically relevant cortical activities in  $\alpha$  and  $\theta$  bands. This is a first important step to develop a multi-metric signature able to quantify PC and distinguish healthy from pathological response.

#### 3.3.2 Introduction

Parkinson's Disease (PD) is a progressive disorder of the nervous system characterized by muscle tremors, muscle rigidity, decreased mobility (bradykinesia), stooped posture, slow voluntary movements, and a mask-like facial expression. It may take time to diagnose because some of its symptoms are associated with the natural process of aging [72]. Globally, disability and death in PD are increasing faster than any other neurological disorder. The World Health Organization (WHO) reports that the prevalence of PD has doubled in the past 25 years and world estimates count over 8.5 million individuals with PD in 2019. In people with early-onset PD, the initial symptoms can arise between the ages of 21 and 40 years, while the first symptoms in juvenile-onset disease occur before the age of 20 years. Nowadays, a standard criterion in the evaluation of PD is still one of the main goals for clinicians. Finding the right category for the progression of the disease is necessary to prescribe the best treatment. Specific signs, symptoms, or test results can help in the classification of the disease. Over the years, accuracy has been improved by new diagnostic protocols that consider qualitative and quantitative aspects [183], [184]. Defining early-stage Parkinson's subjects when the symptoms are silent or weak remains a challenge. PD stages are identified based on clinical observations: according to the Hoehn-Yahr staging system, stages are based primarily on motor symptoms [75]. Pre-Clinical is characterized by the absence of signs or symptoms - genetic testing and counselling are available to identify risk factors. Prodromal corresponds to a stage of neurodegenerative changes. Symptoms are unspecific but the identification of early changes allows to intervene with initial



therapies. Early-Stage symptoms include mild tremors and some walking difficulty. It can affect only one side of the body and produce a decrease of facial expressions. These symptoms do not interfere with daily life much and are not always obvious [75]. In the middle stages, balance and coordination are affected: a moderate-to-severe disability that affects daily life [75]. Later-Stage PD subjects have difficulty standing and walking even with aids. Patients in this stage have severe disability [75]. Fig.3.12 reports the general classification of PD stages according to its main symptoms. A

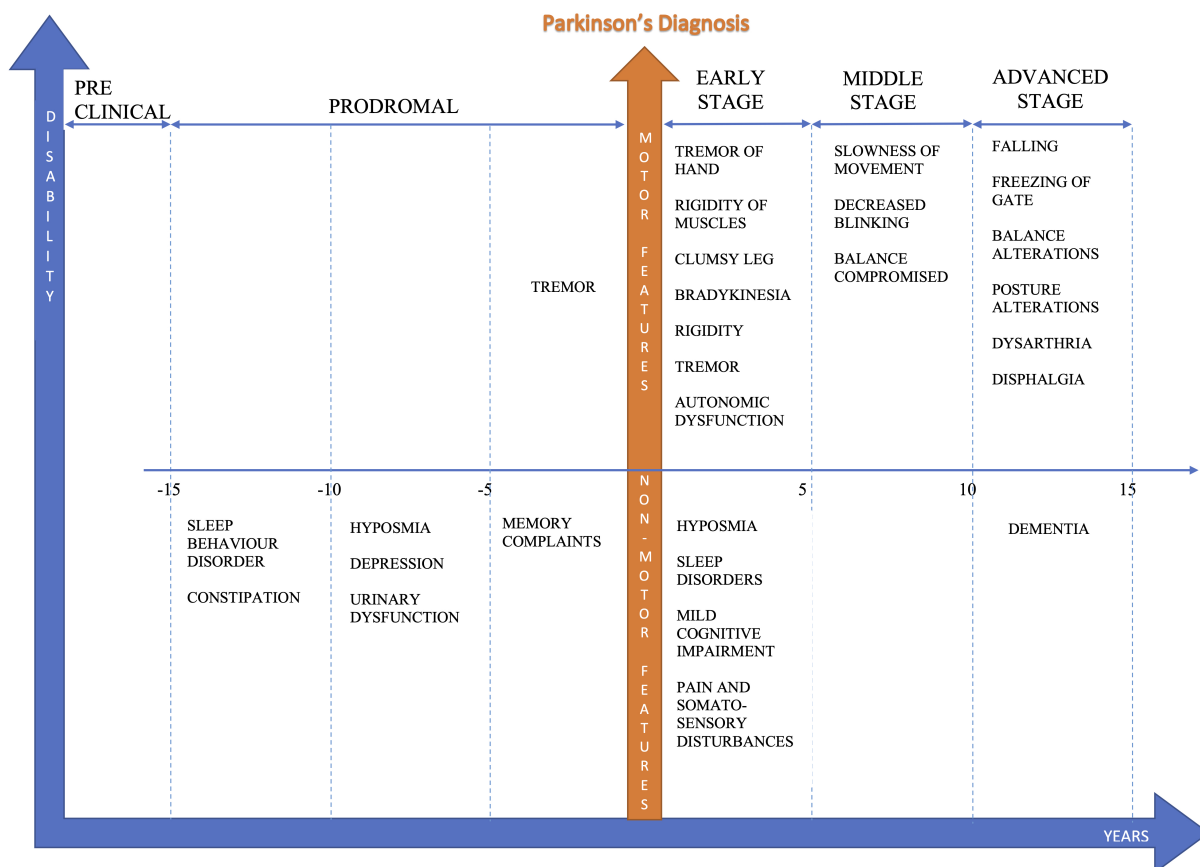


Figure 3.12: Symptoms and Stages before-after Parkinson's diagnosis

preliminary analysis can be carried out by clinicians taking into account qualitative and quantitative aspects of PD, as shown in Fig.3.13 below.

Mobility and gait impairment is also seen to evolve with the progression of the disease are included as parameters of investigation. Issues with gait initiation, freezing of gait, reduced balance, and difficulties in postural control [185] are some of common symptoms. Table 3.7 summarizes the main tests used in mobility and gait analyses. Among the innovative techniques, blood tests show potential to be used for the detection of early-stage PD.

Researchers identified a molecular profile that defines the disease but it is still under investigation and not yet available clinically [186].

In recent years, non-invasive neuroimaging techniques have become more accurate for the detection of differences in brain morphology and functional activities in Parkinson's subjects [187]. Brain positron emission tomography (PET) can estimate the disease progression and can be used to confirm the clinical diagnosis of PD. With specific radioactive drugs (18F-DOPA and 18-FDG) absorbed into the bloodstream, PET can provide very precise brain region and activation in PD subjects [188]. Single

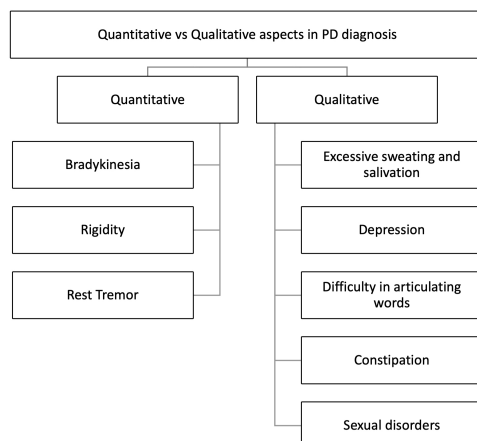


Figure 3.13: Quantitative and Qualitative Aspects in Parkinson Disease Diagnosis [184]

Table 3.7: Gold standard tests for assessing gait ability

ASSESSMENT	TEST	PARAMETER INVESTIGATED
Balance	Timed Up and Go Test Tinetti Balance and Gait Test Retropulsion Test One-leg Stance Åstrand-Rhyming protocol during Graded Exercise Test Balance Evaluation System Test Mini Balance Evaluation Systems Test Berg Balance Scale	Functional mobility Static and dynamic balance Postural stability Static balance Dynamic balance Balance Systems Dynamical balance Static and dynamic balance
Endurance	2-min Walk Test 6-min Walk Test Two-minute Step test Modified Bruce Protocol during Graded exercise test Åstrand-Rhyming protocol during Graded exercise test Borg Ratio Scale	Functional capacity, walking ability Physical capacity and gait Aerobic capacity Cardiac functional capacity Maximal functional capacity Physical capacity
Resistance	Handgrip Strength Test Isokinetic Strength Test Manual Muscle Test  Arm Curl Test Chair Stand Test Five Time Sit to Stand Test One Repetition Maximum Test	Upper limb strength Upper/lower limb strength Individual or grouped muscle strength Upper limb strength Lower limb strength Lower limb strength Maximum lower or upper limb isotonic
Flexibility	Goniometer Inclinometer Leighton flexometer Sit and Reach Test  Back Scratch Test	General Joint Flexibility Angles of slope measurement Joint flexibility Lower back and hamstring muscles tightness Shoulder range of motion

Positron Emission Tomography (SPECT) is also used as method to confirm a Parkinson's diagnosis by highlighting cerebral blood flow and dopamine transporters in the

brain [188]. In patients with Parkinson's disease, a distinct intensity pattern can be noted in the brain region that is deeply affected by degeneration, namely the basal ganglia that controls movement. Magnetic resonance imaging (MRI) is also used to diagnose PD in early onset subjects. MRIs can show small changes and damage in the brain tissue that can indicate PD. Often, these markers are present even before symptoms of PD begin. Transcranial sonography (TCS) has been established as a valuable supplementary tool in the diagnosis of PD. Alterations in the area of the hypochogenic mesencephalic brainstem can be visualized in about 90% of PD patients, which is measured planimetrically to determine the magnitude of the change [189]. Increased iron levels contribute to this sonographic abnormality and indicate that iron can be responsible for the change in the echo signal. Iron accumulation can be a very early indicator in the pathogenesis of PD. Electroencephalography (EEG) can detect damage in the central nervous system and alterations in neurophysiological activity associated with PD. In recent studies, quantitative analysis of EEG data identified significant differences in PD patients versus healthy subjects. In particular, the anterior cingulate and temporal lobe are areas with an established pathology in PD. Changes in cortico-cortical and cortico-thalamic coupling were observed as excessive EEG beta coherence in PD patients [79].

Map structure and functions of the brain are obtained measuring the signals produced by neural activity. Each region can have a particular influence according to the disease and the activation of an area can be considered important in the understanding of the progression of the disease. Although cortical EEG coherence can serve as a reliable measure of disease severity, the use of EEG to study PD has not been fully investigated. Neurophysiological signals provide instantaneous information and can aid in improving the accuracy of the diagnosis.

EEG signals have different specific frequency bands. Features in sub-bands are particularly important to characterize different brain states. The standard frequency bands of interest are  $\delta$ -band (0–4 Hz),  $\theta$ -band (4–8 Hz),  $\alpha$ -band (8–13 Hz), and  $\beta$ -band (13–30 Hz). Moreover, the quantification of EEG rhythms could provide an important biomarker for different neuropsychiatric and neurological disorders, such as schizophrenia, Alzheimer's disease, epilepsy, and Parkinson disease [80]–[82]. The combination of new analysis methods and EEG signal processing can contribute to the detection of early-stage PD. EEG reveals more important information underlying brain dysfunctions, which would be lost if analysis were restricted to traditional methods. Nowadays, many novel methods are suggested for EEG signal processing.

A recent study analyzed the EEG signals from 15 early-stage PD patients and 15 age-matched healthy controls during eyes-closed resting state [83]. Most EEG electrodes showed an increase in  $\theta$ -band relative power for PD patients, while several other electrodes decreased, such as in the frontal and occipital cortex (Fp1, Fp2, F7, F3, Fz, Oz). Moreover, an increase in  $\delta$ -band relative powers were reported, and a decrease in  $\alpha$ -band and  $\beta$ -band relative powers for PD patients compared with healthy patients. Other studies present higher spectral power in the low frequency domain of EEG, compared with controls. Also in these cases, subjects were in the resting awake condition with the eyes closed [84], [85].

Postural Control (PC) and adaptation are part of a complex system to maintain or restore balance from any position or during motor activity. The central nervous system is fundamental in PC strategies and electroencephalography can underline the different cortical brain activities under different postural perturbations [16], [86]. PD usually interferes in this regulatory system, as can be clearly demonstrated by most motor

EEG in resting state (no visual or movement stimulations)	Statistical Tools	$\delta$ -band (0–4 Hz)	$\theta$ -band (4–8 Hz)	$\alpha$ -band (8–13 Hz)	$\beta$ -band (13–30 Hz)	Notes
Eyes Closed	AR Burg method Bonferroni correction	↑	↑	↓	↓	Electrodes activity decreased in the frontal and occipital cortex
Eyes Closed		—	↑ Frontal channels	—	↓ Posterior channels	Power in central and parietal channels decreased
Eyes Closed subject awake sitting comfortably	CNN T-test	↑ in 3.5-4.5Hz Right frontal lobe	—	↓ in 7.5-11Hz Left occipital lobe	—	
Eyes Open & Eyes Closed	ANOVA	↑	↑	↓	—	
Awake patients asked to minimize eye and body movement	ANOVA	↑	↑↑	↑ in 8-10Hz ↓ in 10-13Hz	↓	

Figure 3.14: ASP Bands Analysis in different studies [83], [190]–[193].

symptoms, but to date, no study has yet been conducted on the analysis of postural kinematics in movement disorders. Our aim was to (i) investigate the postural strategy adopted in PD individuals and in healthy subjects; (ii) describe adaptation and how the brain adapts to the induced movement of a platform and visual stimuli using virtual reality (VR). However, postural control and adaptation have been extensively studied in healthy and blind subjects. In a recent study [16], postural kinematics from HD-EEG have been measured during a postural perturbation applied to calf muscles. The main changes in cortical activity were found in Absolute Spectral Power (ASP) over four frequency bands. For postural adaptation, increases in the  $\theta$  band in the frontal-central region for closed-eyes trials, and in the  $\theta$  and  $\beta$  bands in the parietal region for open-eyes trials were reported. In habituation of the stance, no significant variations in ASP were observed during closed-eyes trials, whereas an increase in the  $\theta$ ,  $\alpha$ , and  $\beta$  bands were observed with open eyes [87]. Furthermore, open-eyed trials generally yielded a greater number of significant differences across all bands during both adaptation and habituation, suggesting that cortical activity during postural perturbation may be regulated with visual feedback. This clearly shows a correspondence in cortical activity and postural kinematics during postural perturbation, and could also be developed for pathological postural control.

Other studies show similar results in healthy subjects, suggesting cortex activity as the main change in the frontal-central and frontal-parietal cortical regions during balance perturbation, specifically within  $\alpha$  and  $\theta$  frequencies [112], [151]. Moreover, the increase of the ASP in the central region is demonstrated during high-demand postural correction, such as balance maintenance without allowing corrective foot placement [16]. In accordance, the increase in  $\theta$  activity in the frontal-central regions implies the processing of postural stability during balance control. Thus, ASP differences in the  $\theta$

band signify the planning of corrective steps and the analysis of the consequences of the subject falling. Instead, the significant differences in the  $\alpha$  band reflect an inhibition of error detection within the cingulate cortex due to habituation. Other studies have been carried out with the blind (including both congenital blindness and acquired blindness). Congenitally blind subjects had poorer postural control (anterior-posterior and medio-lateral body swing) compared to sighted subjects. They use a more efficient mechanism for maintaining balance control through joint stiffness. These findings demonstrate that motor coordination, localization, or perception of body segments and movements in visually impaired individuals can be compensated by enhancing the proprioceptive and vestibular systems. Blindness leads to impaired postural balance and imbalance in static and dynamic tasks [194].

Our novel BioVRSea setup introduces a unique multi-biometric system that combines virtual reality and a moving platform to evaluate the postural control response. The system is designed to imitate the sensation of being at sea on a small boat, a situation which involves different balancing strategies. During the experiment, there are six phases (see Table 2.1 Fig.2.1) in which different biosignals are measured such as electromyography (EMG), center of pressure (CoP), and electroencephalography (EEG). Some of our recent studies emphasize the importance of BioVRSea setup allowing cohort differentiation and pathology assessment [106], [156]. The advantage of using BioVRSea is that we are measuring quantitative signals associated with postural control in a challenging environment. The experiment is a prototype and the purpose of the current research with BioVRSea is to gather as much data as possible with many simultaneous measurements in order to extrapolate the most relevant features which could then be used in a clinical setting, with a lower-profile machine that could be accessed easily by those with mobility problems. Current diagnosis of PD relies primarily on the presence of motor symptoms in the patient (such as MDS diagnosis criteria [195] and generally lacks any quantitative measurement such as we perform in the BioVRSea experiment.

### 3.3.3 Methods

#### 3.3.3.1 Participants

Nine early-stage (recently diagnosed) PD participants (6 male, 3 female, between 56 and 76 years of age) and 29 healthy subjects (17 male, 12 female, between 50 and 73 years old) took part in the BioVRSea experiment. Few of them showed physical evidence of early stage PD such as weak tremor or onset of postural instability. All PD patients were taking the drug Levodopa as part of their treatment.

#### 3.3.3.2 BioVRSea Experiment

A 64-channel wet EEG was used record brain response to VR and motion stimulation. Wireless EMG sensors were placed on the tibialis anterior (TA), gastrocnemius lateral (GL), and soleus (S) muscles of both legs. A heart rate sensor strapped around the chest. For the experiment, the participant were asked to stand onto the force plates embedded in the platform. Finally, the participants donned the VR goggles. The experimental protocol was then explained to the participant. Participants stood quietly on the platform with their hands by their side observing a mountain view for the first 2 minutes of the experiment (Baseline). Then, the scene in the VR goggles changed,

beginning the sea simulation but no platform movement. The participants remained standing quietly with their hands by their side for the first 35 seconds of the sea simulation (PRE). After the PRE phase the platform began synchronized movement with the sea scene in the VR goggles, increasing from 25% to 75% of maximal wave amplitude. For a total of 120 seconds the participants held the bars of the platform while continuing to observe the sea simulation. Finally, the platform stopped moving while the sea simulation is still showing and the participant was asked to remove their hands from the bars and attempt to stand quietly with their hands by their side for the final 40 seconds of the experiment. This is called the POST phase of the experiment; it is performed identically to the PRE phase but after the participant has performed movement in the central part of the procedure. A table of the VR experiment protocol is shown below in Table 3.8, shows a schematic of the experimental setup. Each participant took part in a single trial according to the experimental protocol. The subject undergoes different stimuli: visual stimulus (PRE-phase), motor stimulus (movement phase), and balance control (POST-phase). Measured data was post-processed in Matlab and analysis was made in the PRE and POST phases of the experiment. Each analysis pipeline for a particular measurement is explained below.

Table 3.8: BioVRSea Experimental Paradigm

Time (s)	Segment	VR Scene	Position of Hands	Platform
0-120	Baseline	Mountains	by side	Stationary
120-160	PRE	Sea	by side	Stationary
160-200	25%	Sea	on bars	Moving
200-240	50%	Sea	on bars	Moving
240-280	75%	Sea	on bars	Moving
280-320	POST	Sea	by side	Stationary

### 3.3.3.3 Heart Rate

Heart rate was measured using a chest heart sensor (Polar Electro, Kempele, Finland, sampling frequency 1 Hz). The average and standard deviation for the HR for each section of the experiment was calculated.

### 3.3.3.4 EMG Analysis

Muscle electrical activities from the lower limbs were acquired using six wireless EMG sensors (sampling frequency of 1600 Hz) placed on the tibialis anterior (TA), gastrocnemius lateral (GL), and soleus (S) muscles of each leg (Kiso ehf, Reykjavik, Iceland). EMG data processing was performed using Matlab 2021b. EMG data were filtered using a 4th-order Butterworth filter. Seven features were computed in the frequency domain and thirty-six features in the time domain for each muscle and each phase of the experiment. These features are listed in Table 3.10.

**Statistical Analysis** The Shapiro-Wilk test along with visual inspection of the distribution of each variable were used to test the normality of the data. Statistical comparisons between the healthy and PD groups in both the PRE and POST phases were carried out using the t-test with Welch's correction for the normally distributed

variables and the Mann-Whitney U-test for the non-normally distributed variables, with a significance value of  $p < 0.05$ . Effect sizes were calculated through the non-parametric Cliff's delta using the R package 'effsize' [196]. Cliff's delta ranges from +1 if all observations in the first group are larger than all observations in the second group, to -1 if all observations in the first group are smaller than all observations in the second group [197].

### 3.3.3.5 CoP Analysis

CoP measurements were made using 4 sensors located under each foot platform. The sensors give information about the center of mass in the Antero-Posterior and Medio-Lateral axis (Virtualis, Clapiers, France, sampling frequency 90Hz). The processing of the CoP data was performed using Matlab 2021b. During the experiment, the force platform records the movement of the Centre of Pressure (CoP), a projection of the center of mass of the subject on the plane of the machine, also called stabilogram. The CoP data was filtered with a Savitsky-Golay filter with window size 7. Included in the CoP analysis were a number of multi-scale entropy measurements, which have been shown to have great importance in the analysis of CoP data in discriminating between pathological subjects [103]. Multi-scale entropy measurements include features such as complexity index (CI), which indicate the complexity of the CoP signal as calculated using multi-scale entropy methods. We extract several parameters from the stabilogram for evaluating the postural control response of the subject during the experiment. The list of features extracted from the CoP as outlined in the appendix. **Statistical Analysis** Normality was checked through the Shapiro-Wilk test and visual inspection of the variables, and comparisons were made between the healthy and PD groups for all features in the PRE and POST phases using the t-test with Welch's correction and the Mann-Whitney U-test with significance level  $p < 0.05$ . Effect sizes were calculated using Cliff's delta. **Sway profiles** were also outlined using 95% confidence ellipses in PRE and POST, as seen in Fig.3.15.

### 3.3.3.6 EEG Analysis

The CA-204-64 wet electrode cap, Eego™ mylab with sampling frequency of 4096 Hz, measured the brain electrical activity in 64 electrodes. Raw EEG signals were processed using Matlab 2022b, Brainstorm, EEGlab 2022.1 and Automagic toolboxes [125]. The signals were divided in segments for each phase of the experiment, then the signals were down-sampled from 4096 Hz to 1024 Hz. During pre-processing, different settings were applied to the EEG, such as ICA MARA artefact removal and high pass and low pass filters respectively set at 1 Hz and 45 Hz. The data were interpolated finding the locations of bad channels. The EEG data set can be displayed as electrode channel plots, allowing a quick overview of data quality. Then, the absolute power spectral density (PSD) was calculated and compared between PD and Healthy groups in each phase of the experiment for each of the delta, theta alpha and delta bands. A Mann-Whitney U-test with significance level ( $\alpha = 0.05$ ) was used to determine significance. False detection rate (FDR) correction was applied to each electrode.

### 3.3.4 Results

The following results are reported for the analysis of the PRE and POST phases of the experiment with the aim of distinguishing between the PD and healthy groups based on their biosignal responses. Our experiment was able to identify changes in many of the analysed domains.

The protocol is a visual-motor simulation of being on a boat and part of the subjects experienced the feeling of seasickness. Just under half of PD subjects experienced actual discomfort with various symptoms (reported on questionnaires), and a smaller percentage of them reported a self-assessment of motion sickness in daily life.

#### 3.3.4.1 Heart Rate

An increase in beats per minute (bpm) was measured in PD subjects, although not statistically significant. No statistically significant differences were found between groups.

Table 3.9: Average and standard deviation for Heart Rates inside cohorts and between cohorts in PRE and POST phases

Beats per minute (BPM)	Parkinsons	Controls
PRE-phase	88.76 ± 18.09	82.48 ± 14.63
POST-phase	94.19 ± 20.97	82.54 ± 14.35

#### 3.3.4.2 EMG

The right TA muscle showed a number of statistically significant features in the POST phase, with a p value ( $p < 0.05$ ) and the corresponding effect sizes for each variable shown in bold in Table 3.10. The right side could be considered the dominant leg in the prevalence of the group. Significant changes were found also in the left soleus (MN - mean,  $p=0.003$ , cliff delta = -0.64) in the POST phase and the soleus right which had one significant feature (MD -median,  $p=0.007$ , cliff delta = -0.586) in the PRE phase.

#### 3.3.4.3 CoP

**Sway Profile** Fig. 3.15 highlights the CoP evolution between PD and healthy subjects on two of its main characteristics area and axis length of the sway ellipse. Sway is greater in healthy than PD participants.

The only significant feature ( $p < 0.05$ ) for CoP in the PRE phase is the *Direction Entropy (Nats)*, while the statistically significant ones in the POST are listed below with p-values and cliff delta values listed.

#### 3.3.4.4 EEG

The topological plots were computed for all frequency bands during the phases of the acquisition. Each of them displays the difference of power spectral density between PD and healthy cohorts, only for the statistically significant electrodes ( $p \leq 0.05$ , represented by a green point in the figure). Theta and alpha bands presented several significant electrodes in different locations of the brain. In the theta band, significant



Table 3.10: EMG Features - This table shows the features that were significantly different between PD and Healthy groups in the Right Tibialis anterior muscle in the POST phase.

Feature	PRE p-value	POST p-value	cliff delta POST
Maximum Power (Pmax)	-	0.0394	0.464
Average Amplitude Change (AAC)	-	0.0256	0.502
Absolute Value of the Summation of the Exponential Root(ASM)	-	0.0195	0.524
Absolute Value of the Summation of the Square Root (ASS)	-	0.0234	0.0509
Difference Absolute Mean Value (DAMV)	-	0.0256	0.502
Difference Absolute Standard Deviation Value (DASDV)	-	0.0362	0.471
Difference Variance Value (DVARV)	-	0.0362	0.471
Enhanced Mean Absolute Value (EMAV)	-	0.0234	0.510
Enhanced Wavelength (EWL)	-	0.0162	0.0540
Kurtosis (KURT)	-	0.0162	-0.540
Integrated EMG (IEMG)	-	0.0214	0.517
Interquartile Range (IQR)	-	0.0394	0.463
Log Detector (LD)	-	0.0428	-0.02
Log DAMV (LDAMV)	-	0.0256	0.502
Log DASDV (LDASDV)	-	0.0362	0.417
Log Teager Kaiser Energy Operator (LTKEO)	-	0.0394	0.464
Mean Absolute Deviation (MAD)	-	0.0256	0.502
Mean Absolute Value (MAV)	-	0.0256	0.502
Maximum Fractal Length (MFL)	-	0.0362	0.471
Modified Mean Absolute Value (MMAV)	-	0.0234	0.510
Modified Mean Absolute Value 2 (MMAV2)	-	0.0428	0.455
Mean Value of the Square Root (MSR)	-	0.0195	0.524
Waveform Length (WL)	-	0.0256	0.502

Table 3.11: CoP Features Calculated - this table shows the features that were significantly different in the POST phase of the experiment when comparing the PD and Healthy groups

Feature	PRE p-value	POST p-value	Cliff Delta
Square Root Distance between a point and the plane origin (RD)	-	0.0173	0.494
Mean Distance in Medio-lateral Direction (MDIST-ML)	-	0.0339	0.494
Mean Distance in Antero-posterior Direction (MDIST-AP)	-	0.0173	0.494
Root Mean Square Distance respect to origin (RDIST)	-	0.0115	0.540
Root Mean Square Distance in Medio-lateral Direction (RDIST-ML)	-	0.0256	0.517
Root Mean Square Distance in Antero-posterior Direction (RDIST-AP)	-	0.0115	0.533
Medio-lateral Sample Entropy (ML-SampEn)	-	0.0002	-0.709
Medio-lateral Complexity Index (ML-CI)	-	0.0009	-0.793
Ellipse Area	-	0.0083	0.571
Ellipse angle	-	-	0.057
Ellipse Main Axis Length	-	0.0067	0.571
Ellipse Minor Axis Length	-	0.0127	0.571
Standard Deviation in Antero-posterior Direction (SD AP)	-	0.0115	0.532
Standard Deviation in Medio-Lateral Direction (SD ML)	-	0.0257	0.517
SD Magnitude	-	0.0074	0.563
Magnitude Entropy	-	-	-0.510
Direction Entropy	-	-	-0.249
Multivariate Complexity Index (Multivariate CI)	-	0.0128	-0.639
Postero Magnitude	-	0.0141	0.548
Postero Angle	-	-	0.065
Right Magnitude Maximum	-	0.0282	0.448
Right Angle	-	-	-0.494

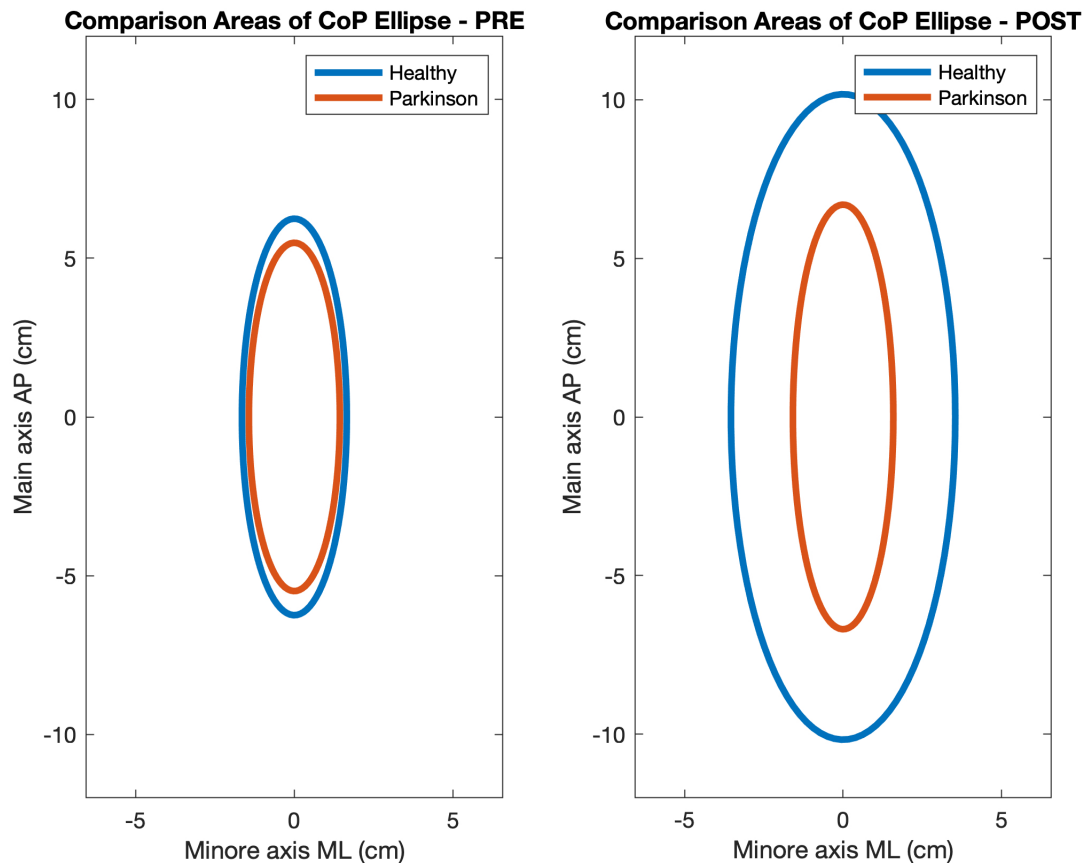


Figure 3.15: Ellipse Areas comparison between Parkinson and Healthy subjects in PRE-POST phases

electrodes are found mostly in the temporal lobe (T7, T8, C6, FT7), one in the frontal lobe (AF3) and one in the occipital (PO6). In the alpha band, significant electrodes are found mostly in the temporal lobe (FC5, T7, T8, FT8), one in the parietal lobe (P4) and one in the occipital (PO6). The p-values of each electrode of the theta and alpha bands are shown in Tables 3.12-3.13, comparing the two cohorts in the PRE and POST phases. They highlight the differences in brain activity in the two phases and underline the significant difference in the POST phase of the experiment between the PD and Healthy groups.

### 3.3.5 Discussion

In previous work, we compared the identical PRE and POST phases in order to characterise different cohorts while they performed unassisted standing under conditions of sensory conflict after exposure to the complex postural control task of the moving platform and VR scene. EEG delta and theta power spectrum analysis and EMG activity in the soleus muscle proved to be strong discriminators between groups [1].

In this paper, we use a similar multi-factorial approach to characterize PD and healthy participants on the basis of their postural control response during the BioVRSea experiment. In particular, we compared the balance response after a visual stimulus only - PRE phase: VR visual sea motion simulation; to the balance response ob-

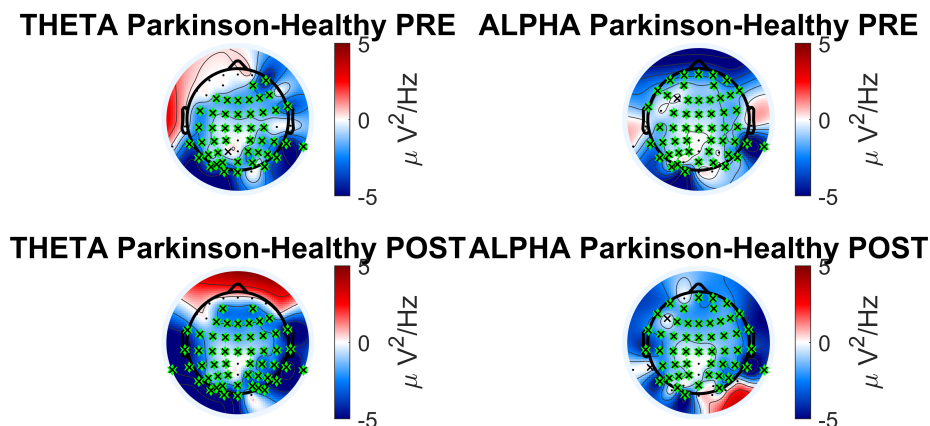


Figure 3.16: Absolute PSD Bands Analysis in Parkinson's vs Healthy cohort for theta and alpha frequency band

Table 3.12: Electrodes for theta band with corresponding p-values comparing the two cohorts in POST and PRE phases - bold shows they were significantly different in the POST phase of the experiment

Electrodes	PRE phase	POST phase
M1	0.124	<b>0.0326</b>
T7	0.0740	<b>0.0169</b>
T8	0.139	<b>0.0215</b>
AF3	0.0947	<b>0.0383</b>
C6	0.0784	<b>0.0247</b>
PO6	0.0983	<b>0.0409</b>
FT7	0.112	<b>0.0476</b>

Table 3.13: Electrodes for alpha band with corresponding p-values comparing the two cohorts in POST and PRE phases - bold shows they were significantly different in the POST phase of the experiment

Electrodes	PRE phase	POST phase
FC5	0.0597	<b>0.0247</b>
T7	0.122	<b>0.0187</b>
T8	0.0703	<b>0.0247</b>
P4	0.0596	<b>0.0391</b>
PO6	0.276	<b>0.0247</b>
FT8	0.0674	<b>0.0165</b>

tained after a complete immersive sensory experience - POST phase: VR visual and correspondent motion stimulation.

This study is part of an extensive work in which a larger population is monitored. We have collected data from 324 volunteers (females 183, males 141, general age  $33 \pm 14$ ). The overall population is between the ages of 18 and 29. Recruiting a larger group of older adults may open a new way to highlight age-related postural control strategies using the same protocol.

### 3.3.5.1 Heart Rate

Although heart rate per minute appears to increase in subjects with Parkinson's from PRE to POST phase, there is no significant result to underscore the difference in the two cohorts.

### 3.3.5.2 Muscle activation

The lower leg muscles are involved in postural and balance control strategies [198]. Different muscles are involved at different times in two cohorts under the same experiment and this may be pathology dependent. The most significant activity was found in the tibialis anterior on the right leg, with some significant activity in the right soleus and the left tibialis anterior. However, only features obtained from the right tibialis anterior (TA) statistically differentiated the two groups. This may be related to the fact that tibialis anterior is the primary dorsiflexor of the foot, and is critical in gait to lift the foot during the swing phase.

We can hypothesize that in the group of subjects considered in this study (Parkinson's and healthy) has overall right-handed prevalence. This is supported in one of the latest reported studies conducted on the human hand, from which it was stated that the precise prevalence is the right hand in the world population. The prevalence of left-handedness is between 10-20% [199]. Thus, we can explain the significant results obtained for the right side through the dominance of the legs.

### 3.3.5.3 Center of Pressure

A common way to evaluate PD is based on gait analysis with accelerometer and force sensors inside the shoe. Gait analysis has revealed higher frequency values for PD compared to healthy controls. However, until now Parkinson was not assessed by measuring the force in a standing position [200].

Our results highlight a reduced sway in PD subjects during the task ant that may be related to a multitude of factors. Some diseases, including PD, interfere in the ability to maintain balance. PD patients have less coordination of agonist and antagonist muscles, making it challenging to maintaining stability. They also frequently suffer from limb and axial rigidity that may reduce mobility [201]. All of those linked to a reduced mobility confidence may account for the reduced sway.

We found significant differences in the POST phase between the PD and healthy cohorts. This is significant as the POST phase is the stage after a motor stimulus and it can be a good index of pathology progression. The most discriminating feature was found to be the complexity index in the medio-lateral direction as seen in Fig. 3.17. The effect size for this variable is also large (-0.793 - the negative value indicating that most of the higher values for this variable were in the PD group) which is classified as a large effect as per [202] which ranks a delta value greater than 0.42 as a large effect. The mediolateral CI in the PD group is higher than in the healthy cohort, which is contrary to a number of studies which show that the complexity of postural dynamics tends to decrease in disease and aging CITE!!!

### 3.3.5.4 Neural response

The strong involvement of the cerebral cortex in postural control responses to perturbation is well-known, but the correlations with pathologies affecting mobility are still

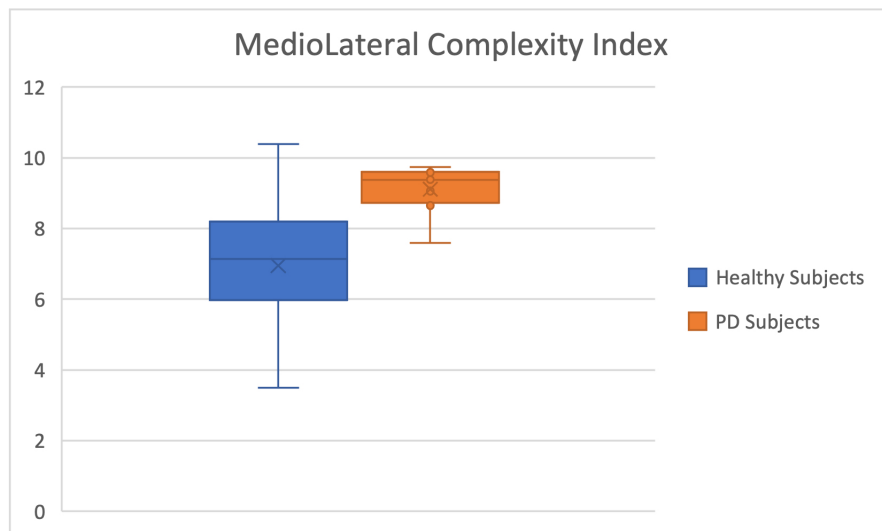


Figure 3.17: Mediolateral Complexity Index of Healthy (Blue) and Parkinson (Orange) Groups

poorly understood [107], [108], [203]. Understanding the network of cortical structures involved in a disease such as Parkinson's and how sensory information are processed can be an important step in diagnostics.

Each band can be associated with a particular neural function and in our research, differences in alpha and theta response prove to be statistically significant when comparing between the two groups. The result for alpha band shows that the activity in the healthy subjects is greater than in the Parkinson subjects in both the PRE and POST phases. On the other hand, the theta band shows different behavior depending on the brain area and phase. Theta and alpha bands are involved in the regulation of the posture, in particular when a visual feedback is altered [204]. Figure 3.16 shows the topological plots of absolute PSD for theta and alpha frequency bands. Each row represents the PSD difference of task (PRE and POST). The PSD differences between Parkinson and healthy subjects are compared for significant electrodes with Benjamin-Hochberd FDR procedure.

**Theta Waves** The theta rhythm is one of the slowest oscillations in the normal waking state, just above the delta rhythm that dominates slow wave sleep. Theta waves are involved in attention and memory processes, especially in memory retrieval episodes [205]. Although the alpha band has been shown to be strongly correlated within postural task conditions, it currently remains less known whether the theta band shows an association with increased postural task difficulty [204]. One of the most recent publications on neurophysiology in healthy subjects showed that the theta band has important electrodes located mainly in the parietal scalp, associated with a slight decrease in PSD [106]. The parietal lobe is activated to plan and process the orientation of the body and sensory information, demonstrating the remarkable role of the theta band in postural strategies.

In our results, parietal activity of the theta band from PRE to POST phase shows a decrease of PSD in healthy subjects, confirming what was found in the work just mentioned. Instead for the frontal lobe, the theta band shows an increased PSD in the healthy group in both tasks. Theta brain rhythms are associated with cognitive and motor functions, and patients with PD would have irregular theta rhythms during lower-limb activations [206].

**Alpha Waves** Different studies have shown that the performance of a generic balance task results in simultaneous changes in the amplitude of alpha oscillations [207], [208]. Alpha activation is associated with cognitive events and has been found to increase during intentional tasks such as mental arithmetic and working memory. Planning actions and their execution also generate alpha [209]. Therefore, alpha waves play a functional role in human cognition and that it does not represent only an 'idling rhythm', as many scientists believed until recently. Maintaining balance is an active process and requires constant awareness of any external stimuli. The alpha band has shown interesting results in postural control studies where a decrease in alpha power was associated with an increased task difficulty during upright stance in young adults [204], [210], [211]. As the PD group has lower overall alpha power (as seen in Fig.3.16, this may indicate higher demand to cope with the balance task compared to the healthy group. In another publication on the neurophysiology of healthy subjects using the BioVRSea experiment [106], the alpha band is important for balance control across the whole scalp. Our study is consistent with these results.

Both the bands (theta and alpha) can be considered parameters to discriminate PD subjects during a complex postural control task and confirm the activation of the frontal, parietal and visual lobe in healthy subjects, underlining the difficulty the PD group experiences when making postural adjustments.





# Chapter 4

## Summary and Conclusion

### 4.1 Summary

In this study, a multifactorial neurophysiological approach was employed to characterize the postural responses of participants during the BioVRSea experiment. The balance responses of participants were analyzed following their performance of an immersive sensory experience following the PRE-MOVE-POST paradigm outlined in the methods section and shown in Fig.2.2. To date over 400 participants have completed the BioVRSea experiment, with pathological cohorts of Parkinson's patients and those who have suffered a sports-related concussion being the focus of this thesis. Recruitment and measurement of these groups allowed for the evaluation of postural control strategies under stressful conditions.

This overarching aim of this thesis is to determine whether a complex task such as BioVRSea that elicits a postural control response that can be measured objectively using neurophysiological means can be used to delineate differences between pathological and healthy groups of participants. This pilot study has clearly shown that this is the case. It is the proposal of the authors of the various studies that make up this thesis that the BioVRSea paradigm is well suited for adaptation to clinical practice, although in a modular (for example, EMG with VR, CoP alone after a perturbation, or other combination) or scaled-down sense.

The BioVRSea paradigm consists of the stages PRE-MOVE-POST using virtual reality and a moving platform to challenge the postural control of the individual in different ways. Firstly, PRE engages purely visual stimulation and causes the subject to adjust posture in response to the scene of a small boat at sea. In this stage of the experiment, the challenge to remaining upright comes purely via the sensory conflict of two competing inputs from the visual and the vestibular systems. Studies using optokinetic stimulation have reported an increase of reported symptoms in vestibular patients compared to healthy controls [212]. Although the study included posturography and all subjects increased their sway during exposure to the visual stimulus, there was no statistical difference in centre-of-pressure measures between patients and their healthy counterparts. Neurophysiological assessments can aid in such cases. A 2020 study involving visual stimulation and base of support manipulations used EEG to detect differences in cortical processing due to a complex balance task [213] in older and younger groups. EEG spectral results showed distinct differences, particularly in tandem stance, between the two groups.

In the second stage, MOVE, the platform and visual seen are coherent, resulting in a visual-motor stimulus to the participant's postural control. This combination can be particularly powerful in determining neurophysiological differences between groups. In a 2014 paper by Baston et al. used the Sensory Organisation Test and a moveable platform to assess the postural control of healthy and parkinsonian subjects. This combination of motor and visual stimulation to challenge postural control was measured using inertial sensors which showed that the healthy groups could modulate their posture using a variety of postural strategies, whereas the parkinsonian groups persisted in a rigid ankle strategy throughout the experiment. [214]

Finally the POST stage results in a standing postural control that is affected by the previous visual-motor stimulation with the BioVRSea platform. In a study looking at the CoP dynamics of PD and healthy participants, [215] the PD group fared worse following an unexpected perturbation (akin to recovery after a motor stimulus) following which they tried to regain balance. The PD group took longer to correct their posture and also experienced higher accelerations following the perturbation. The study even discriminated between PD subtypes, which displayed their own dynamics compared to one another and to healthy controls. This paradigm is useful as it is required in everyday life to react appropriately to external perturbations in order to minimize the risk of fall or injury. Objective assessment of such paradigms are crucial to determine fall risk and quantify any decrease in the quality of life of the individual.

Our concussion study presented a novel concussion assessment method, contrasting self-reported symptoms and neural and postural responses in a BioVRSea environment. We hypothesized that the Icelandic SCAT5 symptoms checklist can distinguish between concussed and non-concussed female athletes, and that changes in CoP, heart rate, EMG, and EEG data can quantitatively measure concussion symptoms. Participants, either with or without a history of concussion, reported significantly different experiences on the SCAT5 scale, despite the non-specificity of symptoms [10], [136]. Notably, concussed athletes reported more symptoms, with headaches being the most common in both groups. Concussion history resulted in a higher severity score for concussion symptoms. CoP features showed significant changes, consistent with previous studies indicating post-concussive alterations in CoP displacement and velocity [137], [138]. We observed differences in TOTEX, RDIST, MVELO, Main Axis, and SD AP, suggesting these could be indicative of postural control impairments [134], [139]–[141]. EEG results showed increased theta band activity in concussed participants, indicating higher cognitive effort during tasks requiring postural control [16], [142]–[151]. EMG measures indicated higher muscle activation in the tibialis anterior (TA) post-concussion, especially in the POST stage. EMG spectral analysis showed significant differences between the PRE and POST stages in the concussion group, with the soleus muscle being particularly discriminative [10], [152]–[155]. Heart rate (HR) data indicated a higher HR in concussed individuals, supporting HR's potential as an additional measure for assessing concussion [52], [66], [67]. In conclusion, our results underscore the effectiveness of neurophysiology measurements to distinguish between athletes based on concussion history and symptoms.

We then applied our BioVRSea paradigm to Parkinson's Disease (PD) and healthy groups. We employed correlation matrices of the metrics recorded during the experiment, comparing the PD group and the healthy over-50s group. Statistical analysis highlighted significant differences ( $p < 0.001$ ) in 11 features from our dataset. Machine Learning (ML) classified participants into PD and healthy groups with up to 94.6% accuracy using the data acquired during the BioVRSea experiment. In examining the

signals measured, EMG analysis indicated contrasting trends related to the right soleus muscle between healthy and PD participants. This muscle, essential for extending the foot and maintaining upright postural control, displayed an inverse correlation in signal skewness with other parameters in the PD and healthy over-50s groups [178]. While the precise physiological implication of this statistical feature remains unclear, it is noteworthy that a muscle crucial for postural control exhibits divergent trends when comparing the POST-PRE (net postural response) between the two groups. The analysis of Center of Pressure (CoP) revealed significant differences in 10 features, most notably in the Complexity Index (CI) in the medio-lateral direction during the POST phase. While decreases in CoP signal complexity have been documented in pathological subjects and the aging population [177], our results indicate a higher CI in the PD group. Previous gait analyses have reported a higher CI for PD compared to healthy controls [179], however, standing CoP measures for PD have not been extensively reported. Our machine learning results, primarily using CoP data related to a postural control task, distinguished between PD and healthy groups with 94.6% accuracy. CoP data, when used in tandem with ML classification, has demonstrated similar accuracy in differentiating PD groups from healthy controls [180], [181]. This study was a preliminary effort in quantitatively evaluating early-stage PD. Despite a limited sample size of 11 patients, the signals acquired via BioVRSea reveal a discernible and predictable difference between PD and healthy groups. The ability of the BioVRSea model to predict early-stage PD conditions is especially significant. BioVRSea paradigms could potentially monitor patients' conditions and identify high-risk situations, such as CoP changes associated with an increased likelihood of falls [182].

Our second publication on BioVRSea and PD characterizes PD and healthy participants using a multi-factorial approach during the BioVRSea experiment. We focused on contrasting postural responses during the purely visual VR sea motion simulation (PRE phase) against those post an immersive visual-motor task (POST phase). Lower leg muscles play pivotal roles in balance and postural strategies [198]. Notably, significant activity was identified in the right tibialis anterior (TA), underscoring its vital function in foot dorsiflexion during gait. The dominance of right-leg results might be attributed to the predominance of right-handedness in the population [199]. Although gait analysis has been instrumental in PD evaluations, standing posture assessments remain relatively unexplored [200]. Our results, particularly from the POST phase, showcased reduced sway in PD subjects, indicative of their challenges in balance maintenance due to factors like rigidity and reduced muscle coordination [201]. Notably, the complexity index in the medio-lateral direction offered significant differentiation between the cohorts (Fig. 3.17). However in contrast to previous studies on pathological groups, the CI index for our PD cohort is higher than the healthy groups. Acknowledging the pivotal role of the cerebral cortex in postural adjustments, we aimed to understand the network's behavior under Parkinson's during the BioVRSea tasks [107], [108], [203]. Both theta and alpha bands yielded significant differences between cohorts, emphasizing their importance in regulating posture especially during altered visual feedback [204]. In the theta band, the evident parietal activity decrease from PRE to POST in healthy subjects echoes findings from previous research [106]. Meanwhile, the frontal lobe exhibited increased PSD in the theta band for the healthy group, with its known associations to cognitive and motor functions [206]. In the context of the alpha band, the consistent reduction in alpha power across various balance tasks highlights its significance in postural regulation [204], [210], [211]. Reduced al-

pha power in the PD group in our study might suggest a heightened cognitive demand during balance tasks.

Ongoing work in our group in feature importance analysis using gradient boosting has revealed some of the most important features for each neurophysiological measurements for the motion sickness prone or not prone groups as determined by participant responses to the questionnaire. EEG PSD features in the frontal beta band in POST and occipital and parietal low gamma band in MOVE and POST were the most important EEG features in the prone group. EMG features in the MOVE phase were very important, particularly in soleus left. CoP features during MOVE and POST particularly directional and angular features were of greatest importance for this group. EEG PSD features in the not prone group have frontal delta band during MOVE, parietal delta band during PRE and alpha frontal during MOVE as their most important features. EMG features from tibialis anterior left and right in the PRE phase, and soleus left and right muscles during the MOVE and POST phases were the most important for the non-prone groups. Finally, sample entropy in POST and antero-posterior angle in MOVE were the most important features for this group. The disparity between the two groups in the most important features is an interesting link with the underlying neurophysiology of their self-reported states. The distinction between the two clearly shows the utility of the BioVRSea paradigm to induce responses that are neurophysiologically detectable and capable of categorizing groups based on their self-reported or suspected state.

Recent work from our lab has shown the potential of using brain network analysis tools to further expand the EEG feature set and understanding of static and dynamic states of the brain during the experiment. [216] combined advanced source-space EEG networks with clustering algorithms to decipher the brain networks states (BNS) that occurred during the BioVRSea experiment. The analysis showed that BNS distribution coincided with the different phases of the experiment with specific transitions between visual, motor, salience, and default mode networks. The study also determined age to be a crucial factor affecting the dynamic transition of a healthy cohort. Fig. 4.1 outlines the pipeline followed to determine BNS.

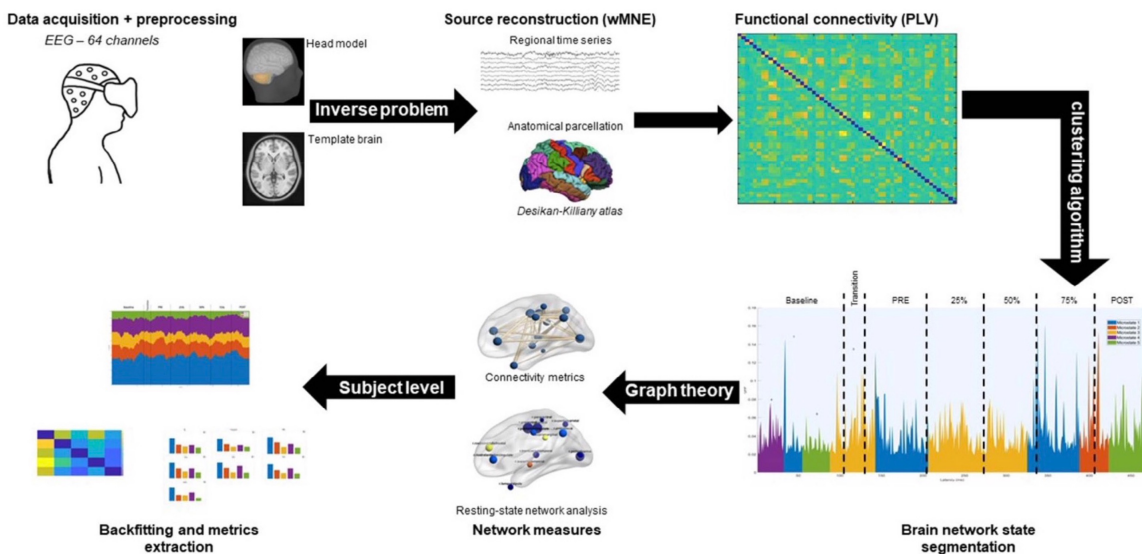


Figure 4.1: Graphic of Workflow for deciphering Brain Network States and Network Measures in Brain Connectivity - reproduced from [216]

Concurrent work using resting state data and brain network analysis from [217] also shows potential in finding new quantitative measures for exploitation in neurophysiological biomarkers of Parkinson's Disease. Future directions for the BioVRSea group will be to expand this brain network analysis to our pathological groups in contrast to the healthy groups in order to determine any potential differences/markers of abnormal functional connectivity behaviour in the participants data. Recruitment is ongoing in both the Parkinson's and concussion subject groups to increase the number of participants and therefore the statistical power of the conclusions drawn from such analyses.

## 4.2 Conclusion

The work outlined in this thesis confirms that the BioVRSea paradigm is effective in differentiating response based on neurophysiological measures. It relates well to self-reported quantities with the potential to be integrated into clinical practice. The BioVRSea paradigm is modular, in that one or more stage from the experiment or one or more neurophysiological measurement may be taken separately from the others in order to be integrated into the clinic. An adapted version of BioVRSea can be appropriately integrated into clinical work of the future to both assist clinicians in diagnosis but also in monitoring and quantifying response to therapies and interventions in neurophysiological disease.



# Bibliography

- [1] D. Jacob, I. S. Unnsteinsdóttir Kristensen, R. Aubonnet, *et al.*, “Towards defining biomarkers to evaluate concussions using virtual reality and a moving platform (biovrsea)”, *Scientific Reports*, vol. 12, no. 1, p. 8996, 2022.
- [2] D. Jacob, R. Aubonnet, M. Recenti, *et al.*, “Assessing early-stage parkinson’s disease using biovrsea”, in *2022 IEEE International Conference on Metrology for Extended Reality, Artificial Intelligence and Neural Engineering (MetroX-RAINE)*, 2022, pp. 271–276. DOI: 10.1109/MetroXRAINE54828.2022.9967502.
- [3] D. Jacob, L. Guerrini, F. Pescaglia, *et al.*, “Adaptation strategies and neurophysiological response in early-stage parkinson’s disease: Biovrsea approach”, *Frontiers in Human Neuroscience*, vol. 17, 2023, ISSN: 1662-5161. DOI: 10.3389/fnhum.2023.1197142. [Online]. Available: <https://www.frontiersin.org/articles/10.3389/fnhum.2023.1197142>.
- [4] T. Paillard, “Effects of general and local fatigue on postural control: A review”, en, *Neuroscience and Biobehavioral Reviews*, vol. 36, no. 1, pp. 162–176, Jan. 2012, ISSN: 01497634. DOI: 10.1016/j.neubiorev.2011.05.009. [Online]. Available: <https://linkinghub.elsevier.com/retrieve/pii/S0149763411001047> (visited on 08/30/2023).
- [5] F. B. Horak, “Postural orientation and equilibrium: What do we need to know about neural control of balance to prevent falls?”, *Age and Ageing*, vol. 35, no. Suppl 2, pp. ii7–ii11, 2006. DOI: 10.1093/ageing/af1077.
- [6] B. E. Maki and W. E. McIlroy, “Postural control in the older adult”, *Clinical Geriatrics Medicine*, vol. 12, no. 4, pp. 635–658, Nov. 1996.
- [7] P. A. Hageman, J. M. Leibowitz, and D. Blanke, “Age and gender effects on postural control measures”, *Archives of Physical Medicine and Rehabilitation*, vol. 76, no. 10, pp. 961–965, Oct. 1995. DOI: 10.1016/s0003-9993(95)80075-1.
- [8] T. Lelard and S. Ahmaidi, “Effects of physical training on age-related balance and postural control”, *Neurophysiologie Clinique*, vol. 45, no. 4-5, pp. 357–369, Nov. 2015. DOI: 10.1016/j.neucli.2015.09.008. [Online]. Available: <https://pubmed.ncbi.nlm.nih.gov/26548366/>.
- [9] R. B. Postuma, D. Berg, M. Stern, *et al.*, “MDS clinical diagnostic criteria for Parkinson’s disease: MDS-PD Clinical Diagnostic Criteria”, en, *Mov Disord.*, vol. 30, no. 12, pp. 1591–1601, Oct. 2015, ISSN: 08853185. DOI: 10.1002/mds.26424. [Online]. Available: <https://onlinelibrary.wiley.com/doi/10.1002/mds.26424> (visited on 03/28/2022).

- [10] P. McCrory and et al., “Consensus statement on concussion in sport—the 5th international conference on concussion in sport held in berlin, october 2016”, *Br J Sports Med*, vol. 51, no. 11, pp. 838–847, 2017. DOI: 10.1136/bjsports-2017-097699.
- [11] P. McCrory and et al., “What is the definition of sports-related concussion: A systematic review”, *British Journal of Sports Medicine*, vol. 51, no. 11, pp. 877–887, 2017. DOI: 10.1136/bjsports-2016-097393.
- [12] C. D. Balaban, R. G. Jacob, and J. M. Furman, “Neurologic bases for comorbidity of balance disorders, anxiety disorders and migraine: Neurotherapeutic implications”, *Expert Review of Neurotherapeutics*, vol. 11, no. 3, pp. 379–394, Mar. 2011. DOI: 10.1586/ern.11.19.
- [13] C. P. McDowell, R. K. Dishman, M. Hallgren, C. MacDonncha, and M. P. Herring, “Associations of physical activity and depression: Results from the irish longitudinal study on ageing”, *Experimental Gerontology*, vol. 112, pp. 68–75, Oct. 2018. DOI: 10.1016/j.exger.2018.09.004.
- [14] T. Brandt and M. Dieterich, “‘excess anxiety’ and ‘less anxiety’: Both depend on vestibular function”, *Current Opinion in Neurology*, vol. 33, no. 1, pp. 136–141, Feb. 2020. DOI: 10.1097/WCO.0000000000000771.
- [15] S. Shefer, C. Gordon, K. B. Avraham, and M. Mintz, “Balance deficit enhances anxiety and balance training decreases anxiety in vestibular mutant mice”, *Behavioural Brain Research*, vol. 276, pp. 76–83, Jan. 2015. DOI: 10.1016/j.bbr.2014.06.046.
- [16] F. Barollo, R. Friðriksdóttir, K. J. Edmunds, *et al.*, “Postural control adaptation and habituation during vibratory proprioceptive stimulation: An hd-eeeg investigation of cortical recruitment and kinematics”, *IEEE Transactions on Neural Systems and Rehabilitation Engineering*, vol. 28, no. 6, pp. 1381–1388, 2020.
- [17] K. J. Edmunds, H. Petersen, M. Hassan, *et al.*, “Cortical recruitment and functional dynamics in postural control adaptation and habituation during vibratory proprioceptive stimulation”, *Journal of Neural Engineering*, vol. 16, no. 2, p. 026 037, Apr. 2019. DOI: 10.1088/1741-2552/ab0678.
- [18] J. A. Langlois, W. Rutland-Brown, and M. M. Wald, “The epidemiology and impact of traumatic brain injury: A brief overview”, *Journal of Head Trauma Rehabilitation*, vol. 21, no. 5, pp. 375–378, 2006. DOI: 10.1097/00001199-200609000-00001.
- [19] M. B. Clay, K. L. Glover, and D. T. Lowe, “Epidemiology of concussion in sport: A literature review”, *Journal of Chiropractic Medicine*, vol. 12, no. 4, pp. 230–251, 2013. DOI: 10.1016/j.jcm.2012.11.005.
- [20] J. N. Ianof and et al., “Sport-related concussions”, *Dementia & Neuropsychologia*, vol. 8, no. 1, pp. 14–19, 2014. DOI: 10.1590/S1980-57642014DN81000003.
- [21] T. Covassin, R. J. Elbin, A. Bleecker, A. Lipchik, and A. P. Kontos, “Are there differences in neurocognitive function and symptoms between male and female soccer players after concussions?”, *The American Journal of Sports Medicine*, vol. 41, no. 12, pp. 2890–2895, 2013. DOI: 10.1177/0363546513509962.



- [22] D. H. Daneshvar, C. J. Nowinski, A. McKee, and R. C. Cantu, “The epidemiology of sport-related concussion”, *Clinics in Sports Medicine*, vol. 30, no. 1, pp. 1–17, 2011. DOI: 10.1016/j.csm.2010.08.006.
- [23] T. Anderson, M. Heitger, and A. D. Macleod, “Concussion and mild head injury”, *Practical Neurology*, vol. 6, no. 6, pp. 342–357, 2006. DOI: 10.1136/jnnp.2006.106583.
- [24] N. A. Shaw, “The neurophysiology of concussion”, *Progress in Neurobiology*, vol. 67, no. 4, pp. 281–344, 2002. DOI: 10.1016/S0301-0082(02)00018-7.
- [25] N. K. McGroarty, S. M. Brown, and M. K. Mulcahey, “Sport-related concussion in female athletes: A systematic review”, *Orthopaedic Journal of Sports Medicine*, vol. 8, no. 7, 2020. DOI: 10.1177/2325967120932306.
- [26] V. C. Merritt, C. R. Padgett, and A. J. Jak, “A systematic review of sex differences in concussion outcome: What do we know?”, *The Clinical Neuropsychologist*, vol. 33, no. 6, pp. 1016–1043, 2019. DOI: 10.1080/13854046.2018.1508616.
- [27] T. Mollayeva, G. El-Khechen-Richandi, and A. Colantonio, “Sex & gender considerations in concussion research”, *Concussion*, vol. 3, no. 1, 2018. DOI: 10.2217/cnc-2017-0015.
- [28] A. Colantonio, “Sex, gender, and traumatic brain injury: A commentary”, *Archives of Physical Medicine and Rehabilitation*, vol. 97, no. 2, S1–S4, 2016. DOI: 10.1016/j.apmr.2015.12.002.
- [29] M. W. Collins and et al., “A comprehensive, targeted approach to the clinical care of athletes following sport-related concussion”, *Knee Surgery, Sports Traumatology, Arthroscopy*, vol. 22, no. 2, pp. 235–246, 2014. DOI: 10.1007/s00167-013-2791-6.
- [30] C. K. Rhea, A. W. Kiefer, F. J. Haran, S. M. Glass, and W. H. Warren, “A new measure of the cop trajectory in postural sway: Dynamics of heading change”, *Medical engineering & physics*, vol. 36, no. 11, pp. 1473–1479, 2014.
- [31] J. S. Richman and J. R. Moorman, “Physiological time-series analysis using approximate entropy and sample entropy”, *American Journal of Physiology-Heart and Circulatory Physiology*, vol. 278, no. 6, H2039–H2049, 2000.
- [32] M. Costa, A. L. Goldberger, and C. K. Peng, “Multiscale entropy analysis of biological signals”, *Physical review E*, vol. 71, no. 2, p. 021 906, 2005.
- [33] S. P. Broglio and T. W. Puetz, “The effect of sport concussion on neurocognitive function, self-report symptoms and postural control”, *Sports Medicine*, vol. 38, no. 1, pp. 53–67, 2008. DOI: 10.2165/00007256-200838010-00005.
- [34] D. R. Temple, B.-C. Lee, and C. S. Layne, “Effects of tibialis anterior vibration on postural control when exposed to support surface translations”, *Somatosensory & Motor Research*, vol. 33, no. 1, pp. 42–48, 2016. DOI: 10.3109/08990220.2016.1171207.
- [35] B. Biagiatti, N. Stocchetti, P. Brambilla, and T. Van Vleet, “Brain dysfunction underlying prolonged post-concussive syndrome: A systematic review”, *Journal of Affective Disorders*, vol. 262, pp. 71–76, 2020. DOI: 10.1016/j.jad.2019.10.058.

- [36] R. J. Echemendia and et al., “The sport concussion assessment tool 5th edition (scat5): Background and rationale”, *British Journal of Sports Medicine*, vol. 51, pp. 848–850, 2017.
- [37] A. C. Conley and et al., “Resting state electroencephalography and sports-related concussion: A systematic review”, *Journal of Neurotrauma*, vol. 36, no. 1, pp. 1–13, 2018. DOI: 10.1089/neu.2018.5761.
- [38] J. N. Ianof and R. Anghinah, “Traumatic brain injury: An eeg point of view”, *Dementia & Neuropsychologia*, vol. 11, no. 1, pp. 3–5, 2017. DOI: 10.1590/1980-57642016dn11-010002.
- [39] T. T. K. Munia, A. Haider, C. Schneider, M. Romanick, and R. Fazel-Rezai, “A novel eeg based spectral analysis of persistent brain function alteration in athletes with concussion history”, *Scientific Reports*, vol. 7, p. 17 221, 2017. DOI: 10.1038/s41598-017-17414-x.
- [40] J. H. Simmons and H. Kerasidis, “Chapter 25—electroencephalography as a biomarker of concussion”, in *Biomarkers for Traumatic Brain Injury*, A. H. B. Wu and W. F. Peacock, Eds., Academic Press, 2020, pp. 367–396. DOI: 10.1016/B978-0-12-816346-7.00025-7.
- [41] D. H. C. Fong and et al., “Steady-state visual-evoked potentials as a biomarker for concussion: A pilot study”, *Frontiers in Neuroscience*, vol. 14, 2020. DOI: 10.3389/fnins.2020.00171.
- [42] A. P. Kontos and et al., “Preliminary evidence of reduced brain network activation in patients with posttraumatic migraine following concussion”, *Brain Imaging and Behavior*, vol. 10, no. 2, pp. 594–603, 2016. DOI: 10.1007/s11682-015-9412-6.
- [43] J. Thompson, W. Sebastianelli, and S. Slobounov, “Eeg and postural correlates of mild traumatic brain injury in athletes”, *Neuroscience Letters*, vol. 377, no. 3, pp. 158–163, 2005. DOI: 10.1016/j.neulet.2004.11.090.
- [44] S. Guay, L. De Beaumont, B. L. Drisdelle, J.-M. Lina, and P. Jolicoeur, “Electrophysiological impact of multiple concussions in asymptomatic athletes: A re-analysis based on alpha activity during a visual-spatial attention task”, *Neuropsychologia*, vol. 108, pp. 42–49, 2018. DOI: 10.1016/j.neuropsychologia.2017.11.022.
- [45] C. Cao, R. L. Tutwiler, and S. Slobounov, “Automatic classification of athletes with residual functional deficits following concussion by means of eeg signal using support vector machine”, *IEEE Transactions on Neural Systems and Rehabilitation Engineering*, vol. 16, no. 4, pp. 327–335, 2008. DOI: 10.1109/TNSRE.2008.918422.
- [46] J. Coenen, F. Van Den Bongard, A. C. Delling, and C. Reinsberger, “Functional connectivity within the default mode network in response to exercise during return-to-sport following concussion”, *Neurology*, vol. 98, no. 18, 2022. DOI: 10.1212/01.wnl.0000801904.27836.ef.
- [47] A. Mansouri, P. Ledwidge, K. Sayood, and D. L. Molfese, “A routine electroencephalography monitoring system for automated sports-related concussion detection”, *Neurotrauma Reports*, vol. 2, no. 1, pp. 626–638, 2021. DOI: 10.1089/neur.2021.0047.

- [48] J. W. Y. Kam and H. C. Todd, “Electroencephalogram recording in humans”, in *Basic Electrophysiological Methods*, E. Covey and M. Carter, Eds., Oxford University Press, 2015, pp. 134–151.
- [49] E. S. Papathanasiou, T. Cronin, B. Seemungal, and J. Sandhu, “Electrophysiological testing in concussion: A guide to clinical applications”, *Journal of Concussion*, vol. 2, p. 2059700218812634, 2018. DOI: 10.1177/2059700218812634.
- [50] J. T. Cavanaugh and et al., “Detecting altered postural control after cerebral concussion in athletes with normal postural stability”, *British Journal of Sports Medicine*, vol. 39, no. 11, pp. 805–811, 2005. DOI: 10.1136/bjsm.2004.015909.
- [51] J. Cavanaugh and et al., “Recovery of postural control after cerebral concussion: New insights using approximate entropy”, *Journal of Athletic Training*, vol. 41, no. 3, pp. 305–313, 2006.
- [52] J. P. Abaji, D. Curnier, R. D. Moore, and D. ElleMBERG, “Persisting effects of concussion on heart rate variability during physical exertion”, *Journal of Neurotrauma*, vol. 33, no. 9, pp. 811–817, 2016. DOI: 10.1089/neu.2015.3989.
- [53] S. D. Wickramaratne, M. S. Mahmud, and R. S. Ross, “Use of brain electrical activity to classify people with concussion: A deep learning approach”, in *ICC 2020 - 2020 IEEE International Conference on Communications (ICC)*, 2020, pp. 1–6. DOI: 10.1109/ICC40277.2020.9149393.
- [54] M. Szczupak, M. E. Hoffer, S. Murphy, and C. D. Balaban, “Posttraumatic dizziness and vertigo”, *Handb Clin Neurol*, vol. 137, pp. 295–300, 2016.
- [55] E. Çınar, L. Grilli, D. Friedman, and I. Gagnon, “Tracking postural stability of children and adolescents after a concussion: Sport-related versus non-sport-related concussion”, *The Turkish Journal of Pediatrics*, vol. 63, no. 3, pp. 471–481, 2021. DOI: 10.24953/turkjped.2021.03.014.
- [56] A. Degani and et al., “The effects of mild traumatic brain injury on postural control”, *Brain Injury*, vol. 31, no. 1, pp. 49–56, 2017. DOI: 10.1080/02699052.2016.1225982.
- [57] S. Slobounov, W. Sebastianelli, and M. Hallett, “Residual brain dysfunction observed one year post-mild traumatic brain injury: Combined eeg and balance study”, *Clin Neurophysiol*, vol. 123, no. 9, pp. 1755–1761, 2012.
- [58] J. J. Sosnoff, S. P. Broglio, S. Shine, and M. S. Ferrara, “Previous mild traumatic brain injury and postural-control dynamics”, *J Athl Train*, vol. 46, no. 1, pp. 85–91, 2011. DOI: 10.4085/1062-6050-46.1.85.
- [59] C. Z. Qiao, A. Chen, J. S. Blouin, and L. C. Wu, “Potential mechanisms of acute standing balance deficits after concussions and subconcussive head impacts: A review”, *Ann Biomed Eng*, vol. 49, pp. 2693–2715, 2021. DOI: 10.1007/s10439-021-02831-x.
- [60] W. Mittenberg, E. M. Canyock, D. Condit, and C. Patton, “Treatment of post-concussion syndrome following mild head injury”, *Journal of Clinical and Experimental Neuropsychology*, vol. 23, no. 6, pp. 829–836, 2001. DOI: 10.1076/jcen.23.6.829.1022.
- [61] T. Paillard and F. Noé, “Techniques and methods for testing the postural function in healthy and pathological subjects [review article]”, *BioMed Research International; Hindawi*, 2015. DOI: 10.1155/2015/891390.

- [62] J. Nguyen, J. Brown, J. W. Mold, and T. L. Welborn, “In patients with concussions, is the probability of permanent neurological damage predicted better by total number of concussions than by severity and duration of individual concussions?”, *The Journal of the Oklahoma State Medical Association*, vol. 106, no. 11, pp. 431–432,
- [63] C. E. Craig, D. J. Goble, and M. Doumas, “Proprioceptive acuity predicts muscle co-contraction of the tibialis anterior and gastrocnemius medialis in older adults’ dynamic postural control”, *Neuroscience*, vol. 322, pp. 251–261, 2016. DOI: 10.1016/j.neuroscience.2016.02.036.
- [64] R. E. Kleiger, P. K. Stein, and J. T. Bigger, “Heart rate variability: Measurement and clinical utility”, *Annals of Non-invasive Electrocardiology*, vol. 10, no. 1, pp. 88–101, 2005. DOI: 10.1111/j.1542-474X.2005.10101.x.
- [65] S. A. Bishop, R. T. Dech, P. Guzik, and J. P. Neary, “Heart rate variability and implication for sport concussion”, *Clinical Physiology and Functional Imaging*, vol. 38, no. 5, pp. 733–742, 2018. DOI: 10.1111/cpf.12487.
- [66] A. K. Memmini, M. F. L. Fountaine, S. P. Broglio, and R. D. Moore, “Long-term influence of concussion on cardio-autonomic function in adolescent hockey players”, *Journal of Athletic Training*, 2021. DOI: 10.4085/1062-6050-0578.19.
- [67] K. L. Pyndiura, A. P. D. Battista, and M. G. Hutchison, “A history of concussion is associated with minimal perturbations to heart rate variability in athletes”, *Brain Injury*, vol. 34, no. 10, pp. 1416–1421, 2020. DOI: 10.1080/02699052.2020.1802661.
- [68] A. J. Martingano and S. Persky, “Virtual reality expands the toolkit for conducting health psychology research”, *Social and Personality Psychology Compass*, vol. 15, no. 7, 2021.
- [69] F. Clay, D. Howett, J. FitzGerald, P. Fletcher, D. Chan, and A. Price, “Use of immersive virtual reality in the assessment and treatment of alzheimer’s disease: A systematic review”, *Journal of Alzheimer’s Disease*, vol. 75, no. 1, pp. 23–43, 2020. DOI: 10.3233/JAD-191218.
- [70] Y. Sawires, E. Huang, A. Gomes, K. Fernandes, and D. Wang, “Development of concussion evaluation tools using life-like virtual reality environments”, in *HCI International 2018 – ‘Posters’ Extended Abstracts*, Springer International Publishing, 2018, pp. 326–333. DOI: 10.1007/978-3-319-92279-9\_44.
- [71] H. Rao, T. Talkar, G. Ciccarelli, and et al., “Sensorimotor conflict tests in an immersive virtual environment reveal subclinical impairments in mild traumatic brain injury”, *Sci Rep*, vol. 10, p. 14773, 2020. DOI: 10.1038/s41598-020-71611-9.
- [72] E. Tolosa, G. Wenning, and W. Poewe, “The diagnosis of parkinson’s disease”, *The Lancet Neurology*, vol. 5, no. 1, pp. 75–86, 2006.
- [73] S. Rinalduzzi, C. Trompetto, L. Marinelli, et al., “Balance dysfunction in parkinson’s disease”, *Biomed Res Int*, vol. 2015, p. 434683, 2015. DOI: 10.1155/2015/434683. eprint: 2015 Jan 14.

- [74] Y. Zhang, M. C. Tartaglia, W. Zhan, and E. Ofori, “Editorial: Neuroimaging in parkinson’s disease and parkinsonism”, *Frontiers in Neurology*, vol. 14, 2023, ISSN: 1664-2295. DOI: 10.3389/fneur.2023.1153682. [Online]. Available: <https://www.frontiersin.org/articles/10.3389/fneur.2023.1153682>.
- [75] C. G. Goetz, S. Fahn, P. Martinez-Martin, *et al.*, “Movement disorder society-sponsored revision of the unified parkinson’s disease rating scale (mds-updrs): Process, format, and clinimetric testing plan”, *Movement disorders*, vol. 22, no. 1, pp. 41–47, 2007.
- [76] J. L. Palmer, M. A. Coats, C. M. Roe, S. M. Hanko, C. Xiong, and J. C. Morris, “Unified parkinson’s disease rating scale-motor exam: Inter-rater reliability of advanced practice nurse and neurologist assessments”, *Journal of Advanced Nursing*, vol. 66, no. 6, pp. 1382–1387, 2010. DOI: <https://doi.org/10.1111/j.1365-2648.2010.05313.x>. eprint: <https://onlinelibrary.wiley.com/doi/pdf/10.1111/j.1365-2648.2010.05313.x>. [Online]. Available: <https://onlinelibrary.wiley.com/doi/abs/10.1111/j.1365-2648.2010.05313.x>.
- [77] A. Siderowf, M. McDermott, K. Kieburtz, *et al.*, “Test–retest reliability of the unified parkinson’s disease rating scale in patients with early parkinson’s disease: Results from a multicenter clinical trial”, *Movement Disorders*, vol. 17, no. 4, pp. 758–763, 2002. DOI: <https://doi.org/10.1002/mds.10011>. eprint: <https://movementdisorders.onlinelibrary.wiley.com/doi/pdf/10.1002/mds.10011>. [Online]. Available: <https://movementdisorders.onlinelibrary.wiley.com/doi/abs/10.1002/mds.10011>.
- [78] C. G. Goetz, B. C. Tilley, S. R. Shaftman, *et al.*, “Movement disorder society-sponsored revision of the unified parkinson’s disease rating scale (mds-updrs): Scale presentation and clinimetric testing results”, *Mov Disord Off J Mov Disord Soci*, vol. 23, no. 15, pp. 2129–70, 2008.
- [79] S. Waninger, C. Berka, M. Stevanovic Karic, *et al.*, “Neurophysiological biomarkers of parkinson’s disease”, *Journal of Parkinson’s disease*, vol. 10, no. 2, pp. 471–480, 2020.
- [80] M. J. Gandal, J. C. Edgar, K. Klook, and S. J. Siegel, “Gamma synchrony: Towards a translational biomarker for the treatment-resistant symptoms of schizophrenia”, *Neuropharmacology*, vol. 62, no. 3, pp. 1504–1518, 2012.
- [81] H. Hampel, R. Frank, K. Broich, *et al.*, “Biomarkers for alzheimer’s disease: Academic, industry and regulatory perspectives”, *Nature reviews Drug discovery*, vol. 9, no. 7, pp. 560–574, 2010.
- [82] F. Kheiri, A. Bragin, J. Almajano, E. Winden, *et al.*, “Non-linear classification of heart rate parameters as a biomarker for epileptogenesis”, *Epilepsy research*, vol. 100, no. 1-2, pp. 59–66, 2012.
- [83] C.-X. Han, J. Wang, G.-S. Yi, and Y.-Q. Che, “Investigation of eeg abnormalities in the early stage of parkinson’s disease”, *Cognitive neurodynamics*, vol. 7, pp. 351–359, 2013.
- [84] K. Serizawa, S. Kamei, A. Morita, *et al.*, “Comparison of quantitative eegs between parkinson disease and age-adjusted normal controls”, *Journal of Clinical Neurophysiology*, vol. 25, no. 6, pp. 361–366, 2008.

- [85] M. Moazami-Goudarzi, J. Sarnthein, L. Michels, R. Moukhtieva, and D. Jeanmonod, “Enhanced frontal low and high frequency power and synchronization in the resting eeg of parkinsonian patients”, *Neuroimage*, vol. 41, no. 3, pp. 985–997, 2008.
- [86] G. Mochizuki, S. Boe, A. Marlin, and W. McIlroy, “Perturbation-evoked cortical activity reflects both the context and consequence of postural instability”, *Neuroscience*, vol. 170, no. 2, pp. 599–609, 2010.
- [87] D. R. Curtis and P. Andersen, “Sir john carew eccles, ac 27 january 1903-2 may 1997”, *Biographical Memoirs of Fellows of the Royal Society*, vol. 47, pp. 161–187, 2001.
- [88] A. Nieuwboer *et al.*, “Motor learning in parkinson’s disease: Limitations and potential for rehabilitation”, *Parkinsonism & Related Disorders*, vol. 15, no. Suppl 3, S53–S58, 2009.
- [89] C. Buck and E. Moro, “Electromyography in parkinson’s disease: Utilization in clinical practice”, *Parkinsonism & Related Disorders*, vol. 46, pp. 1–6, 2018.
- [90] D. Rodriguez-Martin *et al.*, “Home detection of freezing of gait using support vector machines through a single waist-worn triaxial accelerometer”, *PloS one*, vol. 12, no. 2, e0171764, 2017.
- [91] M. Asahina *et al.*, “Autonomic dysfunctions in parkinson’s disease”, in *Parkinson’s Disease: Non-Motor and Non-Dopaminergic Features*. Blackwell Publishing Ltd, 2013, pp. 201–216.
- [92] S. M. Fereshtehnejad and R. B. Postuma, “Subtypes of parkinson’s disease: What do they tell us about disease progression?”, *Current neurology and neuroscience reports*, vol. 17, no. 4, p. 34, 2017.
- [93] P. M. Santos *et al.*, “Heart rate variability and disease characteristics in patients with parkinson’s disease”, *Clinical Autonomic Research*, vol. 28, no. 3, pp. 309–316, 2018.
- [94] L. Rocchi, L. Chiari, and A. Cappello, “Feature selection of stabilometric parameters based on principal component analysis”, *Medical & Biological Engineering & Computing*, vol. 40, no. 3, pp. 358–366, 2002.
- [95] F. Horak, J. Nutt, and L. Nashner, “Postural inflexibility in parkinsonian subjects”, *Journal of the neurological sciences*, vol. 111, no. 1, pp. 46–58, 1992.
- [96] Y. Brenière, M. C. Do, and S. Bouisset, “Are dynamic phenomena prior to stepping essential to walking?”, *Journal of Motor Behavior*, vol. 19, no. 1, pp. 62–76, 1987.
- [97] J. V. Jacobs *et al.*, “Gait dysfunction in parkinson’s disease”, *Physical therapy*, vol. 89, no. 4, pp. 360–374, 2009.
- [98] F. Tadel, S. Baillet, J. C. Mosher, D. Pantazis, and R. M. Leahy, “Brainstorm: A user-friendly application for meg/eeg analysis”, *Computational Intelligence and Neuroscience*, vol. 2011, p. 879716, 2011. DOI: 10.1155/2011/879716. [Online]. Available: <https://doi.org/10.1155/2011/879716>.

- [99] A. Pedroni, A. Bahreini, and N. Langer, “Automagic: Standardized preprocessing of big eeg data”, *NeuroImage*, vol. 200, pp. 460–473, 2019, ISSN: 1053-8119. DOI: <https://doi.org/10.1016/j.neuroimage.2019.06.046>. [Online]. Available: <https://www.sciencedirect.com/science/article/pii/S1053811919305439>.
- [100] P. Welch, “The use of fast fourier transform for the estimation of power spectra: A method based on time averaging over short, modified periodograms”, *IEEE Transactions on Audio and Electroacoustics*, vol. 15, no. 2, pp. 70–73, 1967. DOI: 10.1109/TAU.1967.1161901.
- [101] X.-J. Wang, “Neurophysiological and computational principles of cortical rhythms in cognition”, *Physiological Reviews*, vol. 90, no. 3, pp. 1195–1268, 2010, PMID: 20664082. DOI: 10.1152/physrev.00035.2008. eprint: <https://doi.org/10.1152/physrev.00035.2008>. [Online]. Available: <https://doi.org/10.1152/physrev.00035.2008>.
- [102] G. Buzsáki and A. Draguhn, “Neuronal oscillations in cortical networks”, *Science*, vol. 304, no. 5679, pp. 1926–1929, 2004. DOI: 10.1126/science.1099745. eprint: <https://www.science.org/doi/pdf/10.1126/science.1099745>. [Online]. Available: <https://www.science.org/doi/abs/10.1126/science.1099745>.
- [103] M. A. Busa and R. E. van Emmerik, “Multiscale entropy: A tool for understanding the complexity of postural control”, *Journal of Sport and Health Science*, vol. 5, no. 1, pp. 44–51, 2016.
- [104] Task Force of the European Society of Cardiology and the North American Society of Pacing Electrophysiology, “Heart rate variability: Standards of measurement, physiological interpretation, and clinical use”, *Circulation*, vol. 93, no. 5, pp. 1043–1065, 1996.
- [105] F. Shaffer and J. P. Ginsberg, “An overview of heart rate variability metrics and norms”, *Frontiers in Public Health*, vol. 5, p. 258, 2017. DOI: 10.3389/fpubh.2017.00258.
- [106] R. Aubonnet, A. Shoykhet, D. Jacob, G. Di Lorenzo, H. Petersen, and P. Gargiulo, “Postural control paradigm (biovrsea): Towards a neurophysiological signature”, *Physiological Measurement*, vol. 43, no. 11, p. 115 002, 2022.
- [107] B. E. Maki and W. E. McIlroy, “Cognitive demands and cortical control of human balance-recovery reactions”, *Journal of neural transmission*, vol. 114, no. 10, pp. 1279–1296, 2007.
- [108] J. Jacobs and F. Horak, “Cortical control of postural responses”, *Journal of neural transmission*, vol. 114, no. 10, pp. 1339–1348, 2007.
- [109] R. Goel, R. A. Ozdemir, S. Nakagome, J. L. Contreras-Vidal, W. H. Paloski, and P. J. Parikh, “Effects of speed and direction of perturbation on electroencephalographic and balance responses”, *Experimental Brain Research*, vol. 236, no. 7, pp. 2073–2083, Jul. 2018, ISSN: 1432-1106. DOI: 10.1007/s00221-018-5284-5. [Online]. Available: <https://doi.org/10.1007/s00221-018-5284-5>.

- [110] J. P. Varghese, R. E. McIlroy, and M. Barnett-Cowan, “Perturbation-evoked potentials: Significance and application in balance control research”, en, *Neuroscience & Biobehavioral Reviews*, vol. 83, pp. 267–280, Dec. 2017, ISSN: 01497634. DOI: 10.1016/j.neubiorev.2017.10.022. [Online]. Available: <https://linkinghub.elsevier.com/retrieve/pii/S0149763417305699> (visited on 04/04/2022).
- [111] J. P. Varghese, A. Marlin, K. B. Beyer, W. R. Staines, G. Mochizuki, and W. E. McIlroy, “Frequency characteristics of cortical activity associated with perturbations to upright stability”, en, *Neuroscience Letters*, vol. 578, pp. 33–38, Aug. 2014, ISSN: 03043940. DOI: 10.1016/j.neulet.2014.06.017. [Online]. Available: <https://linkinghub.elsevier.com/retrieve/pii/S0304394014004893> (visited on 03/04/2022).
- [112] T. Hülzdünker, A. Mierau, C. Neeb, H. Kleinöder, and H. Strüder, “Cortical processes associated with continuous balance control as revealed by eeg spectral power”, *Neuroscience letters*, vol. 592, pp. 1–5, 2015.
- [113] A. M. Catai, C. M. Pastre, M. Fernandes de Godoy, E. da Silva, A. C. de Medeiros Takahashi, and L. C. Marques Vanderlei, “Heart rate variability: Are you using it properly? standardization checklist of procedures”, *Brazilian Journal of Physical Therapy*, vol. 24, no. 2, pp. 91–102, 2020.
- [114] B. J. Yates, P. S. Bolton, and V. G. Macefield, “Vestibulo-sympathetic responses”, *Comprehensive Physiology*, vol. 4, no. 2, p. 851, 2014.
- [115] I. G. Amiridis, V. Hatzitaki, and F. Arabatzi, “Age-induced modifications of static postural control in humans”, *Neuroscience Letters*, vol. 350, no. 3, pp. 137–140, 2003.
- [116] H. Nakamura, T. Tsuchida, and Y. Mano, “The assessment of posture control in the elderly using the displacement of the center of pressure after forward platform translation”, *Journal of Electromyography and Kinesiology*, vol. 11, no. 6, pp. 395–403, 2001.
- [117] S. R. Holmes and M. J. Griffin, “Correlation between heart rate and the severity of motion sickness caused by optokinetic stimulation”, *Journal of Psychophysiology*, vol. 15, no. 1, p. 35, 2001.
- [118] Y. Ivanenko and V. S. Gurfinkel, “Human postural control”, *Frontiers in Neuroscience*, vol. 12, p. 171, 2018. DOI: 10.3389/fnins.2018.00171.
- [119] M. Recenti, D. Jacob, R. Aubonnet, *et al.*, “Predicting lifestyle using biovrsea multi-biometric paradigms”, in *2022 IEEE International Conference on Metrology for Extended Reality, Artificial Intelligence and Neural Engineering (MetroX-RAINE)*, 2022, pp. 329–334. DOI: 10.1109/MetroXRAINE54828.2022.9967685.
- [120] H. Kristjánsson and *et al.*, “Self-reported concussion history among icelandic female athletes with and without a definition of concussion”, *The Clinical Neuropsychologist*, vol. 0, no. 0, pp. 1–13, 2020. DOI: 10.1080/13854046.2020.1814873.
- [121] J. K. Dierijck, A. D. Wright, B. Kelsey, and *et al.*, “Effects of acute concussion on centre of pressure variables during quiet stance”, *British Journal of Sports Medicine*, vol. 51, A40, 2017.



- [122] G. S. Jónbjörnsson and T. G. Tómasson, “Íslensk þýðing og áreiðanleikaprófun á scat3 höfuðáverkamælitækinu”, M.S. thesis, University of Iceland, Reykjavik, 2016. [Online]. Available: <http://hdl.handle.net/1946/24722>.
- [123] F. Tadel, S. Baillet, J. C. Mosher, D. Pantazis, and R. M. Leahy, “Brainstorm: A user-friendly application for meg/eeg analysis”, *Comput Intell Neurosci*, vol. 2011, 2011. DOI: 10.1155/2011/879716.
- [124] The MathWorks Inc., *Matlab*, Natick, Massachusetts, 2020.
- [125] A. Pedroni, A. Bahreini, and N. Langer, “Automagic: Standardized preprocessing of big eeg data”, *Neuroimage*, vol. 200, pp. 460–473, 2019. DOI: 10.1016/j.neuroimage.2019.06.046.
- [126] A. D. Vigotsky, I. Halperin, G. J. Lehman, G. S. Trajano, and T. M. Vieira, “Interpreting signal amplitudes in surface electromyography studies in sport and rehabilitation sciences”, *Front Physiol*, vol. 4, 2018. DOI: 10.3389/fphys.2017.00985.
- [127] M. Bilodeau, A. B. Arsenault, D. Gravel, and D. Bourbonnais, “The influence of an increase in the level of force on the emg power spectrum of elbow extensors”, *European journal of applied physiology and occupational physiology*, vol. 61, no. 5, pp. 461–466, 1990.
- [128] C. Sapsanis, G. Georgoulas, A. Tzes, and D. Lymberopoulos, “Improving emg based classification of basic hand movements using emd”, in *2013 35th Annual International Conference of the IEEE Engineering in Medicine and Biology Society (EMBC)*, 2013, pp. 5754–5757. DOI: 10.1109/EMBC.2013.6610836.
- [129] D. J. Hewson, J. Y. Hogrel, Y. Langeron, and J. Duchêne, “Evolution in impedance at the electrode-skin interface of two types of surface emg electrodes during long-term recordings”, *Journal of Electromyography and Kinesiology*, vol. 13, no. 3, pp. 273–279, 2003.
- [130] S. Jerritta, M. Murugappan, K. Wan, and S. Yaacob, “Emotion recognition from facial emg signals using higher order statistics and principal component analysis”, *Journal of the Chinese Institute of Engineers*, vol. 37, no. 3, pp. 385–394, 2014.
- [131] D. M. Williams, S. Sharma, and M. Bilodeau, “Neuromuscular fatigue of elbow flexor muscles of dominant and non-dominant arms in healthy humans”, *Journal of Electromyography and Kinesiology*, vol. 12, no. 4, pp. 287–294, 2002.
- [132] A. Van Boxtel, P. Goudswaard, G. M. Van der Molen, and W. E. Van Den Bosch, “Changes in electromyogram power spectra of facial and jaw-elevator muscles during fatigue”, *Journal of Applied Physiology*, vol. 54, no. 1, pp. 51–58, 1983.
- [133] W. N. Löscher, A. G. Cresswell, and A. Thorstensson, “Electromyographic responses of the human triceps surae and force tremor during sustained sub-maximal isometric plantar flexion”, *Acta physiologica scandinavica*, vol. 152, no. 1, pp. 73–82, 1994.
- [134] C. H. Lee and T. L. Sun, “Evaluation of postural stability based on a force plate and inertial sensor during static balance measurements”, *Journal of physiological anthropology*, vol. 37, no. 1, pp. 1–16, 2018. DOI: 10.1186/s40101-018-0187-5.

- [135] M. U. Ahmed and D. P. Mandic, “Multivariate multiscale entropy analysis”, *IEEE Signal processing letters*, vol. 19, no. 2, pp. 91–94, 2011.
- [136] G. L. Iverson, “Outcome from mild traumatic brain injury”, *Current Opinion in Psychiatry*, vol. 18, no. 3, pp. 301–317, 2005. DOI: 10.1097/01.yco.0000165601.29047.ae.
- [137] M. K. Jónsdóttir, K. H. Kristófersdóttir, S. Runólfssdóttir, *et al.*, “Concussion among female athletes in iceland: Stress, depression, anxiety, and quality of life”, *Nordic Psychology*, vol. 0, no. 0, pp. 1–17, 2021. DOI: 10.1080/19012276.2021.2004916.
- [138] N. Reilly, J. Prebor, J. Moxey, and E. Schussler, “Chronic impairments of static postural stability associated with history of concussion”, *Experimental brain research*, vol. 238, no. 12, pp. 2783–2793, 2020.
- [139] H. Luo, X. Wang, M. Fan, *et al.*, “The effect of visual stimuli on stability and complexity of postural control”, *Frontiers in neurology*, vol. 9, p. 48, 2018.
- [140] T. Yamamoto, C. E. Smith, Y. Suzuki, *et al.*, “Universal and individual characteristics of postural sway during quiet standing in healthy young adults”, *Physiological reports*, vol. 3, no. 3, e12329, 2015.
- [141] H. Chander, S. N. Kodithuwakku Arachchige, C. M. Hill, *et al.*, “Virtual-reality-induced visual perturbations impact postural control system behavior”, *Behavioral Sciences*, vol. 9, no. 11, p. 113, 2019.
- [142] A. Clouter, K. L. Shapiro, and S. Hanslmayr, “Theta phase synchronization is the glue that binds human associative memory”, *Current Biology*, vol. 27, no. 20, 3143–3148.e6, 2017. DOI: 10.1016/j.cub.2017.09.001.
- [143] W. Klimesch, “Eeg alpha and theta oscillations reflect cognitive and memory performance: A review and analysis”, *Brain Research. Brain Research Reviews*, vol. 29, no. 2–3, pp. 169–195, 1999. DOI: 10.1016/s0165-0173(98)00056-3.
- [144] J. Mari-Acevedo, K. Yelvington, and W. O. Tatum, “Chapter 9—normal eeg variants”, in *Handbook of Clinical Neurology*, vol. 160, Elsevier, 2019, pp. 143–160. DOI: 10.1016/B978-0-444-64032-1.00009-6.
- [145] Y.-K. Wang, T.-P. Jung, and C.-T. Lin, “Theta and alpha oscillations in attentional interaction during distracted driving”, *Frontiers in Behavioral Neuroscience*, vol. 12, 2018. DOI: 10.3389/fnbeh.2018.00003.
- [146] G. Manley and *et al.*, “A systematic review of potential long-term effects of sport-related concussion”, *Br J Sports Med*, vol. 51, no. 12, pp. 969–977, 2017. DOI: 10.1136/bjsports-2017-097791.
- [147] N. S. King and S. Kirwilliam, “Permanent post-concussion symptoms after mild head injury”, *Brain Injury*, vol. 25, no. 5, pp. 462–470, 2011. DOI: 10.3109/02699052.2011.558042.
- [148] C. Beaulieu, A. Turcotte-Giroux, F. Carrier-Toutant, B. Brisson, P. Jolicoeur, and L. De Beaumont, “Long-term effects of concussions on psychomotor speed and cognitive control processes during motor sequence learning”, *Journal of Psychophysiology*, vol. 33, no. 2, pp. 96–108, 2019. DOI: 10.1027/0269-8803/a000213.

- [149] A. L. Zhang, D. C. Sing, C. M. Rugg, B. T. Feeley, and C. Senter, “The rise of concussions in the adolescent population”, *Orthopaedic Journal of Sports Medicine*, vol. 4, no. 8, 2016. DOI: 10.1177/2325967116662458.
- [150] N. Sandel, E. Reynolds, P. E. Cohen, B. L. Gillie, and A. P. Kontos, “Anxiety and mood clinical profile following sport-related concussion: From risk factors to treatment”, *Sport, Exercise, and Performance Psychology*, vol. 6, no. 3, pp. 304–323, 2017. DOI: 10.1037/spy0000098.
- [151] A. R. Sipp, J. T. Gwin, S. Makeig, and D. P. Ferris, “Loss of balance during balance beam walking elicits a multifocal theta band electrocortical response”, *Journal of neurophysiology*, vol. 110, no. 9, pp. 2050–2060, 2013.
- [152] I. Di Giulio, C. N. Maganaris, V. Baltzopoulos, and I. D. Loram, “The proprioceptive and agonist roles of gastrocnemius, soleus, and tibialis anterior muscles in maintaining human upright posture”, *The Journal of Physiology*, vol. 587, pp. 2399–2416, 2009. DOI: 10.1113/jphysiol.2009.168690.
- [153] T. A. Buckley, J. R. Oldham, and J. B. Caccese, “Postural control deficits identify lingering post-concussion neurological deficits”, *Journal of Sport and Health Science*, vol. 5, no. 1, pp. 61–69, 2016. DOI: 10.1016/j.jshs.2016.01.007.
- [154] A. P. Kontos, J. M. Deitrick, M. W. Collins, and A. Mucha, “Review of vestibular and oculomotor screening and concussion rehabilitation”, *Journal of Athletic Training*, vol. 52, no. 3, pp. 256–261, 2017. DOI: 10.4085/1062-6050-51.11.05.
- [155] A. Samuel, J. Solomon, and D. Mohan, “A critical review on the normal postural control”, *Physiotherapy and Occupational Therapy Journal*, vol. 8, pp. 71–75, 2015. DOI: 10.21088/potj.0974.5777.8215.454.
- [156] M. Recenti and et al., “Toward predicting motion sickness using virtual reality and a moving platform assessing brain, muscles, and heart signals”, *Front. Bioeng. Biotechnol.*, vol. 9, 2021. DOI: 10.3389/fbioe.2021.635661.
- [157] D. E. Fleck and et al., “Predicting post-concussion symptom recovery in adolescents using a novel artificial intelligence”, *Journal of Neurotrauma*, vol. 38, no. 7, pp. 830–836, 2021.
- [158] R. Boshra, K. Dhindsa, O. Boursalie, et al., “From group-level statistics to single-subject prediction: Machine learning detection of concussion in retired athletes”, *IEEE Transactions on Neural Systems and Rehabilitation Engineering*, vol. 27, no. 7, pp. 1492–1501, 2019.
- [159] K. Dams-O’Connor and et al., “Screening for traumatic brain injury: Findings and public health implications”, *The Journal of Head Trauma Rehabilitation*, vol. 29, no. 6, pp. 479–489, 2014. DOI: 10.1097/HTR.000000000000099.
- [160] I. S. Unnsteinsdottir Kristensen, H. Krisjansdottir, R. Sigurvinsdóttir, H. A. Sigurjonsdottir, L. Ó. Eggertsdottir Claessen, and M. K. Jónsdóttir, “Methodology matters: Added information affects the self-report of concussions and symptoms among female athletes”, *Journal of Head Trauma Rehabilitation*, Under review.
- [161] M. L. Alosco and et al., “Utility of providing a concussion definition in the assessment of concussion history in former nfl players”, *Brain Injury*, vol. 31, no. 8, pp. 1116–1123, 2017. DOI: 10.1080/02699052.2017.1294709.

- [162] C. M. Baugh and et al., “Chronic traumatic encephalopathy: Neurodegeneration following repetitive concussive and subconcussive brain trauma”, *Brain Imaging Behav*, vol. 6, no. 2, pp. 244–254, 2020.
- [163] B. E. Gavett, R. A. Stern, and A. C. McKee, “Chronic traumatic encephalopathy: A potential late effect of sport-related concussive and subconcussive head trauma”, *Clin Sports Med*, vol. 30, no. 1, pp. 179–188, xi, 2011.
- [164] S. Rawlings, R. Takechi, and A. P. Lavender, “Effects of sub-concussion on neuropsychological performance and its potential mechanisms: A narrative review”, *Brain Research Bulletin*, vol. 165, pp. 56–62, 2020.
- [165] T. M. Parker, L. R. Osternig, P. van Donkelaar, and L.-S. Chou, “Balance control during gait in athletes and non-athletes following concussion”, *Medical Engineering & Physics*, vol. 30, pp. 959–967, 2008.
- [166] M. Morin, P. Langevin, and P. Fait, “Cervical spine involvement in mild traumatic brain injury: A review”, *J Sports Med (Hindawi Publ Corp)*, vol. 2016, p. 1590161,
- [167] J. T. McCabe and L. B. Tucker, “Sex as a biological variable in preclinical modeling of blast-related traumatic brain injury”, *Front Neurol*, vol. 11, p. 541050, 2020.
- [168] A. Samii, J. G. Nutt, and B. R. Ransom, “Parkinson’s disease”, *Lancet*, vol. 363, no. 9423, pp. 1783–1793, May 2004. DOI: 10.1016/S0140-6736(04)16305-8.
- [169] J. Jankovic, “Parkinson’s disease: Clinical features and diagnosis”, en, *Journal of Neurology, Neurosurgery & Psychiatry*, vol. 79, no. 4, pp. 368–376, Apr. 2008, ISSN: 0022-3050. DOI: 10.1136/jnnp.2007.131045. [Online]. Available: <https://jnnp.bmj.com/lookup/doi/10.1136/jnnp.2007.131045> (visited on 05/26/2022).
- [170] F. Doná, C. Aquino, J. Gazzola, *et al.*, “Changes in postural control in patients with Parkinson’s disease: A posturographic study”, en, *Physiotherapy*, vol. 102, no. 3, pp. 272–279, Sep. 2016, ISSN: 00319406. DOI: 10.1016/j.physio.2015.08.009. [Online]. Available: <https://linkinghub.elsevier.com/retrieve/pii/S0031940615038213> (visited on 03/14/2022).
- [171] C. C. Harro, A. Kelch, C. Hargis, and A. DeWitt, “Comparing Balance Performance on Force Platform Measures in Individuals with Parkinson’s Disease and Healthy Adults”, en, *Parkinson’s Disease*, vol. 2018, pp. 1–12, Dec. 2018, ISSN: 2090-8083, 2042-0080. DOI: 10.1155/2018/6142579. [Online]. Available: <https://www.hindawi.com/journals/pd/2018/6142579/> (visited on 03/17/2022).
- [172] M. Patel, M. H. Nilsson, S. Rehncrona, *et al.*, “Strategic alterations of posture are delayed in Parkinson’s disease patients during deep brain stimulation”, en, *Sci Rep*, vol. 11, no. 1, p. 23550, Dec. 2021, ISSN: 2045-2322. DOI: 10.1038/s41598-021-02813-y. [Online]. Available: <https://www.nature.com/articles/s41598-021-02813-y> (visited on 03/28/2022).

- [173] K. E. Hawkins, S. S. Paul, E. Chiarovano, and I. S. Curthoys, “Using virtual reality to assess vestibulo-visual interaction in people with Parkinson’s disease compared to healthy controls”, en, *Exp Brain Res*, vol. 239, no. 12, pp. 3553–3564, Dec. 2021, ISSN: 0014-4819, 1432-1106. DOI: 10.1007/s00221-021-06219-0. [Online]. Available: <https://link.springer.com/10.1007/s00221-021-06219-0> (visited on 03/28/2022).
- [174] A. Landolfi, C. Ricciardi, L. Donisi, *et al.*, “Machine learning approaches in parkinson’s disease.”, *Current medicinal chemistry*, 2021.
- [175] L. Donisi, G. Cesarelli, P. Balbi, *et al.*, “Positive impact of short-term gait rehabilitation in parkinson patients: A combined approach based on statistics and machine learning”, *Mathematical Biosciences and Engineering*, vol. 18, no. 5, pp. 6995–7009, 2021, ISSN: 1551-0018. DOI: 10.3934/mbe.2021348. [Online]. Available: <https://www.aimspress.com/article/doi/10.3934/mbe.2021348>.
- [176] M. Amboni, C. Ricciardi, S. Cuoco, *et al.*, “Mild cognitive impairment subtypes are associated with peculiar gait patterns in parkinson’s disease”, *Frontiers in Aging Neuroscience*, vol. 14, 2022, ISSN: 1663-4365. DOI: 10.3389/fnagi.2022.781480. [Online]. Available: <https://www.frontiersin.org/article/10.3389/fnagi.2022.781480>.
- [177] M. A. Busa and R. E. van Emmerik, “Multiscale entropy: A tool for understanding the complexity of postural control”, en, *Journal of Sport and Health Science*, vol. 5, no. 1, pp. 44–51, Mar. 2016, ISSN: 20952546. DOI: 10.1016/j.jshs.2016.01.018. [Online]. Available: <https://linkinghub.elsevier.com/retrieve/pii/S209525461600020X> (visited on 05/27/2022).
- [178] I. Di Giulio, C. N. Maganaris, V. Baltzopoulos, and I. D. Loram, “The proprioceptive and agonist roles of gastrocnemius, soleus and tibialis anterior muscles in maintaining human upright posture”, *The Journal of Physiology*, vol. 587, no. 10, pp. 2399–2416, 2009. DOI: <https://doi.org/10.1113/jphysiol.2009.168690>. eprint: <https://physoc.onlinelibrary.wiley.com/doi/pdf/10.1113/jphysiol.2009.168690>. [Online]. Available: <https://physoc.onlinelibrary.wiley.com/doi/abs/10.1113/jphysiol.2009.168690>.
- [179] Y.-L. Hsieh and M. F. Abbod, “Gait analyses of parkinson’s disease patients using multiscale entropy”, *Electronics*, vol. 10, no. 21, 2021, ISSN: 2079-9292. DOI: 10.3390/electronics10212604. [Online]. Available: <https://www.mdpi.com/2079-9292/10/21/2604>.
- [180] R. Fadil, A. Huether, R. Brunnemer, A. P. Blaber, J.-S. Lou, and K. Tavakolian, “Early detection of parkinson’s disease using center of pressure data and machine learning”, in *2021 43rd Annual International Conference of the IEEE Engineering in Medicine & Biology Society (EMBC)*, 2021, pp. 2433–2436. DOI: 10.1109/EMBC46164.2021.9630451.
- [181] O. C. Li Y Zhang S, “Automated classification of postural control for individuals with parkinson’s disease using a machine learning approach: A preliminary study.”, *J Appl Biomech.*, no. 31, pp. 1–6. 2020. DOI: 10.1123/jab.2019-0400..

- [182] P. H. S. Pelicioni, J. C. Menant, M. D. Latt, and S. R. Lord, “Falls in Parkinson’s Disease Subtypes: Risk Factors, Locations and Circumstances”, en, *IJERPH*, vol. 16, no. 12, p. 2216, Jun. 2019, ISSN: 1660-4601. DOI: 10.3390/ijerph16122216. [Online]. Available: <https://www.mdpi.com/1660-4601/16/12/2216> (visited on 03/28/2022).
- [183] A. M. Maitín, A. J. García-Tejedor, and J. P. R. Muñoz, “Machine learning approaches for detecting parkinson’s disease from eeg analysis: A systematic review”, *Applied Sciences*, vol. 10, no. 23, p. 8662, 2020.
- [184] M. Maffoni, A. Giardini, A. Pierobon, D. Ferrazzoli, and G. Frazzitta, “Stigma experienced by parkinson’s disease patients: A descriptive review of qualitative studies”, *Parkinson’s disease*, vol. 2017, 2017.
- [185] C. Martignon, A. Pedrinolla, F. Ruzzante, *et al.*, “Guidelines on exercise testing and prescription for patients at different stages of parkinson’s disease”, *Aging clinical and experimental research*, vol. 33, no. 2, pp. 221–246, 2021.
- [186] C. Agliardi, M. Meloni, F. R. Guerini, *et al.*, “Oligomeric  $\alpha$ -syn and snare complex proteins in peripheral extracellular vesicles of neural origin are biomarkers for parkinson’s disease”, *Neurobiology of Disease*, vol. 148, p. 105185, 2021.
- [187] M. Politis, “Neuroimaging in parkinson disease: From research setting to clinical practice”, *Nature Reviews Neurology*, vol. 10, no. 12, pp. 708–722, 2014.
- [188] F.-M. Lu and Z. Yuan, “Pet/spect molecular imaging in clinical neuroscience: Recent advances in the investigation of cns diseases”, *Quantitative imaging in medicine and surgery*, vol. 5, no. 3, p. 433, 2015.
- [189] D. Berg, J. Godau, and U. Walter, “Transcranial sonography in movement disorders”, *The Lancet Neurology*, vol. 7, no. 11, pp. 1044–1055, 2008.
- [190] J. Bosboom, D. Stoffers, C. Stam, *et al.*, “Resting state oscillatory brain dynamics in parkinson’s disease: An meg study”, *Clinical Neurophysiology*, vol. 117, no. 11, pp. 2521–2531, 2006.
- [191] C. Chu, Z. Zhang, J. Wang, *et al.*, “Deep learning reveals personalized spatial spectral abnormalities of high delta and low alpha bands in eeg of patients with early parkinson’s disease”, *Journal of Neural Engineering*, vol. 18, no. 6, p. 066036, 2021.
- [192] M. Neufeld, R. Inzelberg, and A. Korczyn, “Eeg in demented and non-demented parkinsonian patients”, *Acta neurologica scandinavica*, vol. 78, no. 1, pp. 1–5, 1988.
- [193] O. Sinanović, A. Kapidzić, L. Kovacević, J. Hudić, and D. Smajlović, “Eeg frequency and cognitive dysfunction in patients with parkinson’s disease.”, *Medicinski arhiv*, vol. 59, no. 5, pp. 286–287, 2005.
- [194] R. B. Parreira, L. A. C. Grecco, and C. S. Oliveira, “Postural control in blind individuals: A systematic review”, *Gait & Posture*, vol. 57, pp. 161–167, 2017.
- [195] R. B. Postuma, D. Berg, M. Stern, *et al.*, “Mds clinical diagnostic criteria for parkinson’s disease”, *Movement Disorders*, vol. 30, no. 12, pp. 1591–1601, 2015. DOI: <https://doi.org/10.1002/mds.26424>. eprint: <https://movementdisorders.onlinelibrary.wiley.com/doi/pdf/10.1002/mds.26424>. [Online]. Available: <https://movementdisorders.onlinelibrary.wiley.com/doi/abs/10.1002/mds.26424>.

- [196] M. Torchiano, *Effsize: Efficient effect size computation*, 2020. [Online]. Available: <https://CRAN.R-project.org/package=effsize>.
- [197] N. Cliff, “Dominance statistics: Ordinal analyses to answer ordinal questions”, *Psychological Bulletin*, vol. 114, 1993.
- [198] I. D. Loram, C. N. Maganaris, and M. Lakie, “Human postural sway results from frequent, ballistic bias impulses by soleus and gastrocnemius”, *The Journal of Physiology*, vol. 564, no. 1, pp. 295–311, 2005. DOI: <https://doi.org/10.1113/jphysiol.2004.076307>. eprint: <https://physoc.onlinelibrary.wiley.com/doi/pdf/10.1113/jphysiol.2004.076307>. [Online]. Available: <https://physoc.onlinelibrary.wiley.com/doi/abs/10.1113/jphysiol.2004.076307>.
- [199] M. Papadatou-Pastou, E. Ntolka, J. Schmitz, *et al.*, “Human handedness: A meta-analysis”, *Psychological bulletin*, vol. 146, no. 6, p. 481, 2020.
- [200] Y.-L. Hsieh and M. F. Abbod, “Gait analyses of parkinson’s disease patients using multiscale entropy”, *Electronics*, vol. 10, no. 21, p. 2604, 2021.
- [201] M. Gandolfi, N. Valè, M. Filippetti, *et al.*, “Postural control in individuals with parkinson’s disease”, in *Different Areas of Physiotherapy*, IntechOpen, 2018.
- [202] A. Vargha and H. D. Delaney, “A critique and improvement of the cl common language effect size statistics of mcgraw and wong”, *Journal of Educational and Behavioral Statistics*, vol. 25, no. 2, pp. 101–132, 2000. DOI: [10.3102/10769986025002101](https://doi.org/10.3102/10769986025002101). eprint: <https://doi.org/10.3102/10769986025002101>. [Online]. Available: <https://doi.org/10.3102/10769986025002101>.
- [203] S. Papegaaij, W. Taube, S. Baudry, E. Otten, and T. Hortobágyi, “Aging causes a reorganization of cortical and spinal control of posture”, *Frontiers in aging neuroscience*, vol. 6, p. 28, 2014.
- [204] M. Kahya, K. Liao, K. M. Gustafson, A. E. Akinwuntan, B. Manor, and H. Devos, “Cortical correlates of increased postural task difficulty in young adults: A combined pupillometry and eeg study”, *Sensors*, vol. 22, no. 15, p. 5594, 2022.
- [205] B. J. Baars and N. M. Gage, *Cognition, brain, and consciousness: Introduction to cognitive neuroscience*. Academic Press, 2010.
- [206] A. Singh, R. C. Cole, A. I. Espinoza, D. Brown, J. F. Cavanagh, and N. S. Narayanan, “Frontal theta and beta oscillations during lower-limb movement in parkinson’s disease”, *Clinical Neurophysiology*, vol. 131, no. 3, pp. 694–702, 2020.
- [207] S. M. Slobounov, E. Teel, and K. M. Newell, “Modulation of cortical activity in response to visually induced postural perturbation: Combined vr and eeg study”, *Neuroscience letters*, vol. 547, pp. 6–9, 2013.
- [208] D. Malisova, T. Petrenko, A. Kondratenko, and O. Bazanova, “Alpha eeg and emg indices of optimal music-performing movement and postural control”, 2017, pp. 967–968.
- [209] G. Pfurtscheller, “Induced oscillations in the alpha band: Functional meaning”, *Epilepsia*, vol. 44, pp. 2–8, 2003.

- [210] C. Del Percio, A. Brancucci, F. Bergami, *et al.*, “Cortical alpha rhythms are correlated with body sway during quiet open-eyes standing in athletes: A high-resolution eeg study”, *NeuroImage*, vol. 36, no. 3, pp. 822–829, 2007, ISSN: 1053-8119. DOI: <https://doi.org/10.1016/j.neuroimage.2007.02.054>. [Online]. Available: <https://www.sciencedirect.com/science/article/pii/S1053811907001668>.
- [211] T. Hülzdünker, A. Mierau, and H. K. Strüder, “Higher balance task demands are associated with an increase in individual alpha peak frequency”, *Frontiers in Human Neuroscience*, vol. 9, 2016, ISSN: 1662-5161. DOI: 10.3389/fnhum.2015.00695. [Online]. Available: <https://www.frontiersin.org/articles/10.3389/fnhum.2015.00695>.
- [212] A. Van Ombergen, A. J. Lubeck, V. Van Rompaey, *et al.*, “The effect of optokinetic stimulation on perceptual and postural symptoms in visual vestibular mismatch patients”, *PLoS One*, vol. 11, no. 4, e0154528, Apr. 2016. DOI: 10.1371/journal.pone.0154528.
- [213] B. R. Malcolm, J. J. Foxe, S. Joshi, *et al.*, “Aging-related changes in cortical mechanisms supporting postural control during base of support and optic flow manipulations”, *European Journal of Neuroscience*, vol. 54, no. 12, pp. 8139–8157, 2021. DOI: <https://doi.org/10.1111/ejn.15004>. eprint: <https://onlinelibrary.wiley.com/doi/pdf/10.1111/ejn.15004>. [Online]. Available: <https://onlinelibrary.wiley.com/doi/abs/10.1111/ejn.15004>.
- [214] C. Baston, M. Mancini, B. Schoneburg, F. Horak, and L. Rocchi, “Postural strategies assessed with inertial sensors in healthy and parkinsonian subjects”, *Gait & Posture*, vol. 40, no. 1, pp. 70–75, Mar. 2014, Epub 2014 Mar 2. DOI: 10.1016/j.gaitpost.2014.02.012.
- [215] V. S. Beretta, R. Vitório, P. C. R. dos Santos, D. Orcioli-Silva, and L. T. B. Gobbi, “Postural control after unexpected external perturbation: Effects of parkinson’s disease subtype”, *Human Movement Science*, vol. 64, pp. 12–18, 2019, ISSN: 0167-9457. DOI: <https://doi.org/10.1016/j.humov.2019.01.001>. [Online]. Available: <https://www.sciencedirect.com/science/article/pii/S0167945718303804>.
- [216] R. Aubonnet, M. Hassan, A. Mheich, G. D. Lorenzo, H. Petersen, and P. Gargiulo, “Brain network dynamics in the alpha band during a complex postural control task”, *Journal of Neural Engineering*, vol. 20, no. 2, p. 026030, Apr. 2023. DOI: 10.1088/1741-2552/acc2e9. [Online]. Available: <https://dx.doi.org/10.1088/1741-2552/acc2e9>.
- [217] M. Hassan, L. Chaton, P. Benquet, *et al.*, “Functional connectivity disruptions correlate with cognitive phenotypes in parkinson’s disease”, *NeuroImage: Clinical*, vol. 14, pp. 591–601, 2017, ISSN: 2213-1582. DOI: <https://doi.org/10.1016/j.nicl.2017.03.002>. [Online]. Available: <https://www.sciencedirect.com/science/article/pii/S221315821730061X>.



# Appendix A

## Detailed Description of Features Calculated During Experiment

### A.1 EEG Features

Table A.1: 50 EEG features calculated according to band, region and relative or absolute

Name	Significance
<b>BANDS</b>	
ALPHA	Drowsy state, Relaxation, Calmness
BETA	Conscious state, Thought process
DELTA	Deep Sleep, Deepest level of Relaxation
LOWGAMMA	Elaboration of two different senses at same time
THETA	REM Sleep, Deep and Raw Emotions, Cognitive processing
<b>REGIONS</b>	
FRONTAL	Higher Mental Functions: Concentration, planning, judgment, emotional expression, creativity, inhibition
TEMPORAL R&L	Association Area: Short-term memory, equilibrium, emotion
PARIETAL	Sensory Area: Sensation from muscles and skin
OCCIPITAL	Somatosensory Association Area: Evaluation of weight, texture, temperature, etc. for object recognition

### A.2 EMG Features

Table A.2: EMG features

Name	Definition	Reference
<b>TIME PARAMETERS</b>		
AAC	Average Amplitude Change	A.1
AE	Average Energy	A.2
ASM	Absolute Value of the Summation of the Exponential Root	A.3
ASS	Absolute Value of the Summation of the Square Root	A.5
CV	Coefficient of Variation	A.6
DAMV	Difference Absolute Mean Value	A.7
DASDV	Difference Absolute Standard Deviation Value	A.8
DVARV	Difference Absolute Standard Deviation Value	A.9
EMAV	Enhanced Mean Absolute Value	A.10
EWL	Enhanced Wavelength	A.12
FZC	New Zero Crossing	A.14
KURT	Kurtosis	A.17
IEMG	Integrated EMG	A.18
IQR	Interquartile Range	A.19
LCOV	Log Coefficient of Variation	A.20
LD	Log Detector	
LDAMV	Log Difference Absolute Mean Value	A.21
LDASDV	Log Difference Absolute Standard Deviation	A.22
LTKEO	Log Teager Kaiser Energy Operator	A.23
MAD	Mean Absolute Deviation	A.24
MAV	Mean Absolute Value	A.25
MFL	Maximum Fractal Length	A.26
MN	Mean	
MD	Median	
MMAV	Modified Mean Absolute Value	A.27
MMAV2	Modified Mean Absolute Value 2	A.29
MSR	Mean Value of the Square Root	A.31
RMS	Root Mean Square	A.32
SD	Standard Deviation	A.33
SKEW	Skewness	A.34
SSI	Single Square Integral	A.35
TM	Temporal Moment	A.36
VAR	Variance	A.37
VARE	Variance of EMG	A.38
VO	V-Order	A.39
WL	Waveform Length	A.40
<b>FREQUENCY PARAMETERS</b>		
PT	Total Power	A.44
Pmax	Maximum Power	A.46
Fmax	Maximum Frequency	A.47
FMD	Median Frequency	A.43
FMN	Mean Frequency	A.42
Fkurt	Frequency Kurtosis	A.48
Fskew	Frequency Skewness	A.49

### A.2.1 EMG Formulas:

Average Amplitude Change ACC

$$AAC = \frac{1}{N} \cdot \sum_{i=1}^{N-1} |x_{i+1} - x_i| \quad (\text{A.1})$$

Average Energy

$$AE = \frac{1}{N} \cdot \sum_{i=1}^N (x_i)^2 \quad (\text{A.2})$$

Absolute Value of the Summation of the Exponential Root

$$ASM = \frac{1}{N} \cdot \sum_{i=1}^N |(x_i)^p| \quad (\text{A.3})$$

where

$$p = \begin{cases} 0.5 & \text{if } 0.25N \leq i \leq 0.75N \\ 0.75 & \text{otherwise} \end{cases} \quad (\text{A.4})$$

Absolute Value of the Summation of the Square Root

$$ASS = \sum_{i=1}^N \sqrt{|x_i|} \quad (\text{A.5})$$

Coefficient of Variation

$$CV = \frac{SD}{\bar{x}} \quad (\text{A.6})$$

Difference Absolute Mean Value

$$DAMV = \frac{\sum_{i=1}^{N-1} |x_{i+1} - x_i|}{N-1} \quad (\text{A.7})$$

Difference Absolute Standard Deviation Value

$$DASDV = \sqrt{\frac{\sum_{i=1}^{N-1} (x_{i+1} - x_i)^2}{N-1}} \quad (\text{A.8})$$

Difference Variance Value

$$DVARV = \frac{1}{N-2} \cdot \sum_{i=1}^{N-1} (x_{i+1} - x_i)^2 \quad (\text{A.9})$$

Enhanced mean absolute value

$$EMAV = \frac{1}{N} \cdot \sum_{i=1}^N |(x_i)^p| \quad (\text{A.10})$$

where

$$p = \begin{cases} 0.75 & \text{if } 0.2N \leq i \leq 0.8N \\ 0.5 & \text{otherwise} \end{cases} \quad (\text{A.11})$$

Enhanced wavelength

$$EWL = \frac{1}{N} \cdot \sum_{i=1}^N |(x_i - x_{i-1})^p| \quad (\text{A.12})$$

where

$$p = \begin{cases} 0.75 & \text{if } 0.2N \leq i \leq 0.8N \\ 0.5 & \text{otherwise} \end{cases} \quad (\text{A.13})$$

New Zero Crossing

$$FZC = \sum_{i=1}^{N-1} w_i \quad (\text{A.14})$$

$$T = \frac{2}{5} \cdot \sum_{i=1}^{10} x_i \quad (\text{A.15})$$

where

$$p = \left\{ \begin{array}{ll} 1 & \text{if } x > T \& x_{i+1} < T \\ 1 & \text{if } x < T \& x_{i+1} > T \\ 0 & \text{otherwise} \end{array} \right\} \quad (\text{A.16})$$

Kurtosis

$$KURT = \frac{x^4}{SD^4} \quad (\text{A.17})$$

Integrated EMG

$$IEMG = \sum_{i=1}^N |x_i| \quad (\text{A.18})$$

Interquartile Range

$$IQR = Q_3 - Q_1 \quad (\text{A.19})$$

Log CV

$$LCOV = \log(COV) \quad (\text{A.20})$$

Log DAMV

$$LDAMV = \log(DAMV) \quad (\text{A.21})$$

Log DASDV

$$LDASDV = \log(LDASDV) \quad (\text{A.22})$$

Log Teager Kaiser Energy Operator

$$LTKEO = \log\left(\sum_{i=1}^N N - 1(x_i)^2 - x_{i-1} \cdot x_{i+1}\right) \quad (\text{A.23})$$

Mean Absolute Deviation

$$MAD = \frac{1}{N} \cdot \sum_{i=1}^N |x_i - \bar{x}| \quad (\text{A.24})$$

Mean Absolute Value

$$MAV = \frac{1}{N} \cdot \sum_{i=1}^N |x_i| \quad (\text{A.25})$$

Maximum Fractal Length

$$MFL = \log\left(\sqrt{\sum_{i=1}^{N-1} (x_{i+1} - x_i)^2}\right) \quad (\text{A.26})$$

Modified Mean Absolute Value

$$MMAV = \frac{1}{N} \cdot \sum_{i=1}^N w_i \cdot |x_i| \quad (\text{A.27})$$

where

$$p = \begin{cases} 1 & \text{if } 0.25N \leq i \leq 0.75N \\ 0.5 & \text{otherwise} \end{cases} \quad (\text{A.28})$$

Modified Mean Absolute Value 2

$$MMAV2 = \frac{1}{N} \cdot \sum_{i=1}^N w_i \cdot |x_i| \quad (\text{A.29})$$

where

$$p = \begin{cases} 1 & \text{if } 0.25N \leq i \leq 0.75N \\ \frac{4i}{N} & \text{if } i < 0.25N \\ \frac{4(i-N)}{N} & \text{otherwise} \end{cases} \quad (\text{A.30})$$

Mean Value of the Square Root

$$MSR = \frac{1}{N} \cdot \sum_{i=1}^N \sqrt{x_i} \quad (\text{A.31})$$

Root Mean Square

$$RMS = \sqrt{\frac{1}{N} \cdot \sum_{i=1}^N (x_i)^2} \quad (\text{A.32})$$

Standard Deviation

$$SD = \sqrt{\frac{1}{N-1} \cdot \sum_{i=1}^N (x_i - \bar{x})^2} \quad (\text{A.33})$$

Skewness

$$SKEW = \frac{\sum_{i=1}^N (x_i - \bar{x})^3}{(N-1) \cdot SD^3} \quad (\text{A.34})$$

Single Square Integral

$$SSI = \sum_{i=1}^N (x_i)^2 \quad (\text{A.35})$$

Absolute Value of Temporal Moment

$$TM = \frac{1}{N} \cdot \sum_{i=1}^N |(x_i)^p| \quad (\text{A.36})$$

where  $p \in \mathbb{N}$  and commonly  $p = 3$

Variance

$$VAR = \frac{1}{N-1} \cdot \sum_{i=1}^N (x_i - \bar{x})^2 \quad (\text{A.37})$$

Variance of EMG

$$VARE = \frac{1}{N-1} \cdot \sum_{i=1}^N (x_i)^2 \quad (\text{A.38})$$

Variance Order

$$VO = \sqrt{\frac{1}{N} \cdot \sum_{i=1}^N (x_i)^p} \quad (\text{A.39})$$

where  $p \in \mathbb{N}$  and commonly  $p = 2$

Waveform Length

$$WL = \sum_{i=2}^N |x_i - x_{i-1}| \quad (\text{A.40})$$

Power

$$p_i = \frac{1}{M} \cdot (X_i)^2 \quad (\text{A.41})$$

Mean Frequency

$$F_{MN} = \frac{\sum_{i=1}^M f_i \cdot p_i}{\sum_{i=1}^M p_i} \quad (\text{A.42})$$

Median Frequency

$$F_{MD} = \frac{1}{2} \cdot \sum_{i=1}^M p_i \quad (\text{A.43})$$

Total Power

$$P_T = \sum_{i=1}^M p_i \quad (\text{A.44})$$

Mean Power

$$P_{MN} = \frac{1}{M} \cdot \sum_{i=1}^M p_i \quad (\text{A.45})$$

Peak Power

$$P_{max} = \max(p_i) \quad (\text{A.46})$$

Peak Frequency

$$F_{max} = \max(f_i) \quad (\text{A.47})$$

Kurtosis Frequency

$$F_{kurt} = \frac{F_{MN}^4}{F_{SD}^4} \quad (\text{A.48})$$

Skewness Frequency

$$F_{skew} = \frac{\sum_{i=1}^M (f_i - F_{MN})^3}{(M - 1) \cdot F_{SD}^3} \quad (\text{A.49})$$

## A.3 CoP Features

Table A.3: 35 COP features

Name	Definition	Reference
<b>TIME PARAMETERS</b>		
TOTEX (cm)	Total Excursion on the support plane	A.57
TOTEX-ML (cm)	Total Excursion on the support ML plane	A.59
TOTEX-AP (cm)	Total Excursion on the support AP plane	A.58
RD (cm)	Square Root Distance between a point and the plane origin	A.56
MDIST-ML (cm)	Mean Distance in Medio-lateral Direction	A.62
MDIST-AP (cm)	Mean Distance in Antero-posterior Direction	A.61
MVELO (cm/s)	Mean Velocity on support plane	A.66
MVELO-ML (cm/s)	Mean Velocity on ML plane	A.68
MVELO-AP (cm/s)	Mean Velocity on AP plane	A.67
RDIST (cm)	Root Mean Square Distance respect to origin	A.63
RDIST-ML (cm)	Root Mean Square Distance in Medio lateral Direction	A.65
RDIST-AP (cm)	Root Mean Square Distance in Antero posterior Direction	A.64
ML-SampEn (nats)	Medio-lateral Sample Entropy	A.65
AP-SampEn (nats)	Antero-posterior Sample Entropy	A.64
ML-CI (nats)	Medio-lateral Complexity Index	
AP-CI (nats)	Antero-posterior Complexity Index	
Ellipse Area ( $cm^2$ )	Area of the 95% confidence ellipse	A.69
Ellipse angle (deg)	Angle between main axis of the 95% confidence ellipse and ML axis	
Ellipse Main Axis Length (cm)	Length of the Main Axis of the 95% confidence ellipse	
Ellipse Minor Axis Length (cm)	Length of the Minor Axis of the 95% confidence ellipse	
SD AP (cm)	Standard Deviation in Antero-posterior Direction	
SD ML (deg)	Standard Deviation in Medio-Lateral Direction	
SD Magnitude (cm)	Standard deviation of the distance of points with respect to the origin	
SD Direction (cm)	Standard deviation of the angle difference between successive points with respect to the ML axis	
Magnitude Entropy (nats)	Sample Entropy of the distance of points with respect to the origin	
Direction Entropy (nats)	Sample Entropy of the angle difference between successive points with respect to the ML axis	
Multivariate CI (nats)	Summation of Sample Entropy computed with increasing time scale on the multivariate ML-AP series	
Antero Magnitude (cm)	Magnitude of the furthest point in the anterior portion of the plane	
Antero Angle (deg)	Angle of the furthest point in the anterior portion of the plane	
Postero Magnitude (cm)	Magnitude of the furthest point in the posterior portion of the plane	
Postero Angle (deg)	Angle of the furthest point in the posterior portion of the plane	
Left Magnitude Maximum (cm)	Magnitude of the furthest point in the left portion of the plane	
Left Angle (deg)	Angle of the furthest point in the left portion of the plane	
Right Magnitude Maximum (cm)	Magnitude of the furthest point in the right portion of the plane	
Right Angle (deg)	Angle of the furthest point in the right portion of the plane	



### A.3.1 CoP Formulas:

ML and AP components (these axes are referenced to the force platform, not the subject) are multiplied with the physical sizes of the machine to express the measurements in centimeters. Thus, the normalized signals  $AP_N$  and  $ML_N$  are:

$$AP_U[n] = AP_N[n] \cdot (41.5/2) \quad (\text{A.50})$$

$$ML_U[n] = ML_N[n] \cdot (32.5/2) \quad (\text{A.51})$$

Equation (A.52) is used to compute the mean of AP component, while equation (A.53) calculates the mean of the ML component. The parameter N represents the number of samples within the time window. The COP coordinate time series, AP and ML, are commonly used to compute measures of postural steadiness, and characterize the static performance of the PC system.

$$\overline{AP} = \frac{1}{N} \sum_{n=1}^N AP_U[n] \quad (\text{A.52})$$

$$\overline{ML} = \frac{1}{N} \sum_{n=1}^N ML_U[n] \quad (\text{A.53})$$

Even though the moving platform has a predetermined sign for foot placement, individual variations in foot positioning result in the stabilogram being rarely centered. To address this, equations (A.54) and (A.55) are utilized to obtain a centered stabilogram.

$$AP[n] = AP_U[n] - \overline{AP}; \quad n = 1, \dots, N \quad (\text{A.54})$$

$$ML[n] = ML_U[n] - \overline{ML}; \quad n = 1, \dots, N \quad (\text{A.55})$$

The resultant distance RD[n] is the Euclidean distance of sample n from the origin:

$$RD[n] = \sqrt{(AP_n^2 + ML_n^2)}, \quad n = 1, \dots, N \quad (\text{A.56})$$

Total Excursion TOTEX is the summation of the elementary excursion (movement) on the support plane between consecutive samples. It represents the total length of the path followed by the CoP. TOTEX is widely recognized as a reliable measurement in various populations and balance conditions. A smaller path length indicates better postural stability. It is also defined for the AP and ML components.

$$TOTEX = \sum_{n=1}^{N-1} \sqrt{(AP[n+1] - AP[n])^2 + (ML[n+1] - ML[n])^2} \quad (\text{A.57})$$

$$TOTEX_{AP} = \sum_{n=1}^{N-1} \sqrt{(AP[n+1] - AP[n])^2} \quad (\text{A.58})$$

$$TOTEX_{ML} = \sum_{n=1}^{N-1} \sqrt{(ML[n+1] - ML[n])^2} \quad (\text{A.59})$$

MDIST represents the average distance of the CoP from the center of the trajectory. It has been defined for the AP and ML axes.

$$MDIST = \frac{1}{N} \sum_{n=1}^N |RD[n]| \quad (A.60)$$

$$MDIST_{AP} = \frac{1}{N} \sum_{n=1}^N |AP[n]| \quad (A.61)$$

$$MDIST_{ML} = \frac{1}{N} \sum_{n=1}^N |ML[n]| \quad (A.62)$$

RDIST is the root mean square (RMS) distance from the mean CoP. It is computed for the support plane, ML axis, and AP axis and corresponds to the standard deviation of the trajectory.

$$RDIST = \sqrt{\frac{1}{N} \sum_{n=1}^N RD^2[n]} \quad (A.63)$$

$$RDIST_{AP} = \sqrt{\frac{1}{N} \sum_{n=1}^N AP^2[n]} \quad (A.64)$$

$$RDIST_{ML} = \sqrt{\frac{1}{N} \sum_{n=1}^N ML^2[n]} \quad (A.65)$$

MVELO is the average velocity of movement (mean velocity of points on the support plane), by dividing the total excursion by the total time T(30 seconds in this analysis).

$$MVELO = \frac{TOTEX}{T} \quad (A.66)$$

$$MVELO_{AP} = \frac{TOTEX_{AP}}{T} \quad (A.67)$$

$$MVELO_{ML} = \frac{TOTEX_{ML}}{T} \quad (A.68)$$

$$EllipseArea = EllipseMainAxis \cdot EllipseMinorAxis \cdot \pi \quad (A.69)$$

## A.4 MOTION SICKNESS QUESTIONNAIRE

### A.4.1 Lifestyle Indexes

Using the data extracted from the MSSQ multiple different indexes are computed relative to lifestyle habits, MS proneness and symptoms.

**Lifestyle Index** The Lifestyle Index (LSI) is a three classes index based on BMI, Sport Activity, Nicotine, Caffeine, and Alcohol assumption.

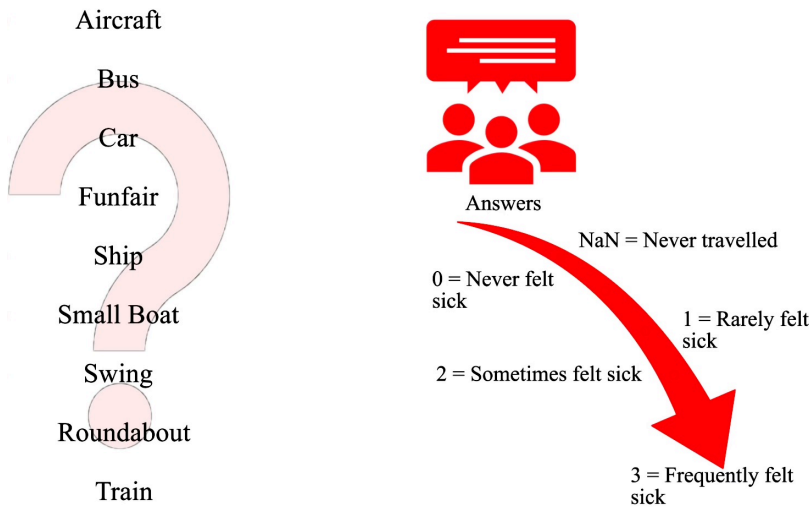
Participants are assigned 1 point if the behavior is considered healthy, and no points otherwise following these next criteria:

$$LifestyleIndex = \sum_{n=1}^N BMI + Sport + Nicotine + Caffeine + Alcohol \quad (A.70)$$

The summation (LS\_Sum) of the points is then computed and the three classes LSI is defined as follow:

It takes into consideration for each patient the BMI, smoking status and physical activities excluding alcohol and caffeine information. A person is considered healthy if two of those characteristics are considered healthy. On the total of 262 participants of the third cohort, 196 has been considered with an healthy lifestyle while the remaining 66 do not have a healthy lifestyle.

**Motion Sickness Proneness Index** The Motion Sickness Proneness Index (MSPI) is a binary index based on the answers relative to MS susceptibility and predisposition on transport and entertainment systems. For each category a point from 0 to 3 is assigned. The summation of these points is computed and divided to the answer given (maximum of 9 categories): the results is defined as (MSP\_Sum).



$$MotionSicknessPronenessIndex = \frac{\sum(Transport/Entertainment) * 9}{9 - \sum(NaN)} \quad (A.71)$$

**Motion Sickness Index** The Motion Sickness Index (IMS) is a binary index that refers to the 13 MS symptoms listed previously. These symptoms are grouped as follow and computed for the PRE (before the simulation) and the POST (after the simulation). Binary indexes referred to these groups of symptoms are created following these steps: first, we compute the average from the individual responses of each index; second, we calculate the maximum among the averages; and third, we divide the cohort into two groups (below and above 1/3 of the maximum). For IGenDis and IDizz, we apply only steps 2 and 3 using the direct response instead of the average. The symptoms groups are the following:

Moreover, we established two more indexes: Physiological/Vegetative Index (IPV) and Neurological/Muscle Strain Index (INM). IPV is based on the responses from sweating, salivation, nausea, burping, stomach awareness, and general discomfort conditions. Similarly, the INM is based on fatigue, eye strain, difficulty focusing, headache, fullness of head, blurred vision, and again general discomfort conditions. IMS is here defined as the weighted sum (SumMS) of all the MSSQ answers (Eq. A.72):

$$\begin{aligned}
 SumMS = & (0.2 * GenDisc + 0.2 * Dizz\&Vert + \\
 & + 0.2 * \sum (StomAwe, Nausea, Sweat, Saliv, Burp) + \\
 & + 0.2 * \sum (Fatigue, EyeSt, DiffFocus) + \\
 & + 0.2 * \sum (Headache, FullHead, BlurrVis)) \quad (A.72)
 \end{aligned}$$

**BioVRSea Effect Index** For each symptom group defined before the difference between POST and PRE is computed (if negative is considered 0). If the difference is >0 the Symptom Group Binary Difference (SG\_BinDiff) is =1, otherwise SG\_BinDiff=0. SG\_BinDiff is computed for each of the five groups and then summed up creating MS\_Diff\_Sum. If MS\_Diff\_Sum=1 it means that 1 symptom group has increased from before (PRE) the simulation to after (POST) it. If MS\_Diff\_Sum=5 it means that all the symptom group has increased, if MS\_Diff\_Sum=0, there are no changes in the MS symptoms after the simulation.

BVSEI is binary defined splitting the population in two considering MS\_Diff\_Sum=1. BVSEI differs people who had a single change in the symptoms (or more than one) between before and after the experiment, from people who did not suffer any symptoms.

Out of the 355 subjects, 233 (65.63%) did have a symptom effect on the BioVRSea experiment (BVSEI=1), 122 (34.37%) did not have any symptom changes (BVSEI=0).

The following tables show the percentages of the 355 subjects when combining the three main indexes: table A.6 shows the percentages and relative gender and age information related to LSI and MSPI, table A.7 do the same in relation to LSI and BVSEI, and finally table A.8 shows the information relative to MSPI and BVSEI.

Table A.4: Motion Sickness Questionnaire based on SCAT5

<b>CONDITION PARAMETERS</b>	
PARKINSON CONCUSSION AMPUTEE	
<b>PHYSIOLOGICAL PARAMETERS</b>	
AGE GENDER HEIGHT WEIGHT BMI	
<b>LIFESTYLE PARAMETERS</b>	
SPORT NICOTINE CAFFEINE ALCOHOL	
<b>INDEX</b>	
LIFESTYLE MS PRONE BIOVRSEA EFFECT	

Lifestyle Conditions	Unhealthy = [0]	Healthy = [1]
<b>BMI</b>	$\geq 25$	$< 25$
<b>SPORT activity</b>	$\leq 3$ times per week	$> 3$ times per week
<b>daily NICOTINE usage</b>	Yes	No
<b>today's CAFFEINE usage</b>	Yes	No
<b>ALCOHOL usage</b>	Today or Yesterday	No or more than 2 days ago

if LS\_Sum=0 or 1

if LS\_Sum=2 or 3

if LS\_Sum=4 or 5

<b>MS Prone = [1]</b> if MSP_Sum $\geq 9$	<b>NOT MS Prone = [0]</b> otherwise
--	--

Table A.5: Motion Sickness Index

Indexes	Symptoms average
Stomach Index (Isto)	Salivation, Sweating, Nausea, Stomach Awareness, Burping
Fatigue Index (Ifatig)	Fatigue, Eye Strain, Diff. Focusing
Head Index (Ihead)	Headache, Blurred Vision, Fullness of Head
General Discomfort (IGenDis)	includes only General Discomfort
Dizziness-Vertigo (IDizz)	includes only Dizziness-Vertigo

Table A.6: Percentages of subjects related to Lifestyle Index and Motion Sickness Proneness Index

	<b>PRONE</b>	<b>NOT PRONE</b>
<b>2*RED</b>	<b>1.97%</b>	<b>3.94%</b>
	AGE: 40,43 +- 14,82 Female: 7 - (100%) Male: 0 - (0,00%)	AGE: 41,14 +- 14,41 Female: 6 - (42,86%) Male: 8 - (57,14%)
<b>2*YELLOW</b>	<b>12.96%</b>	<b>29.01%</b>
	AGE: 37,74 +- 14,12 Female: 29 - (63,04%) Male: 16 - (34,78%) NotSpec: 1 (2,17%)	AGE: 35,29 +- 14,07 Female: 38 - (36,89%) Male: 64 - (62,14%) NotSpec: 1 (0,97%)
<b>2*GREEN</b>	<b>15,77%</b>	<b>36,34%</b>
	AGE: 29,54 +- 14,27 Female: 48 - (85,71%) Male: 8 - (14,29%)	AGE: 28,87 +- 14,18 Female: 70 - (54,26%) Male: 59 - (45,74%)

Table A.7: Percentages of subjects related to Lifestyle Index and BioVRSea Effect Index

	<b>BioVRSea Influenced</b>	<b>BioVRSea Not Influenced</b>
<b>2*RED</b>	<b>3.94%</b>	<b>1.97%</b>
	AGE: 40,50 +- 14,82 Female: 11 - (78,57%) Male: 3 - (21,43%)	AGE: 41,71 +- 14,38 Female: 2 - (28,57%) Male: 5 - (71,43%)
<b>2*YELLOW</b>	<b>26.19%</b>	<b>17.77%</b>
	AGE: 32,82 +- 14,08 Female: 48 - (51,61%) Male: 44 - (47,31%) Not Spec: 1 (1,08%)	AGE: 41,07 +- 14,16 Female: 20 - (35,71%) Male: 35 - (62,50%) Not Spec: 1 (1,79%)
<b>2*GREEN</b>	<b>35.49%</b>	<b>16.61%</b>
	AGE: 28,54 +- 14,21 Female: 88 - (69,84%) Male: 38 - (30,16%)	AGE: 29,70 +- 14,18 Female: 30 - (50,85%) Male: 29 - (49,15%)

Table A.8: Percentages of subjects related to Motion Sickness Proneness Index and BioVRSea Effect Index

	<b>BioVRSea Influenced</b>	<b>BioVRSea Not Influenced</b>
<b>2*Prone</b>	<b>25.35%</b>	<b>40.29%</b>
	AGE: 32,01 +- 14,37 Female: 74 - (82,22%) Male: 15 - (16,67%) Not Spec: 1 - (1,11%)	AGE: 30,30 +- 14,09 Female: 73 - (51,05%) Male: 70 - (48,95%)
<b>2*Not Prone</b>	<b>5.35%</b>	<b>29.01%</b>
	AGE: 39,41 +- 14,38 Female: 11 - (57,89%) Male: 8 - (42,11%)	AGE: 34,62 +- 14,06 Female: 41 - (39,81%) Male: 61 - (59,22%) Not Spec: 1 - (0,98%)